NUCLEAR ELECTRIC MAGNETOHYDRODYNAMIC PROPULSION FOR SUBMARINE

by

ADALBERT A. BEDNARCZYK

B. A. Chemistry, Chaminade University, May 1978

SUBMITTED TO THE DEPARTMENT OF OCEAN ENGINEERING

IN PARTIAL FULFILLMENT OF THE REQUIREMENTS

FOR THE DEGREES OF

MASTER OF SCIENCE IN NAVAL ARCHITECTURE

AND MARINE ENGINEERING

and

MASTER OF SCIENCE IN NUCLEAR ENGINEERING

at the

MASSACHUSETTS INSTITUTE OF TECHNOLOGY

May, 1989

Signature of Author..., Adalbert A. Bednarczyk.....
Department of Ocean Engineering
May, 1989

Certified by.....
Barrick F. Tibbitts, Thesis Supervisor

.....
John E. Meyer, Nuclear Engineering Department Reader

Accepted by.....
A. Douglas Carmichael, Chairman
Departmental Graduate Committee
Department of Ocean Engineering

NUCLEAR ELECTRIC MAGNETOHYDRODYNAMIC PROPULSION FOR SUBMARINE

by

ADALBERT A. BEDNARCZYK

Submitted to the Department of Ocean Engineering and the Department of Nuclear Engineering in May 1989 in partial fulfillment for the Degrees of Master of Science in Naval Architecture and Marine Engineering and Master of Science in Nuclear Engineering.

ABSTRACT

This thesis analyzes the superconducting technology for a shipboard magnetohydrodynamic propulsion system. Based on the principles of magnetohydrodynamics (MHD), the concept of open water efficiency was used to optimize the preliminary design of a MHD thruster. After the baseline submarine hull, modeled after the Los Angeles class submarine, was selected propulsive efficiency and the top speed for four variant MHD submarines were evaluated. The design criteria were set at a 100 MWt nuclear reactor power upper limit and a requirement of 30 knots for the top speed. This required advanced reactor plant and advanced energy conversion system. The selection of High Temperature Gas Reactor (HTGR) and Liquid-Metal Fast Breeder Reactor (LMFBR) was based on the combined merits of safety, environmental impact, high source temperature and maximum volume power density (KW/L). With the reactor outlet temperatures of 2000 K direct cycle energy conversion systems gave the best results in terms of thermal efficiency and propulsion plant power density. Two energy conversion systems selected were closed-cycle gas turbine geared to a superconducting generator, and closed-cycle liquid-metal MHD generator. Based on submarine reliability and safety the option of using an intermediate heat exchanger was also considered. Finally, non-nuclear support systems affected by the advanced power plant and MHD propulsion, stressing submarine safety, are proposed.

Thesis supervisor: Tibbitts, Barrick F.
Title: Profesor of Naval Construction and Engineering

Thesis reader: Meyer, John E.
Title: Professor of Nuclear Engineering

ACKNOWLEDGEMENT

I would like to express my gratitude to Professor Barrick Tibbitts and Professor John Meyer for their expertise, advice, and interest in this research project.

My sincere thanks go to Dr. Daniel Swallom, Dr Isaac Sadovnik, and Judis Gibbs of AVCO Inc. for their assistance, friendship, and much needed technical support, without which my work would have been much more difficult.

Sincere appreciation and thanks to Dr. James Meng and Mr. Phillips of NUSC for sharing their expertise and technical library with the author during the last six months.

Special thanks to Professor Paul Sullivan and Frank Camelio for always finding time to help me with my work or personal problem.

Finally, I would like to thank Jerri Traina for her unending support and love.

Adalbert A. Bednarczyk

May 1989

TABLE OF CONTENTS

LIST OF FIGURES

LIST OF TABLES

NOMENCLATURE

Symbol	Meaning
A	Cross-sectional area
A_c	MHD active channel flow area
A_N	Diffuser flow area
A_o	Capture area
A_{MHD}	Wetted surface area of MHD channel
A_{ws}	Wetted surface area of the hull
a'	Effective magnetic angle
B	Magnetic flux density
b	Boundary layer thickness
C_{app}	Appendage drag coefficient
C_D	Ship's drag coefficient
C_{delf}	Friction correlation allowance
C_f	Friction coefficient
C_p	Pressure coefficient
C_r	Residual resistance
c_p	Prismatic coefficient
D	Diameter
d	MHD electrode separation
E	Electric field
EHP	Effective Horse Power
F	Lorentz Force
f	Friction factor
G	Interaction parameter
H_L	Headloss
h	MHD channel height
I_o	Electric current

J	Electric current density
J_m	Magnetic coil current density
K	MHD generator loading parameter
$K_{()}$	Pressure loss coefficient
K_w	Wake energy
L_m	Inductance
L_{ship}	Ship's length between perpendiculars
l	MHD active channel length
m	Pressure attenuation coefficient
N_{ab}	Unit vector from a to b
N_d	Thruster drag efficiency
N_e	Electrical efficiency
N_h	Hull efficiency
N_{hy}	Hydrodynamic efficiency
N_o	Open water efficiency
N_p	Propulsive efficiency
N_{pl}	MHD generator polytropic efficiency
N_r	Rotative efficiency
P	Electric power density
P'	Non-dimensional power
p	Pressure
p_{amb}	Ambient pressure
PC	Propulsive coefficient
P_g	MHD generator power density
p_{in}	Inlet pressure
P_j	Joule heating power density
p_{out}	Outlet pressure
P_t	Effective thrust power density

R_{ab}	Ship's after body radius
P_{fb}	Ship's forward body radius
Q	Mass flow rate
R_{pmb}	Ship's parallel middle body radius
R_x	Reynold's Number
r_i	Inside radius of MHD channel (hull radius)
r_o	Outside radius of MHD channel
s	Electrical conductivity
SHP	Shaft Horse Power
SVR	Velocity ratio squared
T	Thrust
U_c	MHD channel average velocity
U_N	Diffuser velocity
U_o	Free stream velocity (velocity at A_o)
U_y	Turbulent boundary layer velocity
U_{ship}	Ship's speed
V	Velocity
V_o	Voltage
1-t	Thrust deduction factor
1-w	Wake factor
Φ	Electric potential
ρ	Density

1. INTRODUCTION

The past few decades of submarine hydrodynamic evolution have resulted in a ship of teardrop shape with unobstructed skin. The fact that a modern submarine resembles an airplane is not a coincidence. Underwater the submarine maneuvers much like an aircraft. It dives, climbs, banks and turns by manipulating control surfaces. These control surfaces are a vertical rudder aft and horizontal diving planes forward and aft. There is a fixed fin forward, commonly referred to as fairwater, or simply the sail. The outer hull at the bow houses major sonar equipment and forms the nose of the teardrop. The parallel middle body houses all the equipment required for control, stability, propulsion, and weapon systems. The after end of the outer hull tapers to a point, providing a hydrodynamically effective flow path to the stern control planes and the propeller.

Ship motion causes turbulence and friction, two conditions especially undesirable in the military submarine: turbulence creates noise and friction creates resistance which reduces speed. The submarine is moved through the water by one (or more) propellers, driven (on a nuclear submarine) by steam turbines. The steam is generated by water brought to a boil by other highly pressurized water which is heated by a nuclear reactor. All U.S. submarines are powered by a pressurized water reactor (PWR) coupled to a steam turbine. Although, it

may no longer be the most efficient and compact system technology, the PWR design has a long history of safe, reliable operation. Torque generated by the steam turbine is transmitted to the screw by the propulsion train (reduction gear and shafting). The work of the screw on the sea water results in thrust necessary to overcome ship's drag.

It should be mentioned that a screw propeller design has evolved along with the ship and it has been perfected to give a very high propulsive efficiency. The Los Angeles (SSN 688) class submarine is capable of more than 30 knots top speed. The main disadvantage of screw propulsors is their radiated noise (broad band as well as cavitation). Noise signature, vis-a-vis one's adversary's, plays a predominant role in submarine warfare.

The application of magnetohydrodynamic (MHD) propulsion for marine use is in it's infancy. Consequently, MHD is not yet competitive with conventional propeller systems, particularly in terms of propulsive efficiency. However, advances in superconducting magnet technology have generated renewed interest in developing MHD propulsion systems. By eliminating the mechanical propulsion train and propeller and their associated radiated noise, MHD proponents anticipate developing underwater vehicles of great acoustic stealth.

The basic principles of MHD are straightforward. First, a unidirectional current is established through an electrically conducting fluid such as sea water.

Then, a high intensity magnetic field perpendicular to the current is imposed through the fluid. This combination of orthogonal magnetic field, electric field, and a relative motion of ions results in a Lorentz force with direction defined by the cross-product of current and magnetic field vectors.

If the device containing the electromagnetics and enclosing the fluid is fixed, the fluid is essentially pumped. However, if the device is free or has minimal resistance to motion, it will recoil according to Newton's second law of motion. In this case, the device is referred to as a pump-jet or thruster.

The major structural components of a MHD thruster consist of an inlet nozzle, main body which houses the active MHD channel, and a nozzle diffuser. The superconducting magnet and electrodes are arranged in the main body as to achieve orthogonality between electric and magnetic fields. Figure 1-1 shows a simple schematic of a MHD thruster.

In the absence of imposed electric field but with a conducting fluid moving in orthogonal direction to the imposed magnetic field, electric field will be generated. In this case, the device is referred to as a MHD generator.

Chapter 2 provides a brief analytical derivation and a historical background of the MHD concept. The main focus is on a MHD propulsion thruster with a recognition that a MHD generator is a also a strong candidate for

future energy conversion systems. Based on the relationships developed, the remainder of Chapter 2 is devoted to preliminary optimization of a MHD thruster based on its open water efficiency. The open water efficiency of a screw propeller or a MHD thruster is evaluated in the free stream, hence detached from the ship's hull.

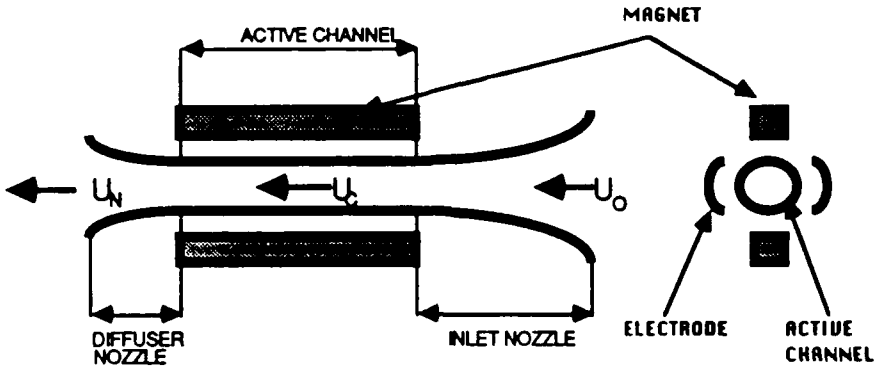

Figure 1-1 Simple Schematic of MHD Thruster

When a thruster is attached to the submarine hull it is no longer advancing into undisturbed water. The thruster is now working in a medium which has been disturbed by the passage of the hull, and in general the water around the ship has acquired a forward motion in the same direction as the ship. This forward-moving water is called the wake. The effects of this wake, and the formation of a turbulent boundary layer over the hull, will alter the efficiency of a MHD thruster. This corrected efficiency is commonly known as a propulsive

coefficient (PC).

The intent of Chapter 3 is to analyze the interaction between the hull and a MHD thruster. Because of coupling between the hull and thruster's performance, a baseline hull is selected and analyzed for its hydrodynamic performance. A hull similar to the Los Angeles class submarine (SSN 688) is chosen in order to compare the propulsive coefficient of the ship with a conventional screw to a MHD propulsion system. The hydrodynamic performance and dimensions of this hull are used to complete the optimization process to achieve maximum propulsive coefficient. Since the propulsive coefficient of a MHD thruster is projected to be lower than for a conventional screw propeller, other options are examined to achieve 30 knots top speed. Finally, all options are evaluated for the maximum speed if a 100 MW pressurized water reactor and a conventional steam turbine generator are used to supply power for the MHD propulsion.

Chapter 4 provides a short review of advanced technology for reactor systems and energy conversion systems. Safety of operation, high efficiency and high volume power density (kW/L) are the selection criteria used to determine the most optimum reactor plant and energy conversion system combination(s). The preliminary designs of the best candidates are based on very high source temperatures and the marine environment. A limit of 2000^{o} K is placed on the reactor outlet temperature which is projected to be upper limit of material tech-

nology in early decades of the next century. The estimates for a maximum speed of all variant ships with MHD propulsion are then calculated using a 100 MW equivalent advanced reactor plant.

Unique issues associated with MHD propulsion and advanced power systems, starting with a preliminary design for advanced energy conversion systems, are discussed in Chapter 5. The major non-nuclear systems required for MHD submarine propulsion are a cryogenic plant and MHD magnet charging and discharging electrical network. Non-nuclear systems affected significantly by the MHD propulsion and the advanced power systems are: the sea water cooling system, emergency propulsion system, and ship's electrical system.

The last topic in Chapter 5 examines magnetic leakage from the MHD propulsion which increases the ship's magnetic signatures and can be used in anti-submarine warfare. An estimate of magnetic leakage internal to the ship is needed also to determine its environmental impact on personnel and machinery.

The main purpose of this study is to determine the feasibility of a MHD propulsion for use on a military submarine. Small prototypes followed by large scale ones will be required to demonstrate the stealth of MHD propulsion. The propulsive efficiency is a secondary consideration since the technological evolution is bound to produce much more efficient design than the one proposed in this study.

2. DIRECT CURRENT MAGNETOHYDRODYNAMICS, MHD

2.1 HISTORY OF PROBLEM

MHD electrical power generation was first recognized by Michael Faraday as technically feasible during his original investigation of electromagnetic induction in 1831. The first recorded attempt to develop an MHD generator was conducted at the Westinghouse Research Laboratories before and during World War II. Ambitious large-scale programs were undertaken in the United States for the next decade but they were plagued with many problems and marginal successes.

After 1959, MHD programs developed rapidly. Of particular importance in the area of commercial MHD was the joint effort between the AVCO Corporation and a group of private utilities to develop MHD generators for coal-fired plants. The program did not receive government support because the major governmental effort was focussed on the development of nuclear power plants.

Of the major countries that at one time embarked on commercial MHD programs, Great Britain, France, and Germany have recently reduced their efforts. The United States, Japan, Poland and the Soviet Union are continuing their programs on a relatively large scale.[1]

The MHD generator or pump is very simple and compact, and has a high power density. As such, it is especially attractive for military applications. The United

States has considered MHD for ship propulsion since 1960; here compactness and the absence of rotating machinery were felt to be important from a viewpoint of reducing noise, especially important in submarine propulsion. The Soviet Union has been a major source of MHD research and there is evidence of a large R&D effort today. The lack of recent publications implies that the military applications have caused current MHD developments to be confidential in nature.

The feasibility of MHD propulsion was first demonstrated by Stewart Way who published a very complete and mathematically rigorous analysis of an external duct, DC propulsion system.[2] Way constructed a small 3-meter long, 900 lb. displacement submarine model (EMS-1) in 1966. Using conventional magnet coils and battery power, the EMS-1 model achieved almost 2 knots with a very weak (0.02 T) magnetic field. Finally, Yoshiro Saji's work on MHD propulsion should be mentioned. In 1979, Saji constructed the first superconducting model of an external duct, DC design. Saji's model, the ST-500, achieved about 1.5 knots.[3]

Recent developments in super-conductivity and superconducting magnets are responsible for intense research in MHD propulsion and generation. The Japanese research group JAFSA has made a major contribution to the development of MHD thrusters for high speed ships.[4] JAFSA constructed a 3 meter operable model (1.2 T, 100 Amps, 48 Volts) which achieved the speed of 0.5 meters per

second (0.97 knots). The next model, Yamato I, is scheduled for operational test in 1990. This model (length=46m) will be outfitted with two six barrel propulsors (4 Tesla, 4 kA/m^2, 26 meter ducts).

2.2 MAGNETOHYDRODYNAMIC THEORY

In this section a simplified mathematical description of an ideal MHD pump and generator is given. This also serves to introduce some of the basic terms and concepts. In principle, the relationship between the pump and a generator is analogous to an electrical motor being driven and operated like a generator. The initial focus will be on the operation of a MHD pump because it is less complex, and has a larger application in MHD propulsion. Recent research revealed many complications which may significantly reduce the achievable efficiency of a MHD pump. Projected efficiency is still attractive enough for submarine propulsion applications.

The following equations are applicable to any fluid of scalar electrical conductivity s (S/m) at a given point, and velocity vector V (m/sec). If the fluid is exposed to the combination of the electric field vector E (V/m), and the magnetic flux density vector B (T), then the induced electric current density J (A/m^2) is a vector with a magnitude and direction defined by the following equation:[5]

$$J = s(E+VxB) \quad . \qquad (1)$$

The cross product (V x B) in equation (1) is manifested as an apparent electric field, which is analogous to the back EMF associated with electric motors, where the motor armature is analogous to the flowing fluid. When E, V, and B are mutually orthogonal (the most

favorable situation), the back EMF will be in the direction opposite to the imposed electric field. The magnitude and direction of the current density depends primarily on the relative magnitudes of the imposed electrical field E, and the back EMF. The direction of current density J determines if the system behaves as a pump or a generator. Equation (1) is very simple to use if the directions and the magnitudes of E, V, and B are uniform throughout the channel. This is very difficult to accomplish in the actual design; equation (1) must be integrated over the entire volume of the working fluid.

If the working fluid is gaseous, additional terms must be added to equation (1). They were omitted here because the media applicable to MHD thrusters is sea water. Note that if the sea water becomes stationary, equation (1) reduces to a simple Ohm's Law customarily used in a DC circuit theory.

Assuming that the flow channel does not experience significant flow perturbations, or that the applied electric field does not result in a breakdown (arcing) event in sea water, the value of electric current density can be calculated with an adequate degree of accuracy. Two phase flow resulting from excessive gas production on the electrodes, or flow irregularities, require significant modeling effort and sophisticated computer codes to obtain an accurate solution.

When electric current passes through an electrically neutral conducting medium in the presence of the mag-

netic field, a vector body force per unit of volume F (N/m^3) is felt by the medium. F is customarily referred to as a Lorentz Force and it is given by the following equation:[5]

$$\bar{F} = \bar{J} \times \bar{B} \quad . \tag{2}$$

It is this force which is applied to accelerate sea water in the MHD duct to generate thrust. Similarly, the Lorentz Force will decelerate the working medium if the resulting direction of J converts the MHD duct into a generator.

The total electrical energy input to the MHD pump per unit volume is called the Electric Power Density P (W/m^3). Fcr a DC circuit, it is expressible as:

$$P = \bar{E}*\bar{J} \quad . \tag{3}$$

As expected, part of the total power input will be manifested by the resulting thrust power. Unfortunately, the remainder will be lost due to heating in the MHD duct. In the MHD pump the resistive losses are referred to as Joule heating power density P_j (W/m^3), i.e.

$$P_j = J^2/s \quad . \tag{4}$$

The difference between the total power input and Joule heating power losses constitutes an ideal Effective Thrust Power Density P_t (W/m^3). Taking a dot product of both sides of equation (1) with J gives:

$$J^2 = \bar{J}*s(\bar{E}+\bar{V}x\bar{B}) \quad .$$

Dividing both sides by d and rearranging after substituting equation (3) for the Electric Power Density P, yields:

$$P = \bar{V}*\bar{J}x\bar{B}+J^2/s \quad ,$$

$$P_t = \bar{V}*\bar{J}x\bar{B} \quad ; \qquad (5)$$

where P_t is the Effective Thrust Power Density.

An alternative expression for P_t is found by substituting equation (2) into equation (5).

$$P_t = \bar{V}*\bar{F} \quad . \qquad (6)$$

Equations (5) and (6) are very simple and easy to work with. Iney can be used in simple analysis and still apply in a complicated cases which require computer or physical modeling.

As mentioned before, the MHD generator works on the same principles but in reverse of the MHD pump. In order for the MHD duct to operate in a generator mode, the imposed electric field E due to an electrical load on the generator must be smaller than the back EMF. Equation (1) still applies.

It is customary to define a loading parameter K:[6]

$$K = E/(\bar{V}x\bar{B}) = [E]/[V][B] \quad .$$

After substituting value of K into equation (1), and working with vector magnitudes only since the system is orthogonal, one may write

$$J = (1-K)sVB \quad . \qquad (7)$$

Then the power delivered to the load, per unit volume of the generator, is

$$P = JE = K(1-K)sV^2B^2 \quad . \qquad (8)$$

Equations (1) and (8) may be rearranged to give the output voltage and power per unit volume as a function of electric current density. The results are:

$$E = VB - J/s \quad ,$$

$$P = JVB - J^2/s \quad .$$

The Lorentz Force, since the direction of J is reversed, will be opposed to the fluid motion and given by:

$$\bar{F} = \bar{J}x\bar{B} = JB = (1-K)sVB^2 \quad .$$

Assuming a constant diameter MHD duct, for fluid to move against this force, there must be a pressure difference (dp) between axial positions in the duct a distance dx apart given by:

$$dp = Fdx \quad .$$

Assuming constant values of B, V, s, one can approximate the total pressure drop across the MHD generator (p_{in}-p_{out}) by:

$$(p_{in}-p_{out}) = Fl = (1-K)sVB^2l \quad ;$$

where l is the flow length of the generator. The rate at which the fluid does work per unit volume P_g is

$$P_g = FV = (1-K)sV^2B^2 \quad .$$

The ratio of power output to the power delivered by working fluid is defined as the electrical efficiency N_e:

$$N_e = P/P_g = K \quad .$$

In applications where working fluid is at very high temperature, a MHD generator can be used as an energy topper in conjunction with another energy conversion system (energy bottoming cycle). Because the Joule losses in MHD generator occur within the working fluid the energy is still partially useful, but it does represent a departure from thermodynamic reversibility.

2.3 MHD PUMP ANALYSIS

In a MHD channel with constant electric and magnetic fields the magnitude of Lorentz Force is constant. If the pump is designed to operate with orthogonal vector fields, then the Conservation of Energy relationship can be used to evaluate the velocity function with respect to position in the channel. The total ideal power output of the pump is found by integrating equation (6) with respect to the position in the MHD duct.

MHD pumps with a varying flow area ducts can be constructed so as to maximize the pump head or to maximize the increase in the kinetic energy of the fluid. The design will be based primarily on the application and on the optimization process.

The thrust necessary to move the submarine through water is supplied by a single large pump or a cluster of smaller propulsors. A MHD thruster consists of a flow channel, a super-conducting magnet system, electrodes, electrical connections to the power supply, and supporting structure. Generally, the magnet makes up 20% of the thruster mass and the remaining is primarily structural support to restrain the magnet from "flying apart". The field strength of 10 Tesla is easily achievable with super-conducting magnets (SCEMT). Several magnet configurations are possible, each having its advantages and drawbacks. The selection of best coil configuration for a MHD thruster application is driven by magnet's weight,

efficiency and magnetic fringe field leakage. More on this subject is given in subsequent chapters. Three possible magnetic coils configurations ("Saddle", "Racetrack Toroid", and "Solenoid") are shown in Figures 2-1, 2-2, and 2-3.

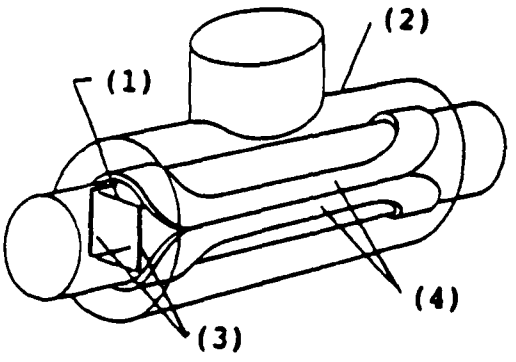

(1) Duct
(2) Cryostat
(3) Electrode
(4) Superconducting coils

Figure 2-1 "Saddle" Magnet Application
(taken from ref. 9)

In a real pump flow may be irregular or flow singularities may develop during transient operations. The magnetic field is generally not uniform from inlet to outlet or across the channel. Since J is coupled with V

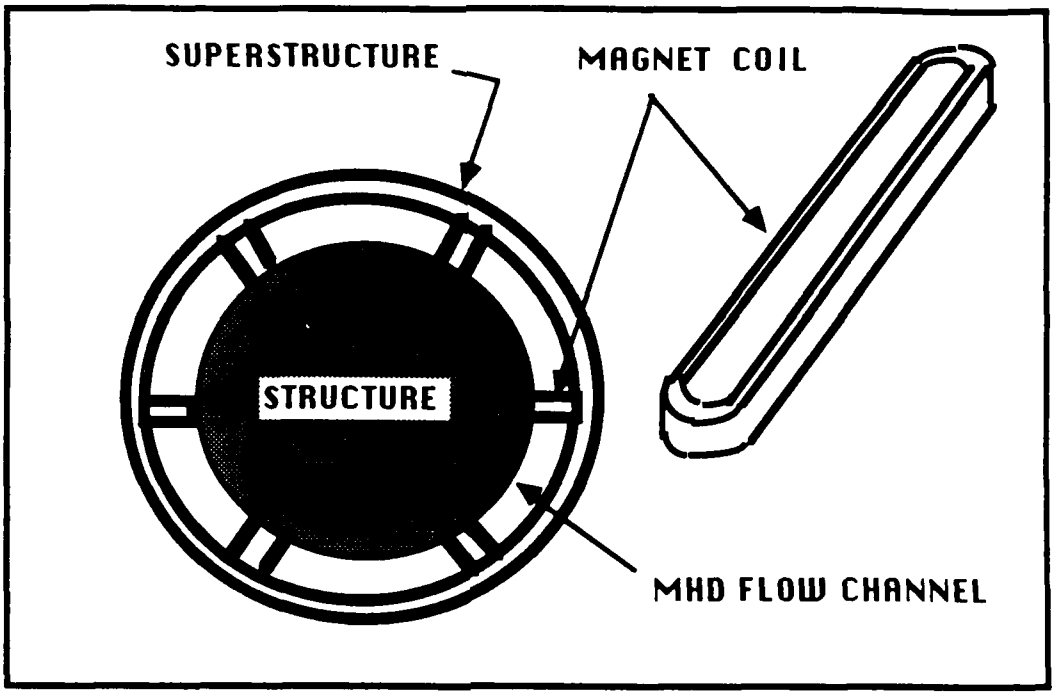

Figure 2-2 "Racetrack Toroid" Magnet Configuration

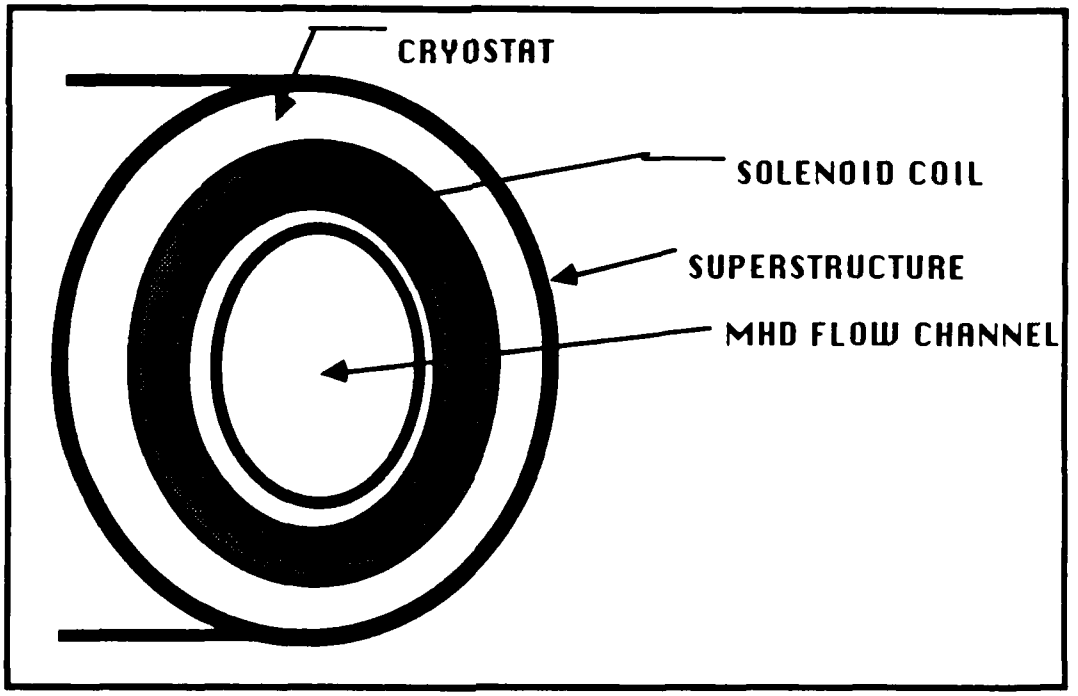

Figure 2-3 "Solenoid" Magnet Configuration

and B, the solution of equation (5) for the total power delivered is not a simple one. The first approximation for quasi-steady magnetic flux distribution is usually computed using the Biot-Savart Law,[8] i.e.

$$B = C_1 \int\int\int_v (J_m N_{ab}/r^2) dv$$

where C_1 is magnetic permeability divided by 4 , v is the volume of integration, J_m is current density in a magnetic coils, N_{ab} is the unit vector from point a to point b, and r is the distance from a to b.

The electric field E can be calculated from equation (1) and the steady-state forms of two of Maxwell's equations,[8] i.e.

$$\nabla \times E = 0 \quad , \tag{9}$$

$$\nabla \cdot J = 0 \quad , \tag{10}$$

provided the velocity V and magnetic flux density B are known throughout the computational domain. Equation (9) implies the existence of an electric potential O satisfying the equation:

$$E = -\nabla\phi \quad . \tag{11}$$

Substitution of J from equation (1) into equation (10), coupled with equation (11), results in a second order partial differential equation in ϕ.

$$\nabla^2\phi = \nabla \cdot V \times B \quad .$$

A detailed description of how such a numerical solution is performed is soon to be published by Daniel.[8]

2.4 MAXIMUM PUMP EFFICIENCY AND POWER

The pump efficiency will be compared for two separate propulsor designs. One will be a preliminary design proposed by the Naval Underwater System Center (NUSC). It uses a cluster of six or more small propulsors and is a good candidate for MHD propulsion. All six propulsors are identical. To arrive at the total thrust only one propulsor needs to be analyzed. The efficiency of the entire assembly corresponds to the efficiency of a single propulsor since hydrodynamic interference is not anticipated.

The second MHD propulsion assembly was proposed separately by the AVCO Corporation and NUSC. The thrust is provided by a single propulsor in a form of a cylinder encompassing the submarine hull. The six segments of the thruster can operate in unison or separately depending on the operational requirements.

It should be mentioned that both designs are still under development and by no means are considered final. The efficiency optimization of any MHD pump is the primary goal of this section.

Both designs are assumed to employ the most optimum configuration by maintaining orthogonality between B, E, and V throughout the channel. The conductivity of sea water will be assumed constant at 4 S/m (seeding of the sea water is not considered to be practical in submarine propulsion). The only variable parameters remaining are

the general dimensions and geometry of the thrusters, the magnetic field B, and the length of the active area. The values for E and J will depend on the electrical power input and the size and separation of the electrodes.

The final thruster characteristics will be developed in Chapter 3 to obtain the maximum performance when the thruster is coupled to the submarine hull. For now, the analysis will be analogous to an open water efficiency evaluation for a conventional propeller.

Consider the electric efficiency of the pump N_e. It is expressed by a ratio of thrust power P_t to a total electrical power input P. From equation (5) electrical efficiency can be found by:[9]

$$N_e = P_t/P = VJB/(VJB+J^2/s) \quad ,$$

Here velocity V must be equal to the average velocity in the active channel U_c, hence

$$N_e = 1/(1+J/U_cBs) \quad . \qquad (12)$$

From this it is apparent that MHD pump is more efficient with low values of J. This implies that larger electrodes will give better performance. Higher velocity and magnetic field strength in active portion of MHD duct should also give better results.

Assuming a frictionless MHD channel, one can write:

$$N_e = A_c(p_{out}-p_{in})U_c/(I_oV_o) \quad ; \qquad (13)$$

where A_c stands for flow area of the active MHD duct, $(p_{out}-p_{in})$ is the pressure difference across the duct, V_o stands for electrical voltage and I_o is electric

current supplied to the MHD electrodes. The pressure difference across the duct is the dynamic head provided by the thruster, i.e.

$$p_o - p_{in} = (\rho/2)(U_N^2 - U_o^2) \quad ; \qquad (14)$$

where ρ stands for density of sea water, U_N and U_o are MHD thruster outlet and inlet velcities respectively. From Lorentz Force equation:

$$p_o - p_{in} = sBl[(V_o/d) - U_c B] \quad ; \qquad (15)$$

where l is the length of active channel, d is electrode separation, and V_o is electrical voltage.

Combining equations (14) and (15) and substituting into equation (13), electric efficiency may be written

$$N_e = 1/\{1+[C_2/(2U_c/U_o)][(U_N/U_o)^2-1]\} \quad ; \qquad (16)$$

where C_2 is the dimensionless ratio of inertial force to electromagnetic force and it is given by:

$$C_2 = \rho U_c/(slB^2) \quad .$$

Two things can be concluded from equation (16). First, electrical efficiency decreases with increases in the ratio of outlet to inlet velocities. This implies that for a given thrust it is optimum to increase the mass flow rate through the channel by maximizing its diameter and decrease the velocity rise across the MHD duct. Second, the electrical efficiency increases with increases in the length and the magnetic flux density of the MHD channel.

To illustrate the scale effects on thruster electric efficiency, the thrust and coil current densities are held fixed. All dimensions are scaled by a factor k. The

volume of the thruster and its magnetic coils are scaled by factor of k^3.

From the Biot-Savart Law magnetic flux density at any point scales to $B'=kB$. Since the volume of sea water scales by k^3, and B scales by k, J must scale as $J'=k^{-4}J$ to maintain the same thrust. Using the two conditions in equation (1) gives a solution for E'. By substitution in the electrical efficiency equation, the following efficiency relationship is obtained:[8]

$$N_e' = N_e/[k^{-5}+(1-k^{-5})N_e \qquad (17)$$

Thus, the electrical efficiency increases with increasing scale factor k. One big propulsor should be more efficient than a cluster of smaller ones.

The maximum thrust power depends on the power input and the efficiency of the MHD duct. The increase in ship's speed will be accomplished by increasing the voltage on the electrodes. The current density increases resulting in a higher thrust power. Depending on impurities, at about E_{max}=1kV/m excessive water breakdown may occur which drains the energy from a duct.[8]

This breakdown value for E_{max} places a constraint on the maximum thrust power achievable. This can be seen from the following:

$$E = E_{max} \ ,$$

$$N_e = VJB/EJ = VB/E \ ,$$

$$J = P_t/VB \ ,$$

$$P_t = VBs(E-VB) = E^2s[VB/E-(VB/E)^2] \ , \qquad (18)$$

$$P_t = E^2s(N_e-N_e^2) \ . \qquad (19)$$

The maximum thrust power density subject to the $E=E_{max}$ constraint can be found by finding the maximum efficiency, i.e.

$$dP_t/dN_e = 0 = E^2s(1-2N_e) \quad ,$$

$$N_e = .5\ P_{t(max)} = 0.25\ E^2s \quad .$$

This places a limit on the power delivered to the MHD electrodes. Increasing electrical power of the propulsion plant beyond a certain point may actually have diminishing returns in performance. However, increasing the size of a thruster will increase the total thrust power. The only other thing that can be done is to increase the magnetic field.

In order to evaluate the hydrodynamic efficiency, the MHD pump has to be mounted to the hull. The thrust power of the propulsor becomes a propulsive power exerted on the submarine. The speed of the ship is steady when the total thrust force equals the total drag on the submarine and its thrusters.

The frictional losses in the MHD duct will depend on the velocity of the sea water. The flow can be turbulent or laminar. In either case, the corresponding friction and form losses inside the MHD propulsor will reduce the head generated by the MHD work.

The hydraulic losses may be significant depending on the final design of a thruster. The thrust energy decrease due to these losses is commonly labeled as headloss H_L. Headloss can be found by following equations:[10]

$$H_L = KV^2/2 \quad ; \quad K = K_e+K_d+K_c+K_n \tag{20}$$

$K_e = .05$ Entrance loss coeff.,

$K_d = .03[(A_{in}/A_{out})-1]$ Diffuser loss coeff.,

$K_c = fL/D_h$ Channel loss coeff.,

$K_n = .04[1-(D_2/D_1)^4]$ Nozzle loss coeff.;

where A is the cross-sectional area, f is a friction factor which is a function of duct relative roughness and Reynold's Number, D_h is a hydraulic diameter, and D stands for diameter.

In addition to these losses, external skin friction losses and form losses will add to the total drag of the submarine.

The thrust provided T may be written in terms of flow parameters as

$$T = Q\ (U_N-U_o) \quad ,$$

$$Q = \rho UA \quad ;$$

where is density and Q is mass flow rate of sea water passing through the thruster.

The hydrodynamic efficiency N_{hy} is defined as the ratio of the power delivered for propulsion TU_{ship} to the sum of propulsive power and kinetic energy left in the wake K_w.[9] Assuming, for now, that thruster inlet velocity equals the ship's velocity;

$$N_{hy} = TU_o/(TU_o+K_w) \quad ,$$

$$K_w = [(\rho/2)(U_N-U_o)^2+w]U_NA_N \quad ,$$

w is the turbulent kinetic energy in the wake assumed as negligible when compared to the total kinetic energy in the wake, and A_N is the diffuser flow area. In steady

state, the effects of dissipitation (all losses) are included implicitly when thrust is equal to total drag. The expression for N_{hy} becomes:

$$N_{hy} = 2/(1+U_N/U_o) \quad . \tag{21}$$

This reinforces the statement that minimum ratio of velocities across the MHD thruster is advantageous.

The propulsive efficiency N_p is found by:

$$N_p = N_e N_{hy} \quad .$$

To optimize the performance of the thruster, design parameters must be varied to achieve the maximum efficiency and maximum speed based on the operational requirements for the submarine. The above analysis imply that increasing magnetic flux density will always increase the electrical efficiency. However, the magnetic forces on the windings require a structure that provides support directed radially inward with a magnitude proportional to B^2. This effectively increases the size of the structural supports and increases the total drag of the thruster.[9] Therefore, there must be an optimum B for a particular application.

2.5 MHD ELECTRICAL GENERATOR

MHD power generation has been gaining popularity over the past several years especially in commercial topping cycles (energy of the working fluid is extracted in two steps, first across the MHD generator then across the steam plant generator). The working fluid is generally a gas or a mixture of combustion products. A major drawback to MHD generation is the high operating temperatures.

The discussion on MHD power generation will be brief. Most power plants which are adaptable to submarine propulsion systems operate at temperatures well below 2,000 K. The MHD topping cycle, depending on the type, requires temperatures ranging from 1,000 K to 2,000 K. An ultra-high temperature gas reactor may be the only nuclear plant that approaches this temperature. This is based on the state of the art, but in the future, advances in material technology may allow much higher reactor fuel temperatures and make MHD energy conversion system far more attractive than it is today. These possibilities are discussed in Chapters 4 and 5.

The basic principles of MHD power generation have been addressed in Section 2.3 and will not be repeated here. The electric field created by a flowing conductor, (V x B) is usually named the Faraday electric field and its direction is orthogonal to B and V.

In addition to the Faraday electric field, the mag-

netic field causes a Hall current to flow co-linearly with the working fluid. In a linear generator this current can be suppressed by employing segmented electrodes.[6] In the "Hall" variation of the linear generator, the Faraday current is short-circuited, and the Hall current provides the power.

Other generator geometries are also possible. In a vortex or spiral geometry the gas is introduced tangentially and withdrawn along the surface of an inner coaxial cylinder. When the inner cylindrical diameter is much smaller than the outer cylinder, the fast moving gas makes several revolutions; thus, this geometry permits a longer magnetic interaction length. This allows for a more compact magnetic field. By maintaining a sufficiently high exit velocity, Hall current in tangential direction is suppressed.

In a vortex generator the gas is injected radially outward from the inner cylinder. The Faraday current flows tangentially, and the Hall current flows radially; the latter interacts with the magnetic field to rotate the flow. The Lorentz Force caused by the Hall current is equal to the centrifugal force in the fluid. All three types of MHD generator geometries are shown in Figure 2-4.

It should be mentioned that the MHD generator analysis are even more complex than those outlined for the MHD pump. The current density is coupled with the magnetic flux density and they are different at each point

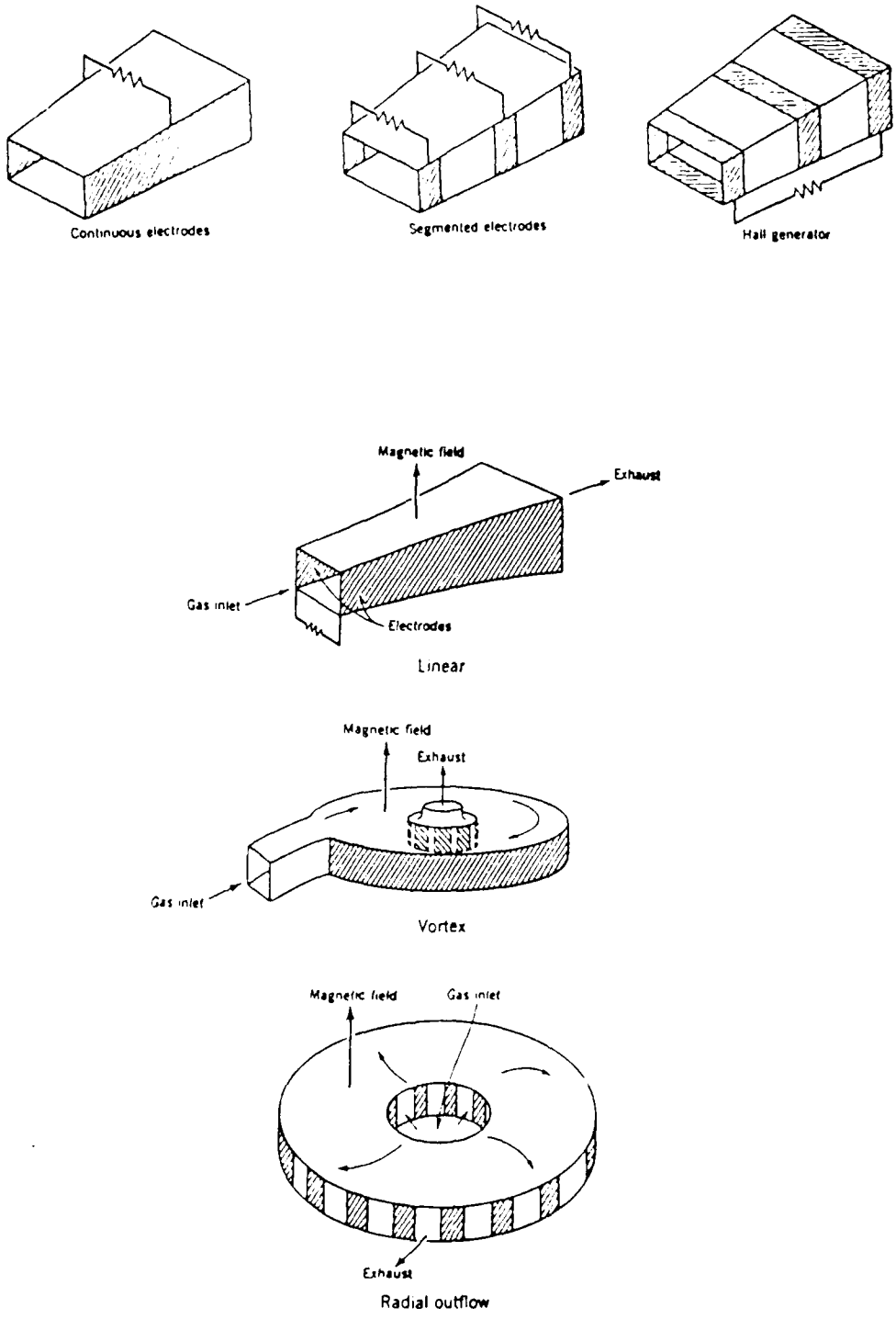

Figure 2-4 MHD Generator Geometries

(taken from ref. 5)

in the channel. The equation $N_e=K$ applies only to a given point in the duct and should be thought of as a local efficiency. In addition, there are a similar losses due to viscous flow that should be taken into account. It is customary to express the efficiency of the ideal constant duct diameter generator by its polytropic efficiency N_{pl}:[6]

$$N_{pl} = N_e/\{[1+(y-1)/2]M^2(1-N_e\} \quad ; \qquad (22)$$

where y is a ratio of specific heats, and M stands for the average Mach number in the active channel. For a gas with electrical efficiency of .8, y of 1.2, and M equal to 2, the polytropic efficiency is 25% less than electrical efficiency.

2.6 MHD GENERATOR REQUIREMENTS

In principle, the MHD generator can operate between arbitrary source and sink temperatures, but most working fluids appropriate for heat engines do not become sufficiently electrically conductive until they have attained extremely high temperatures. Accordingly, some method is required to seed the working fluid, except in the case of metal vapors, which show adequate conductivity at about 2000 K.[1]

Most popular seeding method is often referred to as plasma MHD. It involves the introduction of very small amounts of an alkali metal, potassium and cesium being preferred because of their low ionization potential. At about 2500 K, this seed material is completely ionized thermally and provides the electrons required for plasma conductivity. These electrons can attain temperatures significantly higher than that of the working gas and, under these non-equilibrium conditions, adequate conductivity is possible at temperatures as low as 1500 K.

The development of a low temperature liquid-metal MHD generator is well on its way. One is being tested by Argonne National Laboratory. This generator will operate between 110 C and 51 C,[6] but higher operating temperatures are not precluded. This type of generator can be coupled directly to a liquid metal cooled reactor or a high temperature gas reactor.

A two-phase flow comprising of liquid-metal matrix with trapped gas bubbles can be used as a working mixture. This arrangement is limited only by the melting and boiling points of the metal selected. The range of temperatures for MHD generation can be as low as 800 K. The application of MHD generator energy conversion cycle system will be discussed in detail (Chapters 4 and 5) in conjunction with different propulsion plant schemes.

The MHD power generation can be extremely efficient. Sixty to seventy percent thermal efficiency is achievable because Joule losses are only slightly irreversible and a heat generated can be converted into work in the bottoming heat cycle. Smaller efficiencies would be expected if the MHD generator is the only energy conversion system, but increasing with higher source temperatures.

3. SUBMARINE POWER REQUIREMENTS

3.1 MHD THRUSTER SELECTION

A study of MHD thruster parameters was recently conducted by the Naval Underwater Systems Center (NUSC). The results of this study suggest that, within a typical submarine's size and geometric constraints, a magnetic flux density of between 8 and 10 T results in an optimum propulsive efficiency.[7] Figure 3-1 illustrates one of several options for integrating a MHD thruster with the hull of a submarine.

The MHD thruster shown in Figure 3-1 can be designed to employ the following attributes for efficient propulsion discussed in Chapter 2: simple flow path, maximum flow area, orthogonal electric and magnetic fields, and one large propulsor. The hydraulic efficiency is increased by minimizing exit velocity U_N with a diffuser. The magnetic coils are of "Racetrack Toroid" configuration.

The" Saddle" magnet configuration is competitive if a cluster of smaller propulsors is used. The "Solenoid" configuration results in a complex flow path through a MHD thruster and relatively high magnetic fringe field in all directions. The "Racetrack Toroid" configuration allows for segmentation of the thruster and simple flow path for the sea water. Based on high efficiency and low magnetic leakage, the "Racetrack Toroid" configura-

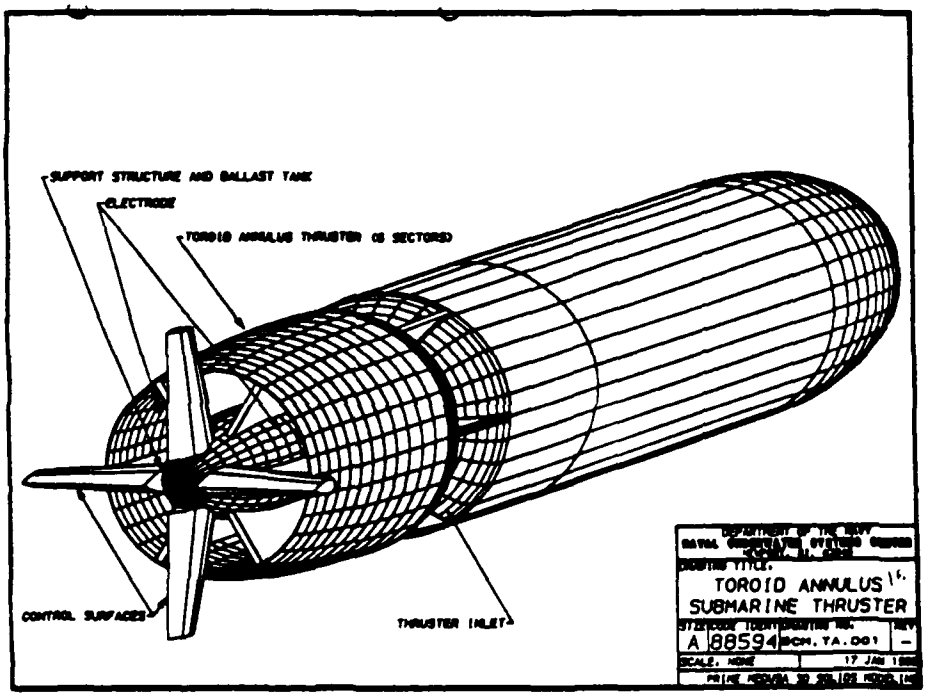

Figure 3-1 Naval Underwater Systems Center MHD Propulsion Concept

(courtesy of NUSC)

tion is superior for a single large MHD thruster design. The thruster is mounted on the after-body of a submarine where it acts like a conventional propeller.

There is far more flexibility in the arrangement of the MHD thruster than with a conventional propeller. The thruster assembly can be mounted over the parallel mid-body of a submarine or anywhere along the hull aft of the sail. The degree of mutual dependence between a thruster and ship's hull must be established before the final dimensions can be determined. The size and location of the MHD thruster may have a significant impact on the hull performance and vice-versa. The focus of the subsequent sections is to arrive at the most efficient combination.

Figure 3-2 illustrates a segment of MHD thruster. U, p, A, and l represent velocity, pressure, area, and MHD active duct length respectively. Figure 3-2 is very similar to Figure 1-1; however, the inlet nozzle is an imaginary nozzle formed by the streamlines of the sea water while accelerating toward the active MHD channel. This acceleration of the sea water is caused by the pressure differential across the MHD channel. In this model the inlet area A_o becomes the capture area and U_o is a free stream velocity. From the Mass Continuity;

$$U_C = U_o(A_o/A_C) \quad ,$$

$$U_N = U_o(A_o/A_N) \quad .$$

From a Momentum Balance and substituting for U_C and U_N ;

$$(\rho/2U_o^2)[(A_o/A_N)^2-1]=JBl-(\rho/2)C_f U_o^2(A_o/A_c)^2(A_{MHD}/A_c) \quad ; \tag{23}$$

where ρ is density of sea water, C_f is a channel friction factor (a "Fanning" friction factor accounting for the frictional losses in the MHD channel), A_{MHD} is the wetted surface area of the active channel, and (JBl) represents the pressure increase due to Lorentz Force. For now, the wall friction in the nozzle and diffuser is neglected. A_{MHD} depends on the channel's geometry and for a cylindrical propulsor;

$$A_{MHD} = 2\pi(r_o+r_i)l_{channel} \quad .$$

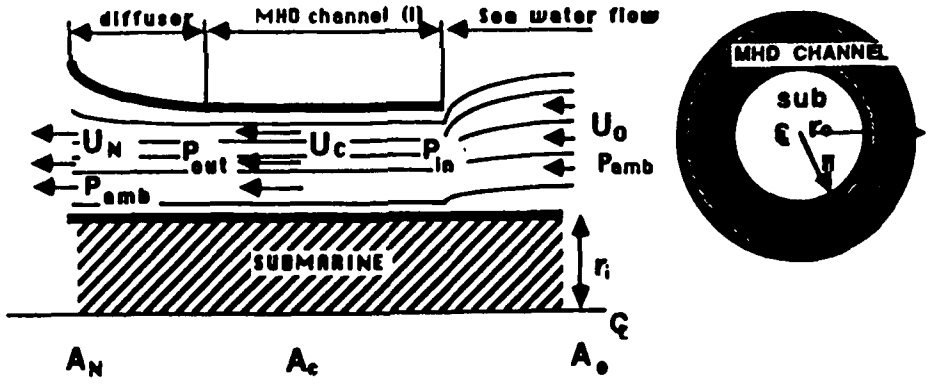

Figure 3-2 Simplfied Schematic of MHD Thruster Mounted on Submarine Hull

The capture area A_o can be found from Force Balance Equation. The capture area is a flexible parameter that will depend on the velocity through the thruster and

the diffuser design. This area will adjust so as to satisfy the Conservation of Mass requirement for different operating conditions or designs. Since the thrust equals the ship's drag and assuming that U_o is equal to the ship's speed;

$$\rho U_o^2 A_o[(A_o/A_N)-1] = \rho/2 C_D U_o^2 A_{WS} \quad , \qquad (24)$$

$$A_o = A_N[.5+(.25+.5C_D A_{WS}/A_N)^{1/2}] \quad ; \qquad (25)$$

where C_D is ship's total drag coefficient, and A_{WS} is the wetted surface area of the ship. It is important to realize that equations (24) and (25) account for an increase in velocity due to fluid acceleration from U_o to U_c, but ignore additional drag and effects of the wake "behind" the hull.

To solve for the power required to propel the ship (based on open water efficiency) some non-dimensional parameters must be defined. Once the equation for non-dimensional power P' is known, it can be used to optimize the design of MHD thruster.

The non-dimensional parameters are:

$$A_{NC} = A_N/A_C \quad ,$$

$$r' = (r_o - r_i)/L_{sub} \quad ,$$

$$L' = l_{channel}/L_{sub} \quad ,$$

$$i = (sB^2 L_{sub})/(\rho U_o) \quad ,$$

$$C_D' = C_D\{1+2L'r'[L_{sub}/(2r_i)]/[r'(1+r'L_{sub}/2r_i]\} \quad ,$$

$$P' = P/(2\pi\rho U_o^3 r_i L_{sub}) \quad ;$$

where L_{sub} is submarine length, r_i stands for submarine radius which also corresponds to the inner radius of a MHD channel, and r_o is the outer radius of a MHD chan-

nel. The concept is further simplified by assuming that submarine hull is a cylinder (c_p=1, c_p is a prismatic coefficient which is calculated by a ratio of ship's volume to an equivalent cylinder). From equation (8), the non-dimensional power expression can be calculated.

• Power :

$$\tilde{P} = \frac{\Delta\tilde{r}\left(1+\Delta\tilde{r}\frac{L_{sub}}{2r_i}\right)}{4}\left\{\frac{1}{i\tilde{L}}\left[\frac{1}{4}\left(1+\sqrt{1+\frac{2C'_D}{A_{NC}}}\right)^2\left(1+\frac{2C_f A_{NC}^2\tilde{L}}{\Delta\tilde{r}}\right)-1\right]^2+\ldots\right\}$$
$$\left\{\ldots+A_{NC}\left[1+\sqrt{1+\frac{2C'_D}{A_{NC}}}\right]\left[\frac{1}{4}\left(1+\sqrt{1+\frac{2C'_D}{A_{NC}}}\right)^2\left(1+\frac{2C_f A_{NC}^2\tilde{L}}{\Delta\tilde{r}}\right)-1\right]\right\}$$

By using a computer spreadsheet, the power equation can be solved in terms of parameters which define the optimum thruster design. For example, the following input parameters were used:

L_{sub} = 100 m

r_i = 5.0 m

B = 8 T

C_D = .003

C_f = .0018 .

Figures 3-3 through 3-8 show graphical results for different parameters. Of particular importance are the features which identify important design parameters such as the height of the MHD channel (Figure 3-3), the optimum diffuser to channel area (Figure 3-4), and the optimum MHD active channel length (Figure 3-5).

For this submarine, the optimum MHD channel length is 18 m, and 1.2 m is the optimum electrode separation

based on maximum beam and draft constraints of 10 to 13 m.

The non-dimensional power expression can be modified to evaluate optimum design parameters for a ship with a MHD thruster mounted internally to the outer hull. This is possible with a double hull design. Figures 3-9 and 3-10 illustrate results for a MHD thruster mounted internally on the same hull. For MHD channel height of 1.2 m, the optimum diffuser area to MHD channel area ratio decreased to 0.80. The optimum length of the MHD channel increased significantly (from 18 m to 24 m) to compensate for the reduction in flow area.

The last step in the optimization process is to evaluate the impact of thruster segmentation. The thruster is split into port and starboard sections and an effective magnetic angle a' was allowed to vary from 0 to 180 degrees. The effective magnetic angle accounts for peripheral losses due to structural material necessary to protect the magnet coils which pass through the height of the MHD channel in order to complete the loop. Two things can be concluded from Figure 3-11 which gives electrical power dependence on a' and A_N/A_C. First, the power decreases as a' increases. Second, A_N/A_C determines an optimum a' and this ratio should be larger than 1.0 for small values of a', and less than 1.0 to achieve the best efficiency for values of a' approaching 180 degrees.

The above observations suggest that a MHD thruster

can extend over the necking down region of the submarine hull. The flow area of a thruster will decrease gradually since the hull diameter decreases aft of the parallel middle body area. Results from AVCO's one-dimensional computer model indicate that efficiency may actually increase, Figure 3-12. Major reservations stem from complex, due to curvature of the magnetic coils, SCEMT design which will make the manufacturing process a difficult one.[36]

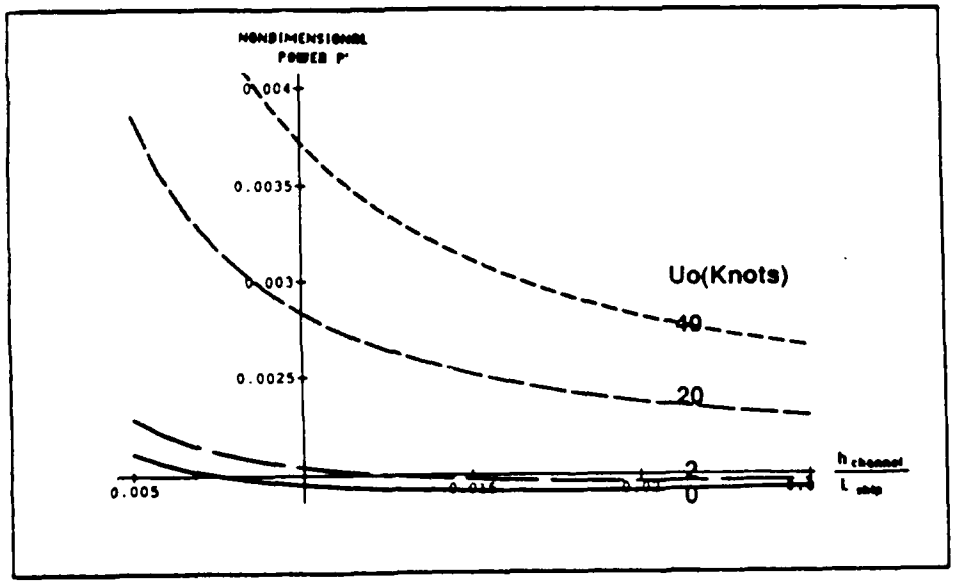

Figure 3-3 Curve for Optimum MHD Channel Height
(based on Submarine Length and Speed)
(courtesy of AVCO Inc.)

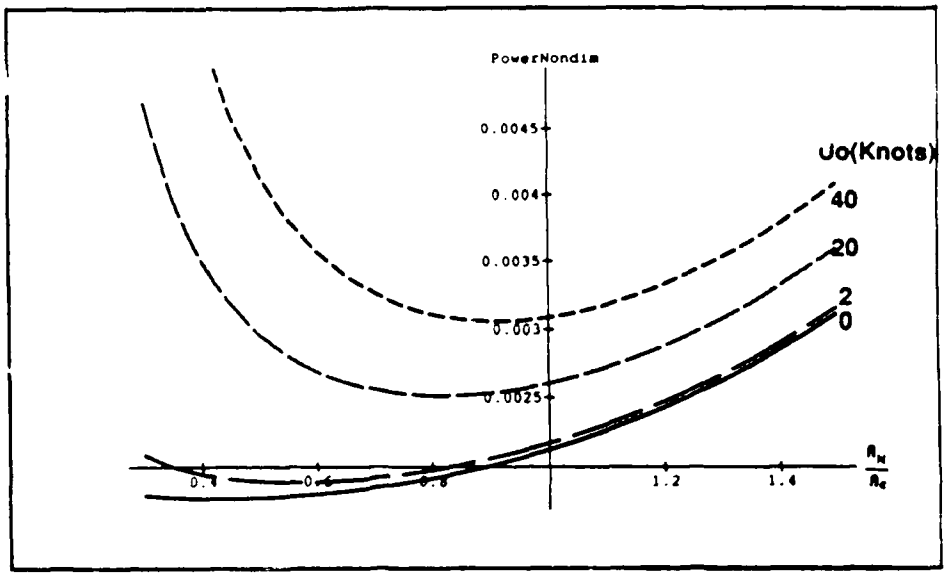

Figure 3-4 Curve for Optimum Diffuser Area

(based on Submarine Power and Speed)

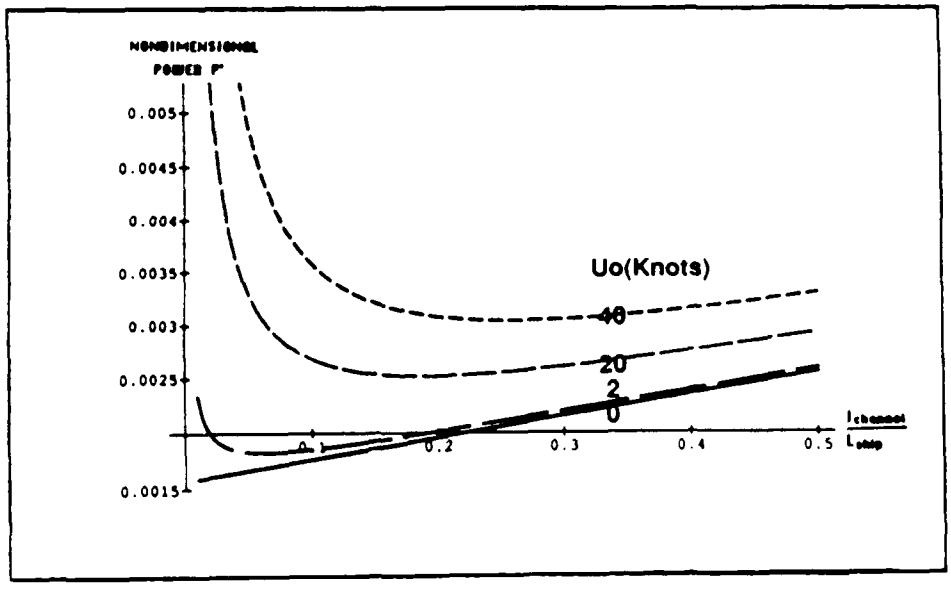

Figure 3-5 Curve for Optimum MHD Channel Length

(based on Submarine Length and Speed)

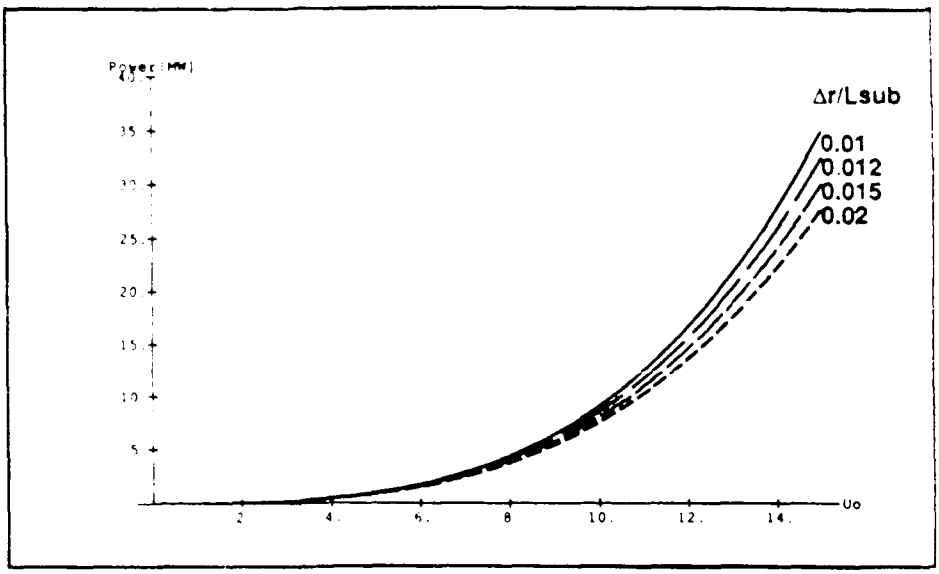

Figure 3-6 Curve for Optimum MHD Channel Height (based on Submarine Length and Speed)

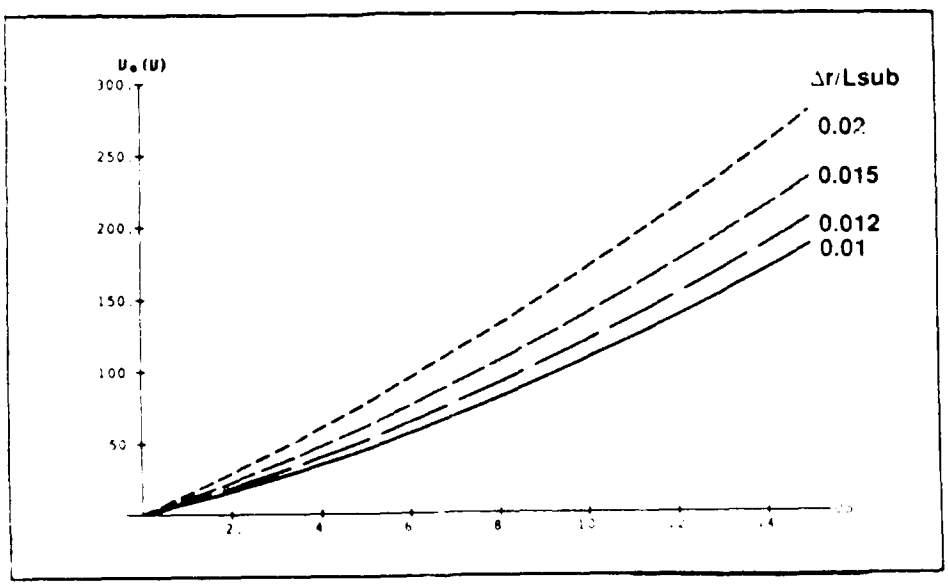

Figure 3-7 MHD Electrode Voltage vs. MHD Channel Height (courtesy of AVCO Inc.)

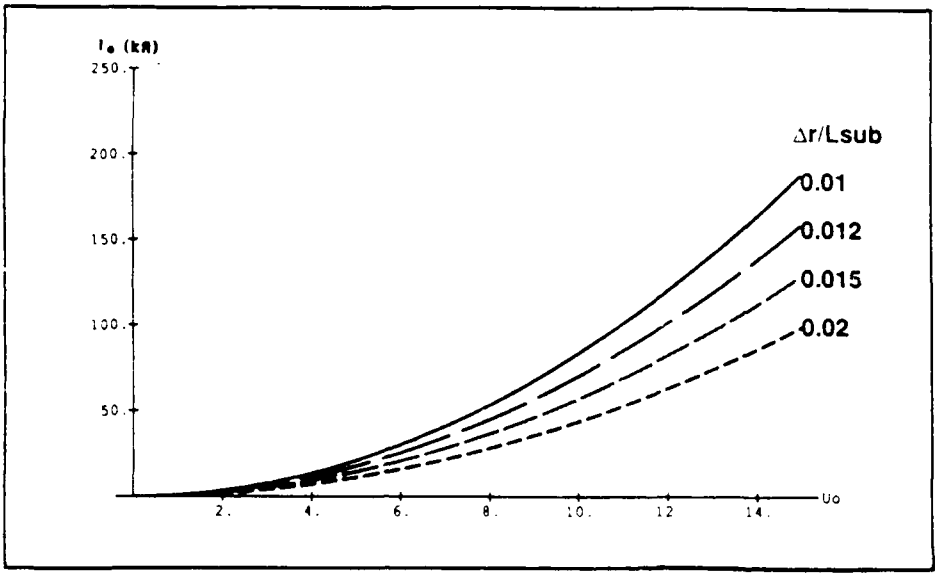

Figure 3-8 MHD Power Supply Current vs. MHD Channel Area (courtesy of AVCO Inc.)

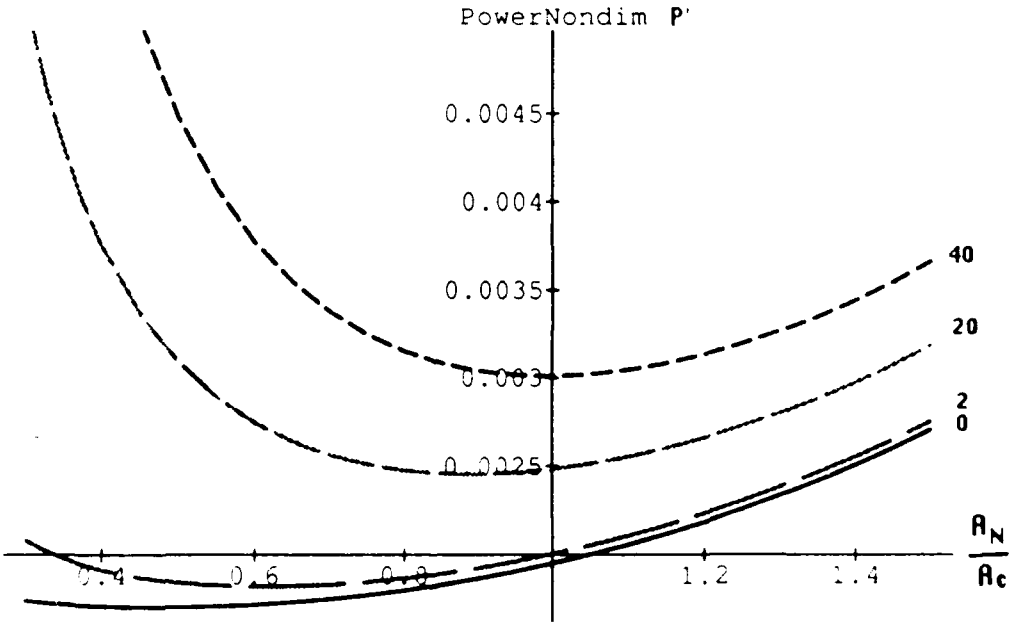

Figure 3-9 Curve for Optimum Diffuser Area based on MHD Channel Area and Submarine Speed (Thruster mounted internally to the hull)

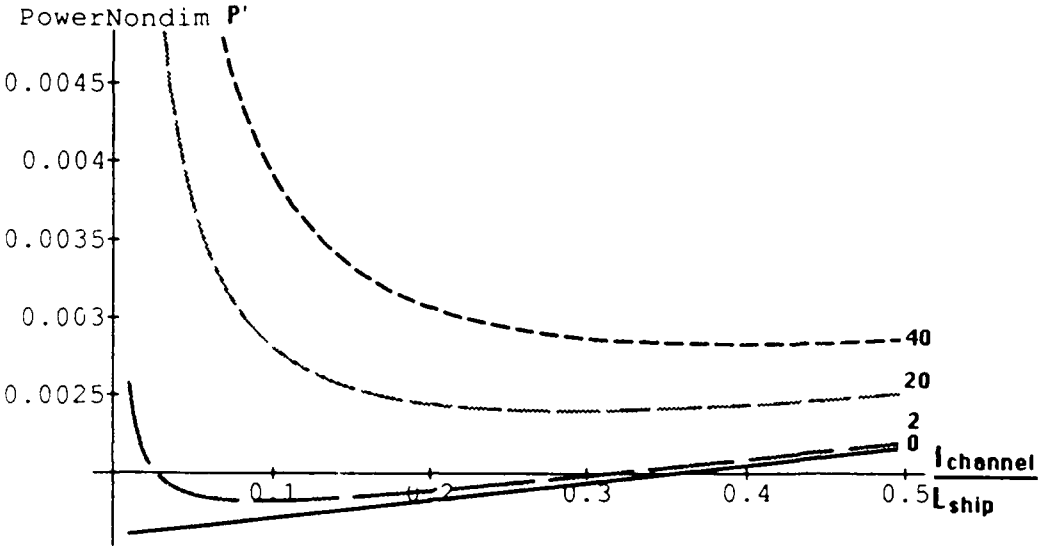

Figure 3-10 Curve for Optimum MHD Channel Length based on Submarine Length
(Thruster mounted internally to the hull)

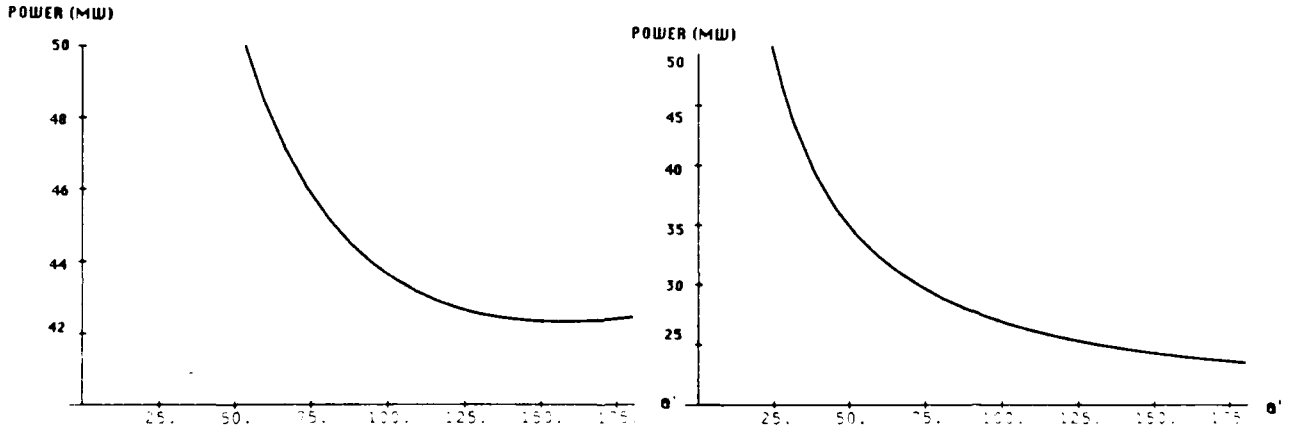

(a) (b)

Figure 3-11 Curves for Optimum Effective Magnetic Angle based on Diffuser Area to MHD Channel Area Ratio (a) A_N/A_C=1.2
(b) A_N/A_C=0.8 (courtesy of AVCO Inc.)

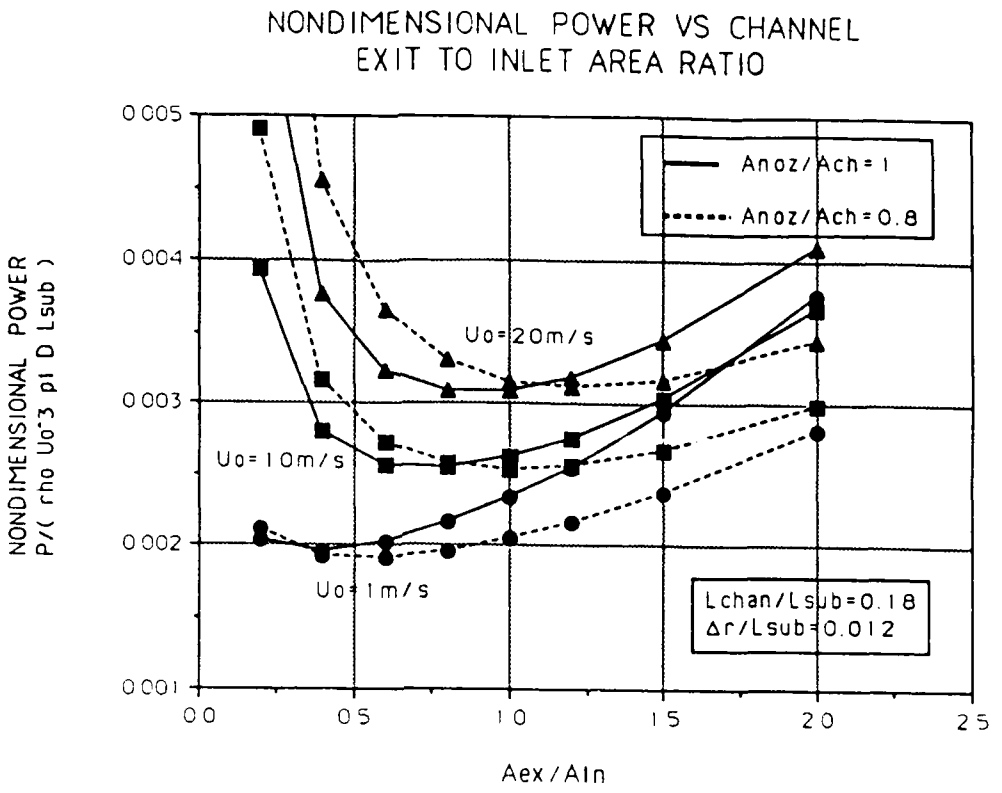

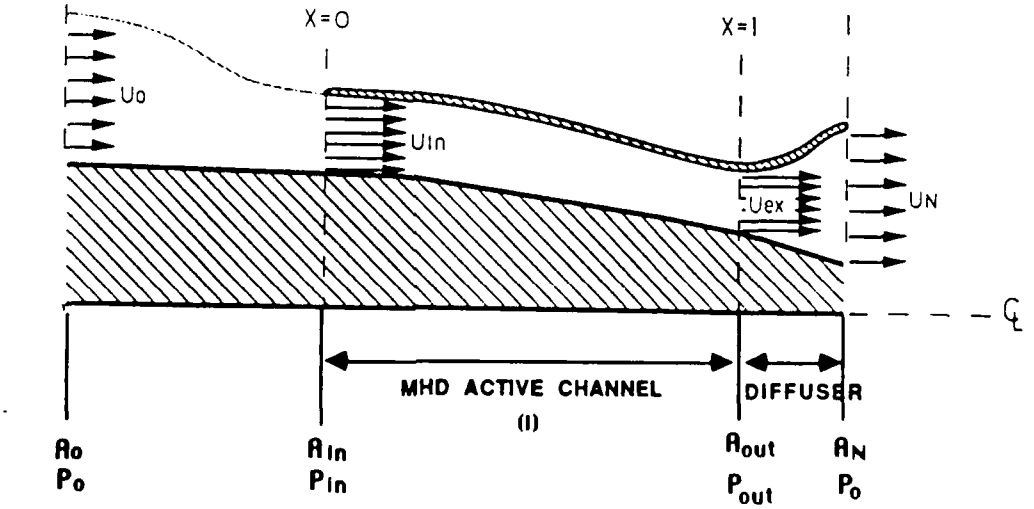

Figure 3-12 Curve for Optimum MHD Channel Area Variation based on Diffuser Area and MHD Power (Thruster installed over the necking down region of the submarine hull)

3.2 MHD PROPULSIVE COEFFICIENT

The absence of moving parts is the only thing separating the MHD thruster from a conventional propeller. The complexity of propeller interaction with the ship's hull has been reduced by uncoupling major effects. These effects are now discussed briefly to establish a connection between a propeller and MHD thruster.

The ratio of the Effective Horse Power (EHP) to the Shaft Horse Power (SHP) is defined as a Propulsive Coefficient (PC). By equating the power available at the shaft with the electrical power delivered to the MHD electrodes, the definition of PC is preserved when applied to MHD propulsion.

The EHP value is normally generated by model testing and appropriate scaling. It corresponds to the power necessary to overcome the total drag on a submarine.

The value of SHP is easily calculated by subtracting the energy losses from a primary mover's delivered power. The primary mover may be a steam turbine or electric motor. PC for the ship is calculated by:

$$PC = EHP/SHP = N_o N_r N_h \quad ,$$

where N_o, N_r, and N_h represent open water efficiency, relative rotative efficiency, and hull efficiency respectively. The division of the quasi-propulsive coefficient into factors in this way is of great assis-

tance, both in understanding the propulsion problem, and in making estimates of propulsive efficiency for design purposes.

The N_o for the propeller uncouples the propeller from the hull. N_p for the MHD thruster serves the same function. Therefore, both efficiencies are synonymous.

The N_r accounts for a difference in thrust found by rotating a propeller "behind" a hull. The properties of fluid flow, behind or over any section of the hull, may vary significantly from an undisturbed open water flow. This factor also accounts for the velocity increase in an oncoming flow due to a differential pressure across the propeller blades. An analogous factor can be derived for a MHD thruster since it will be subjected to similar phenomena.

The N_h accounts for two different effects stemming from propeller-hull interaction. First, the formation of the turbulent boundary layer over the hull results in a velocity gradient in the flow approaching a propeller or a MHD thruster. Second, the pressure wave generated by the propulsor travels upstream and affects the velocity ahead. This velocity increase causes additional skin friction drag on a ship.

The fact that the inlet velocity to a thruster does not necessarily equal the velocity of a ship may affect the overall efficiency (PC). The propulsive efficiency N_p is evaluated using a ship's velocity corrected for an acceleration of sea water due to MHD pump suction.

If the nozzle inlet area equals the captured area A_o, then the intake velocity will equal the free stream velocity; however, the latter is not equal the ship's speed.

N_r and N_h uncouple the propulsor from the hull and account for the difference in performance after integrating with the ship's hull. Uncoupling into N_h and N_r will result in a more flexible and simpler model.

The presence of magnetic field flux has one undesirable impact. The effect of a large B is to thin the boundary layer, which in turn leads to an increase in friction;[11]

$$C_f = .0064[(sB^2x)/(\rho U_c R_x)]^{.2} \quad ; \qquad (26)$$

where R_x is Reynold's Number (direct function of velocity and position, and inversely dependent on kinematic viscosity), x is an axial position in the MHD active duct, and all other symbols have the same meaning as was defined before. In the absence of a magnetic field;[12]

$$C_f = .075(\log_{10}R_x - 2)^{-2} \quad . \qquad (27)$$

Equation (26) applies only for highly conductive medium with a magnetic interaction parameter (Hartmann number) larger than 1. Hence, it only applies at speeds below 10 knots and becomes negligible at higher speeds; therefore, it will not be considered in future calculations since only high speed results are of interest in this study.

An important thing to realize is that the total

losses, other than electrical losses, in the MHD duct are not included in calculation of N_p, but are implicit in the total drag. Thus, drag efficiency N_d for a MHD propulsor will be defined as:

$$N_d = [C_{D(ship)} + C_{D(thruster)}]/C_{D(ship)} \quad , \qquad (28)$$

where ship's drag accounts for hull and appendage drag only. N_d is useful only for comparing two alternate designs.

MHD channel exit velocity U_c, determines C_f and the skin friction in the MHD channel. The drag in a nozzle and diffuser is based on a corresponding local velocities determined by the geometry of their flow areas.

The open water efficiency model assumes a uniform velocity field equal to ship's speed approaching a MHD channel. This is possible if a thruster's location is some distance away from the ship's hull. When adjacent to the hull, the approaching velocity field has the distribution of a turbulent boundary layer.[13] Figure 3-13 illustrates the development of a turbulent boundary layer along the hull.

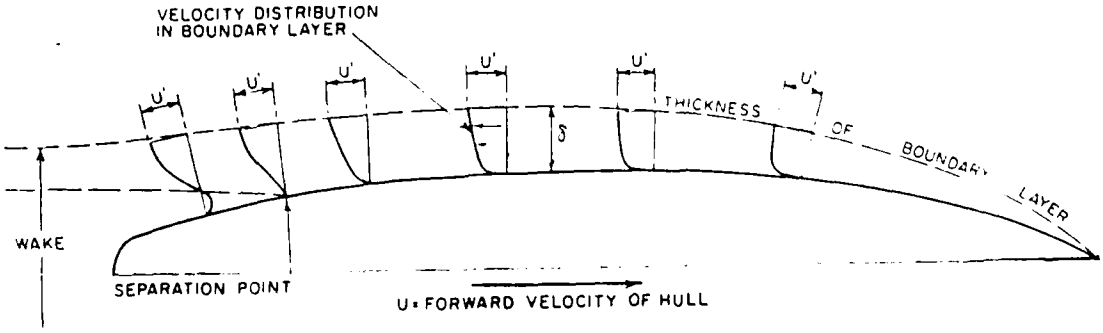

Figure 3-13 Schematic Diagram of Boundary Layer Flow (taken from ref. 13)

Flow analysis of a MHD duct can be very complex and can require a solution to the Navier-Stokes equation. Alternatively, a much simpler boundary layer approach can be used. For this study, the assumption is made that flow separation does not occur anywhere in a thruster. Hence, equation (20) in Chapter 2 can be used to find the total headloss.

For a conventional propeller, N_h can be estimated using parametric equations:[13]

$$N_h = (1-t)/(1-w) \quad ,$$

where (1-t) is a thrust-deduction factor and (1-w) is a wake factor. The (1-t) value stems from a differential pressure across propeller blades which introduces an additional drag on a ship. With a MHD propulsor, the effect of differential pressure developing in the channel can be modeled as a frictionless nozzle. From Figure 3-2, the nozzle inlet area must be equal to the capture area A_o. The equation for the nozzle flow area can be modeled considering sound attenuation in sea water:

$$p_{(x)} = p_{(o)}e^{-(mx)} \quad ,$$

where $p_{(x)}$ is a function of position, p_o is a pressure field at the origin, and m is a pressure attenuation coefficient.

Making further assumptions that the MHD channel is designed to give an optimum 20% increase in velocity,[10] and that the active MHD channel height is equal to 1.2 m, an estimate of average increase in velocity along

the hull is possible. Since the change in power to overcome additional drag is proportional to a change in the average velocity cubed, (1-t) can be evaluated.

The imaginary stream-line nozzle in Figure 3-2 can be modeled by the following equation:

$$A_{(x)} = A_c[(2-e^{(-mx)})]^{.5} \quad , \tag{29}$$

where x is the distance in an upstream direction referenced from the MHD channel, and $A_{(x)}$ is the flow area as a function of x.

Using the Continuity equation and substituting from equation (25);

$$[U_{ship}/U_{(x)}]^2 = (A_N/A_o)(2-e^{-mx}) \quad .$$

The average of squared velocity ratio SVR is found by:

$$SVR = [U_{ship}/U(x)]^2_{avg} = \int_0^x (SVR)^2 dx / \int_0^x (SVR) dx \quad .$$

After Taylor expansion for exponential factors, and assuming $m=0.0092\ km^{-1}$;

$$SVR = .857(A_o/A_N)^2 \quad . \tag{30}$$

Since thrust is proportional to velocity squared, it follows that:

$$SVR = (1-t) \quad ,$$

and substituting equation (24) for capture area into equation (26) gives, after simplification ;

$$(1-t) = .857(.25+2G+G^2) \quad , \tag{31}$$

where G is an interaction parameter and defined as:

$$G = C_D L/(2h+h^2/r_i) \quad . \tag{32}$$

C_D is ship's total drag coefficient, L and r_i stand for submarine length and radius, and h is an MHD channel

height. The wetted surface of the submarine (A_{WS}) is based on a surface of cylinder with the same length and diameter. This simplification introduces only a small error (on the order of 1%) to the value of (1-t).

The value (1-t) will be less than unity unless nozzle inlet area equals the captured area. The additional drag losses will be reflected in a nozzle losses and accounted for in N_d.

To find a parametric equation for N_h, an estimate for (1-w) is necessary. In a "conventional propeller" case, the velocity distribution in a boundary layer U_y is directly related by:[13]

$$(1-w) = U_{y(bl)}/U_{ship} \quad ,$$

where $U_{y(bl)}$ is a mean velocity up to a point y in the turbulent boundary layer. The thickness of the turbulent layer at the inlet to a thruster must be known. The velocity U_y distribution can be approximated by:[14]

$$U_y/U_{ship} = (y/b)^{1/7} \quad , \tag{33}$$

where y is measured away from the hull, and b is the local turbulent boundary layer thickness.

To arrive at reasonably simple considerations on boundary layer intake, it is necessary to define $U_{y(bl)}$. This mean value should represent the momentum as well as the kinetic energy of the incoming flow, leading to two different definitions, namely for the momentum;

$$U_{y(bl)} = \int_0^{y_1} U_y^2 dy \quad / \int_0^{y_1} U_y dy \tag{34}$$

On the other hand, the kinetic energy is represented by

the definition:

$$U_{y(bl)} = \int_0^{y_1} U_y^3 dy \quad / \int_0^{y_1} U_y dy$$

where y_1 is the distance measured away from the hull. Fortunately the two different definitions for $U_{y(bl)}$ lead, for normal boundary layer distributions, to practically the same value for mean intake velocity.

The advantage of boundary layer intake as discussed here is based on the fact that by such an arrangement the inlet velocity to the propulsor is reduced. Since for a given rate of flow through the propulsor the thrust is proportional to the difference between the discharge and inlet velocity, whereas the energy needed to produce this velocity increase is proportional to:

$$U_N^2 - U_o^2 = [2U_o + (U_N - U_o)](U_N - U_o) \quad .$$

The ratio of thrust to the work required to produce that thrust is defined in Chapter 2 as N_{hy} (assuming a frictionless thruster). The effect of the wake (1-t) is defined as a ratio of hydraulic efficiencies without and with a boundary layer intake;

$$(1-t) = N_{hy(bl)}/N_{hy} = (U_{ship}/U_{y(bl)})(1-U_{y\ avg})/(1-U_{ship}). \qquad (35)$$

This relationship assumes that the outlet velocity is the same for both scenarios.

If the thruster's height h is not excessive, and if the boundary layer thickness exceeds the value of h, the $U_{y(bl)}$ can be calculated with equation (34). A flat plate analysis can be used to find a first estimate of the thickness of a turbulent boundary layer, or sophis-

ticated computer codes designed to evaluate hydrodynamics for bodies of revolution can be employed.

The advantage of the thruster arrangement, if properly developed, is to prevent separation behind a fairly blunt body. Hence, submarine after-bodies can be made fuller without risking flow separation. This effect can be determined by large scale model testing but is not reflected here in the ship power calculations.

With a smooth flow entering the MHD duct, NUSC's computer simulation predicts minor flow separation near the exit.[7] This separation results in the formation of undesirable "eddies"; therefore, more drag. It was indicated in Chapter 2 that in a uniform velocity MHD channel J varies as $1/r$ because B varies as $1/r^2$. This gives rise to a non-uniform Lorentz Force. With a boundary layer intake, velocity increases as $r^{1/7}$ which should give a more even distribution in back EMF as seen in equation (1). Consequently, J is more uniform and the Lorentz Force, predominant in the axial direction, has some "flow smoothing" properties.

Because the boundary layer intake effect lowers the nozzle inlet velocity U_o, the electrical efficiency will increase. U_N/U_o remains consistent for the entire range of speed since it depends on the geometry of the diffuser. The decrease in U_N/U_o with an increase in speed is relatively small and becomes negligible at high speeds. This is based on a solution to quadratic equa-

tion in U_N derived from a force balance with U_o being an independent variable. Based on the above, equation (16) can be simplified to:

$$N_e = 1/(1+k_1k_2U_o) \quad ,$$

$$k_1 = \rho/(2slB^2) \quad ,$$

$$k_2 = (U_N/U_o)^2-1 \quad .$$

By defining N_r as a ratio of $N_{e(bl)}$ with boundary layer intake to N_e based on free stream velocity;

$$N_e = (1+k_1k_2U_o)/(1+k_1k_2U_{o(bl)}) \quad . \qquad (36)$$

The effect of boundary layer intake will be reflected in N_r values being larger than unity.

The quasi-propulsive coefficient for MHD submarine, treating a thruster as an appendage, can be found by:

$$PC = N_pN_hN_r \quad . \qquad (37)$$

Each factor in the above equation depends on the ship's hull geometry and on the thruster design. The scope of subsequent sections is to select a submarine hull and a MHD propulsion thruster. Based on a final combination, each factor in the above equation can be evaluated. Finally, the ship's speed versus SHP relationship can be determined.

3.3 SUBMARINE EHP AND SHP

In submarine design, the resistance is composed of three parts: frictional resistance, roughness allowance, and residual resistance. The frictional resistance R_f is proportional to the product of the wetted surface area A_{ws}, the square of the speed, and the frictional resistance coefficient C_f, a function of Reynold's Number;

$$R_f = (\rho/2)A_{ws}U_{ship}^2C_f \quad . \tag{38}$$

The roughness allowance accounts for the surface roughness resulting from such irregularities as sea chests, valves, flood ports, and any other hull surface fouling. It is usually included in a frictional resistance by augmenting the friction coefficient by an amount determined from experience. For submarines, correlation allowance $C_{(delf)}=.0004$ is adequate.

If C_f in equation (38) is replaced with the residual coefficient C_r, the residual resistance R_r can be calculated. However, the residual coefficient is a complex quantity consisting of three parts:

(1) A small portion which depends upon the hull form.

(2) A portion which is a measure of the natural wave making attributes of the hull.

(3) A portion which is dependent on speed-length ratio which reflects the interference effects of bow and stern wave trains.

When running at sufficient depth, about four hull diameters, no waves are generated and R_r depends only on hull form.

The best way to determine C_r is to perform model testing. Results of hull form performance or model testing are collected in a data bank of many available computer codes. The code determines the best fit and provides a first estimate for C_r and C_f.

The total drag coefficient C_D for the submarine can be found by:

$$C_D = C_f + C_{(delf)} + C_r + C_{app} \quad , \tag{39}$$

where C_{app} represents an additional drag due to appendages such as: sail, fairwater planes, stern planes, rudder, and external MHD propulsor.

For a body-of-revolution form, zero parallel middle body length is associated with a minimum residual drag and the effect of reducing the length/diameter ratio L/D is to decrease surface area and hence skin friction resistance down to optimal L/D of about 6, with a prismatic coefficient c_p of about 0.60. This is a subject of many trade-offs during the design process.

The fact that sea water forms a boundary layer around the hull, leads to the preferred "tear-drop" shape to avoid large adverse pressure gradients, to reduce boundary layer growth and to delay boundary layer separation.

The residual drag is generally 2% to 4% of the total resistance. This percentage will drop even lower

if a design has a long parallel middle body. The resistance due to appendages, no matter how streamlined and carefully executed, approaches 50% of the bare hull resistance. The only real solution is to eliminate appendages. One possibility is to design a retractable sail. A MHD thruster mounted internally to the hull may result in significant savings in total drag since N_d=1.0.

Since different nuclear propulsion plants will be analyzed, a hull form similar to a Los Angeles class submarine will be used as a demonstration base-line. A similar hull form, 7 ft. (2.13 m) larger in diameter, will be examined to determine possible advantages in mounting a large MHD thruster internal to the outside hull.

Demonstration base-line SSNX will be:[15]

Length 360 feet (109.8m)

Beam 33 feet (10.1m)

Parallel middle body length 160 feet (48.8m)

Length of forward body 65 feet (19.8m)

Length of after body 135 feet (41.1m).

The length of the parallel middle body was derived from specific volume of 3.5 ft^3/SHP and a location of the sail which was assumed to be directly above the Operations compartment.[16] Additional volume was factored in to account for the space required if retractable sail option is exercised.

Parametric equations for hull offsets were used to

generate the body-of-revolution:[19]

$$R_{fb} = R_{pmb}[1-(x/65)^{2.75}]^{1/2.75} \quad ,$$

$$R_{ab} = R_{pmb}\{1-[(x-225)/135]^{2.5}\} \quad ,$$

where x is in feet and measured from the forward perpendicular. The coefficients 2.75 and 2.5 determine the fullness of the forward and after bodies. The value of 2.75 was selected for the forward body based on the increasing size of a sonar equipment. The value of 2.5 and the length of after body was selected based on a criterion of flow separation. The cone half-angle should not exceed 18 degrees.[17] It should be mentioned that the fullness of the forward body has significant impact on the resistance; on the other hand, the variations of the after-bodies (within reasonable limits) do not influence the resistance significantly.

The Transition Analysis Program System,[18] TAPS-1, was used to determine all hydrodynamic parameters (for a baseline submarine) required for this study. Figure 3-14 illustrates one of many outputs generated by TAPS-1. The pressure coefficient C_p determines the axial pressure and velocity distribution outside the turbulent boundary layer.

The pressure distribution around the hull can be used to predict the boundary layer separation or local cavitation, either one is undesirable. From Bernoulli's equation:

$$p+(\rho/2)U^2 = p_{amb}+(\rho/2)U_{ship} \quad ,$$

$$C_p = (p-p_{amb})/(.5\ U_{ship}^2) = 1-(U/U_{ship})^2 \quad ;$$

where C_p is a pressure coefficient, p stands for pressure and p_{amb} is a static pressure for a given depth.

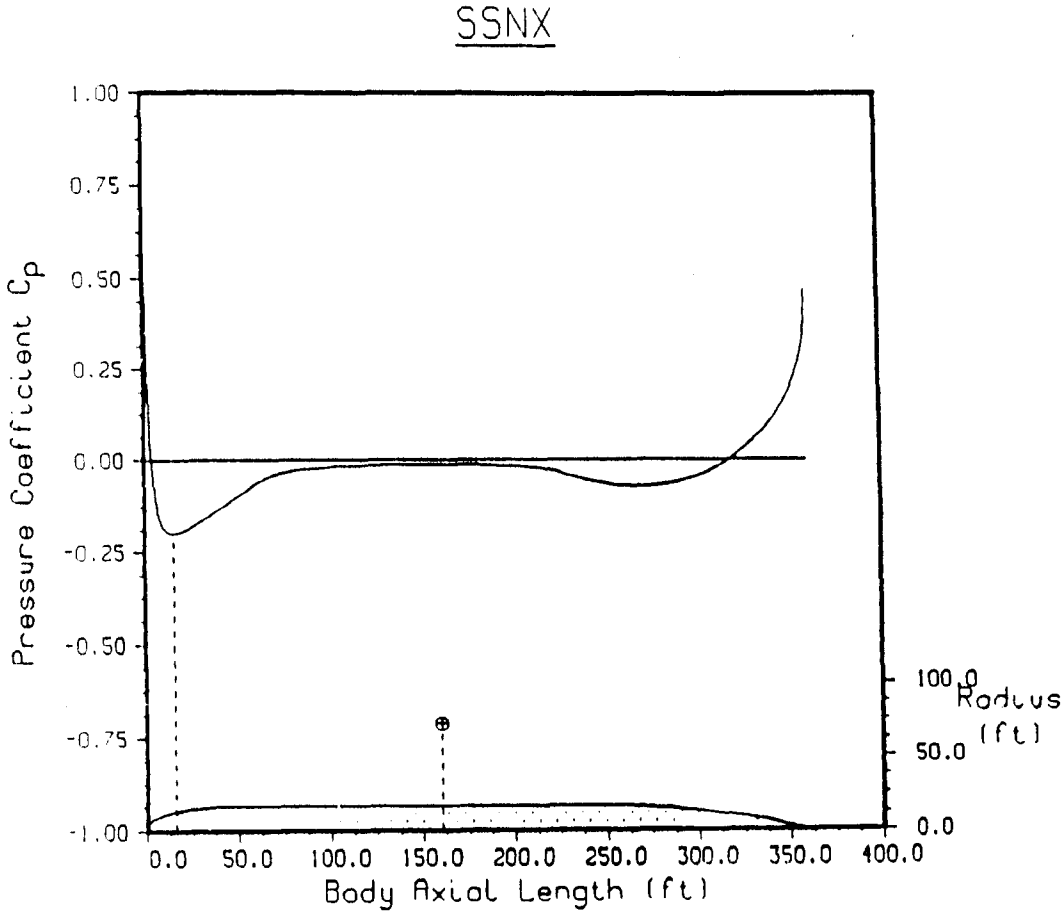

C_{pmin} = -0.198 at X = 15.595 ft
Number of Coordinates = 101
Maximum Diameter = 396.00 in
Total Axial Length = 359.91 ft
Total Body Arclength = 368.46 ft
Body CG Location is at 159.81 ft
Total Body Volume = 248860.300 ft^3
Total Body Surface Area = 32685.580 ft^2
Total Body Displacement = 15536350.000 lbs
Data Located in File ssnx.017

Figure 3-14 TAPS 1 Program Output for Baseline Ship

Figure 3-14 predicts a separation at about 325 ft. (99 m) from the forward perpendicular; however, the pumping action of MHD thruster will prevent this occurrence. Based on C_p, tangential velocity distribution is known.

TAPS-1 calculates C_f and C_r at each increment along the total length of the hull. The output given is in an integrated form of $\int_0^x C_D(x)A(x)dx$. The values of C_D below 20 knots were considered less important and can be found using parametric equations.

Mounting a thruster externally to the outer hull increases the effective beam of the submarine by approximately 7 feet. The SUBSHAPE computer program was used to compare the values of EHP if the maximum beam of SSNX was increased to 40 ft. (12.2 m) and all other dimensions were unchanged. Propulsive coefficient was set at an optimistic value of 0.8 which has no bearing on the relative values of SHP.

The SUBSHAPE is less precise than TAPS-1 since it is based on parametric equations and a best fit to a hull in a Standard Series 58. The results of both programs are in agreement within 5% and are summarized as a function of speed versus EHP for a bare hull, Figures 3-15 and 3-16.

By mounting a thruster as far aft as possible where it will not increase the effective beam will result in a smaller thruster. However, back aft is where the boundary layer thickness is maximum and the inlet axial

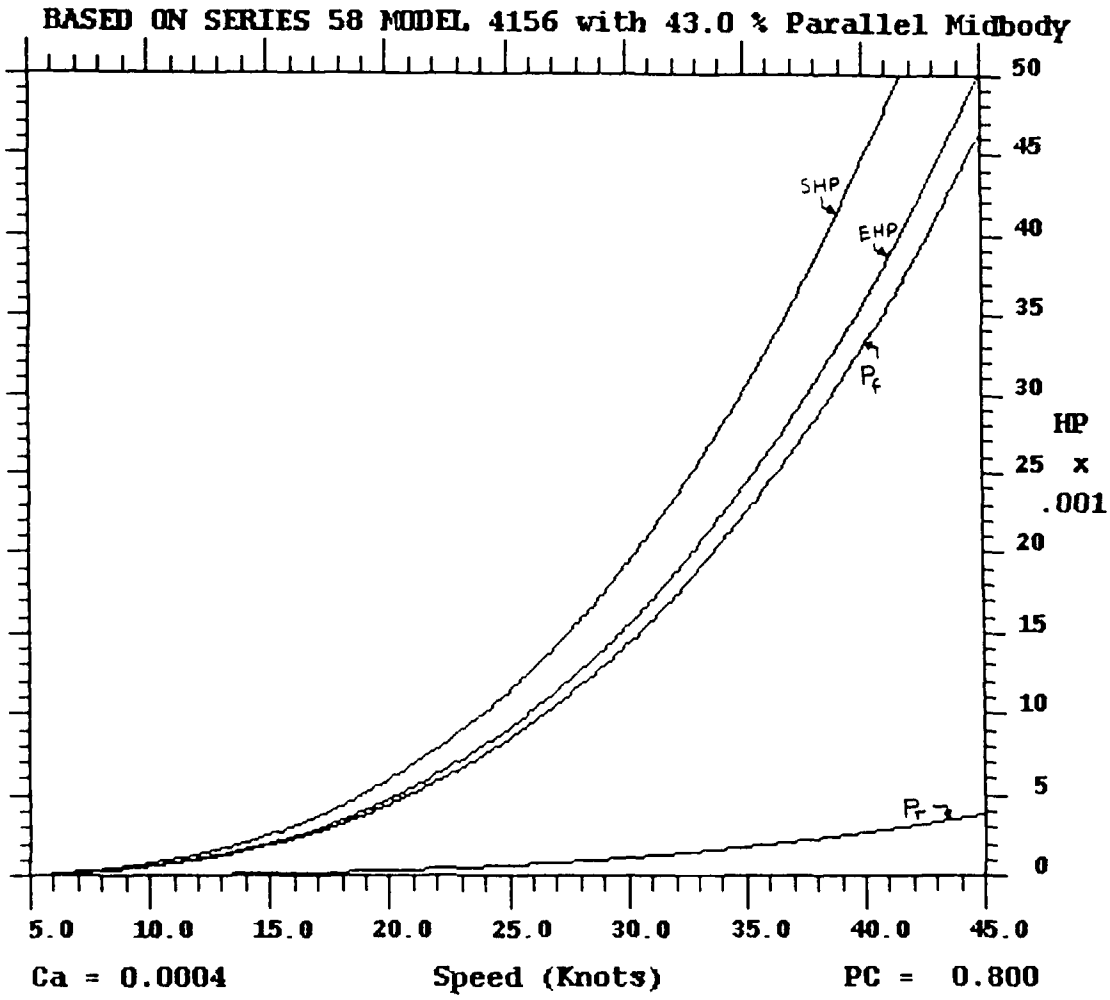

D = 33.00 nf = 2.75 na = 2.50 rho = 35.00

Parameter	Forebody	Midbody	Afterbody	Total Hull
Length	65.00	160.00	135.00	360.00
Surf Area	6047.21	16587.61	10059.26	32694.08
Volume	43402.17	136847.78	68729.35	248979.30
Displmnt	1240.06	3909.94	1963.70	7113.69
LCB	38.00	145.00	270.00	160.85
Cp	0.781	1.000	0.595	0.809
Cws	0.897	1.000	0.719	0.876

Tail Cone Angle (Half) (degrees) : 16.99

Figure 3-15 SUBSHAPE Program Output for Baseline Ship (beam 33 ft.)

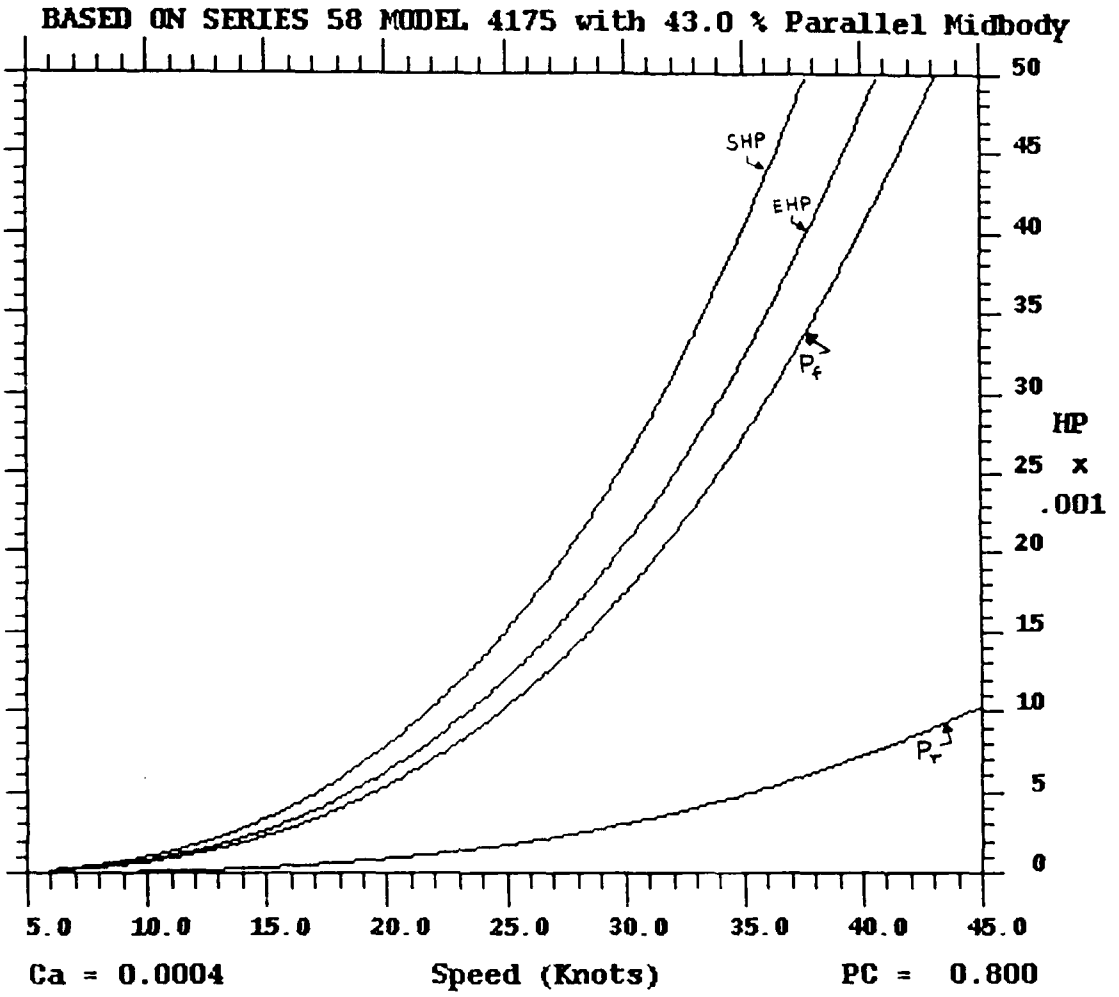

D = 40.00 nf = 2.75 na = 2.50 rho = 35.00

Parameter	Forebody	Midbody	Afterbody	Total Hull
Length	65.00	160.00	135.00	360.00
Surf Area	7422.91	20106.19	12228.00	39757.11
Volume	63768.12	201061.93	100979.76	365809.81
Displmnt	1821.95	5744.63	2885.14	10451.71
LCB	38.00	145.00	270.00	160.85
Cp	0.781	1.000	0.595	0.809
Cws	0.909	1.000	0.721	0.879

Tail Cone Angle (Half) (degrees) : 20.32

Figure 3-16 SUBSHAPE Program Output for Variant Ship (beam 40 ft.)

velocity is minimum. It is the change in axial velocity, not tangential velocity, which determines the magnitude of thrust delivered. This propulsion scheme provides the best match with a submarine hull but, due to geometric constraints, N_e will be small.

Since E depends inversely on the separation between electrodes, for a given power input, J will increase as electrode separation increases. Equation (12) shows that high values of J are undesirable. NUSC's preliminary efficiency calculations showed N_p=20.7%.[7] With this propulsion scheme, a large reactor plant will be required to achieve speeds in the neighborhood of 30 knots.

The optimum combination of a large flow area and a minimum electrode separation can be achieved by mounting a MHD thruster over the parallel middle body. The tangential velocity over the entire length of middle body remains relatively constant and a location of the suction inlet is flexible. Discharging in the vicinity of 280 ft. (85.3 m) aft of the forward perpendicular will give a minimum velocity gradient between the exiting jet and a local velocity. This is predicated on a design which integrates the outer surface of a thruster with the outer hull of a submarine.

An integrated internal thruster hull design can employ lateral suction. NUSC has shown that this approach will result in a better propulsive efficiency.[20] Since the suction accelerates sea water in a

direction normal to the hull, (1-t) factor should decrease. On the other hand, studies in aerodynamics indicate the total drag on a body can be significantly larger with a lateral intake than with a nose intake.[10] Nose intake also provides for superior performance during thrust reversal which may be required in emergency situation.

With a MHD thruster mounted over the parallel middle body, four different options will be evaluated:

1. SSNX-1 is a baseline SSNX with a MHD thruster mounted externally.
2. SSNX-2 is the same design as SSNX-1 but with a retractable sail.
3. SSNX-3 is a baseline ship with a beam increased to 40 feet and a MHD thruster is mounted internally to the outer hull. The sail is retractable.
4. SSNX-4 is a baseline ship with a MHD thruster mounted internally to the outer hull.

Options 3 and 4 will require reduction in the main pressure hull diameter starting in vicinity of 180 feet aft of the forward perpendicular, hence classify as a double hull submarine.

The final dimensions were based on the output of optimization program. MHD active channel length was set to 18.29 m for the first three options and 24 m for the fourth option. The dimensions of inlet nozzle were derived from convergence angle of 10.9 degrees which

was modeled after a similar design.[21] Diffuser convergence angle was set at 5 degrees.

The values of C_f and C_D were generated by TAPS-1 for the bare hull and by parametric relationships, based on a flat plate analysis, for the appendages. The appendage surface areas were derived from a data bank for different submarines by adjusting size in proportion with ship's displacements. For the same reason, SSNX-3 appendage area was increased by the displacement ratio to the baseline ship.

The MHD thruster entrance loss was absorbed in a form drag which was derived from the frictional losses due to thruster's externals. The inlet nozzle and diffuser loss, based on relationships in Section 2.4, was added to the frictional loss inside the MHD channel. By doing so, the energy loss inside the thruster is uncoupled from the total drag on the ship; therefore, N_d is implicit in the values of EHP obtained.

Using equation (25), A_o can be calculated since C_D is known. Since thruster internal losses are known, equation (23) solves for the required J; a corresponding value of E is found from equation (1). The total electrical power input to the MHD thruster is calculated using equation (3).

The calculated electrical power must be adjusted for N_h and N_e. These were calculated for speed of 25 knots and assumed relatively constant for all speeds. The turbulent boundary layer thickness at the inlet

nozzle was estimated at 2.5 feet using TAPS-1, Figures 3-17 and 3-18.

The result of equation (34) was averaged with a free stream velocity to obtain a corrected inlet velocity. Because the inlet nozzle is located far from the stern, the correction for the inlet velocity was very small, namely $0.944U_{ship}$. Using equation (30), $(1-t)=.995$ was calculated. From equation (31) value of $(1-w)=.944$ was obtained, hence $N_h=1.054$. From equation (36), $N_r=1.036$ resulted; therefore, the electrical power was adjusted by $N_hN_r=1.091$.

Because C_D and thruster internal losses vary with ship's speed, the calculations require a computer spreadsheet which was used to evaluate the performance of all four designs. The results are summarized in Table 3-1 through 3-4, and Figures 3-19 through 3-22. Since the propulsive coefficient for the MHD thruster is lower than for the conventional propeller used on SSN-688 , all four variant submarines can not make the speed of 30 knots if the Shaft Horse Power is limited to 35,000 HP.[26]

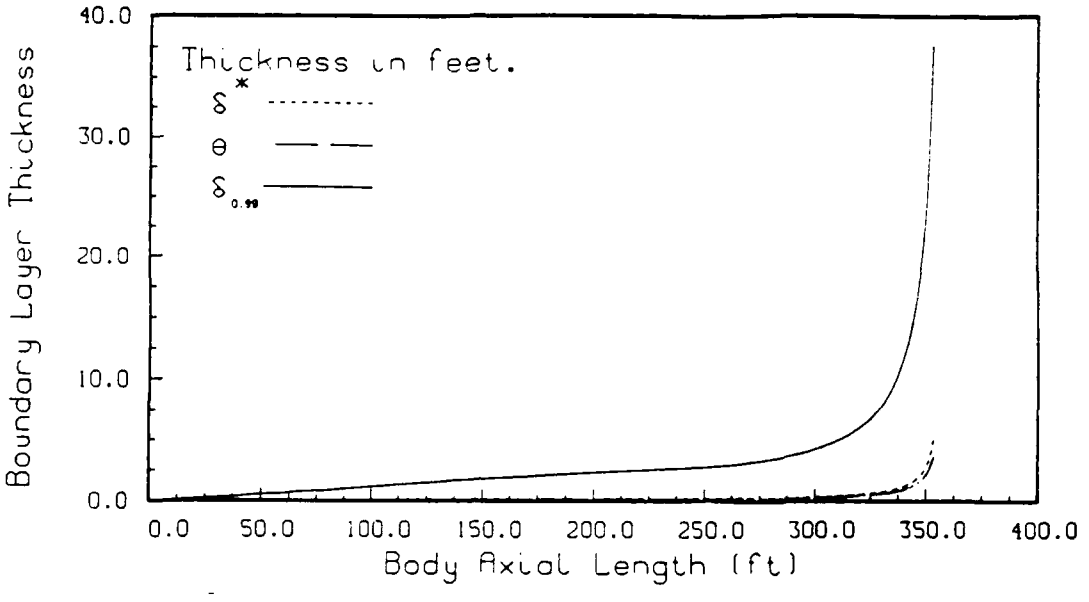

Figure 3-17 TAPS 1 Program Results for Boundary Layer Thickness vs. Axial Position along the Hull (Baseline Submarine, speed=25 kts.)

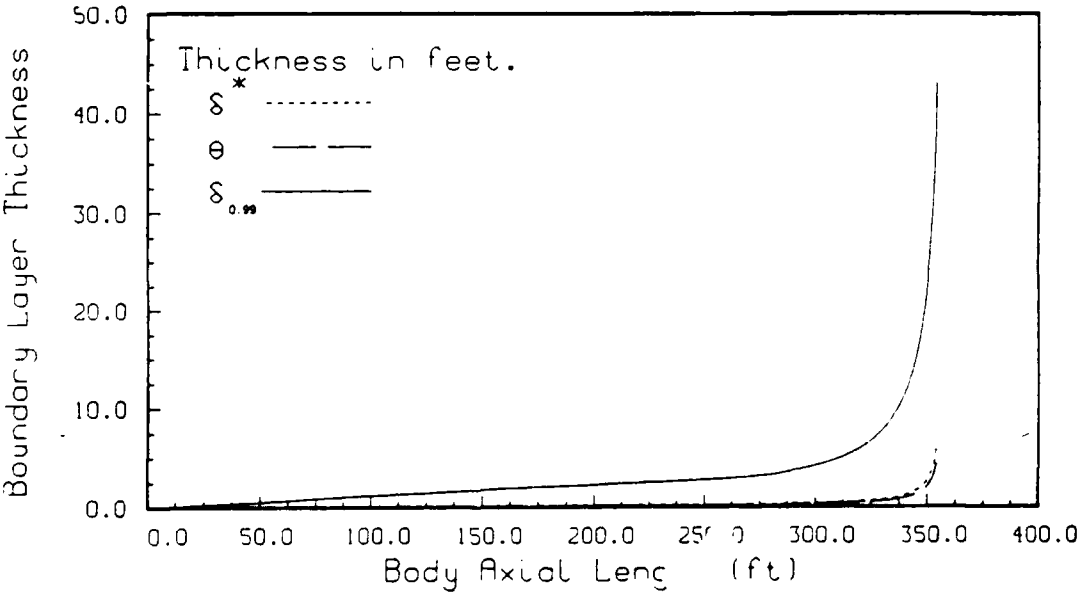

Figure 3-18 TAPS 1 Program Results for Boundary Layer Thickness vs. Axial Position along the Hull (Baseline Submarine, speed=30 kts.)

SSNX-1 SPEED-POWER REQUIREMENT

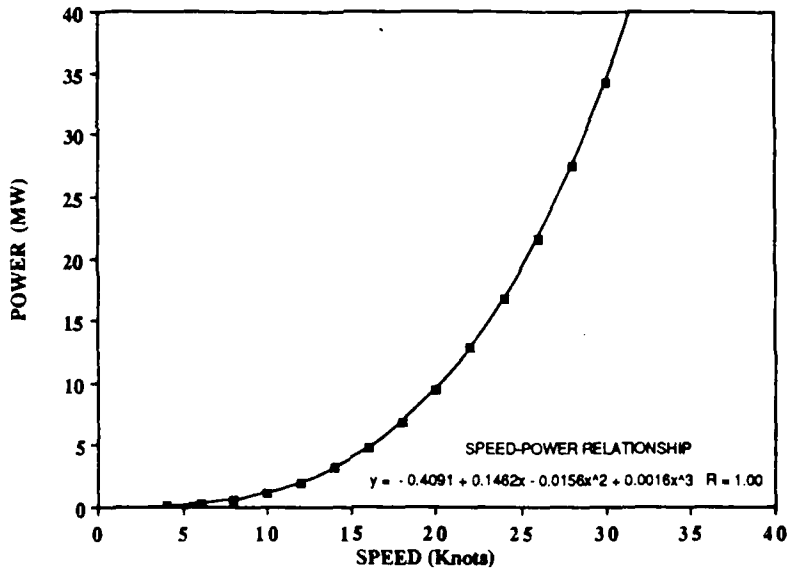

Figure 3-19 SSNX-1 Speed-Power Requirement Curve

SSNX-2 SPEED-POWER REQUIREMENT

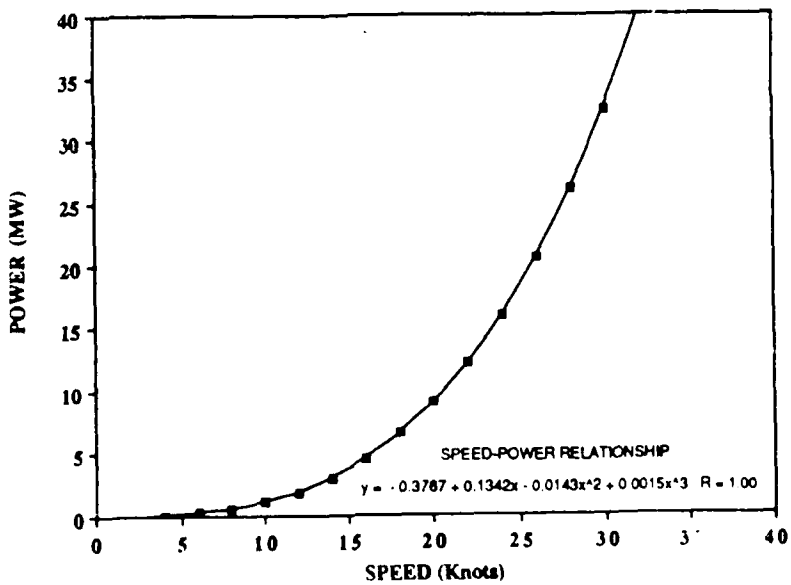

Figure 3-20 SSNX-2 Speed-Power Requirement Curve

SSNX-3 SPEED-POWER REQUIREMENT

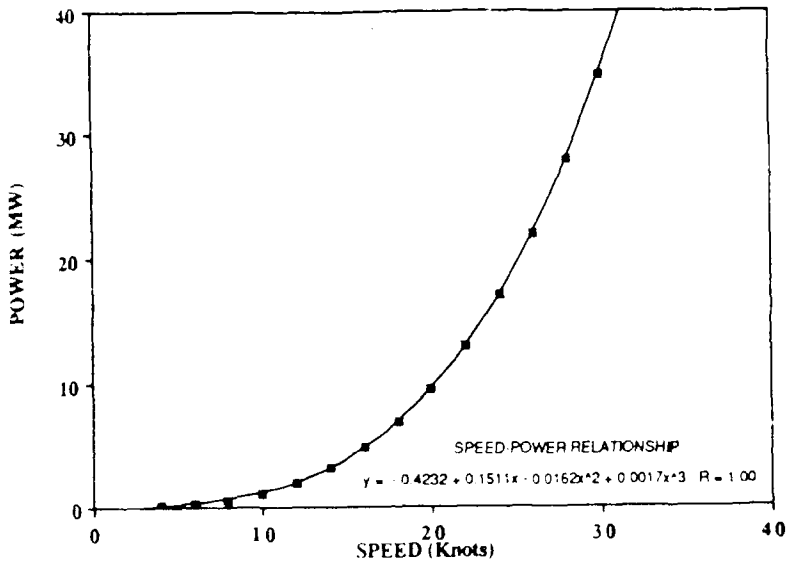

Figure 3-21 SSNX-3 Speed-Power Requirement Curve

SSNX-4 SPEED-POWER REQUIREMENT

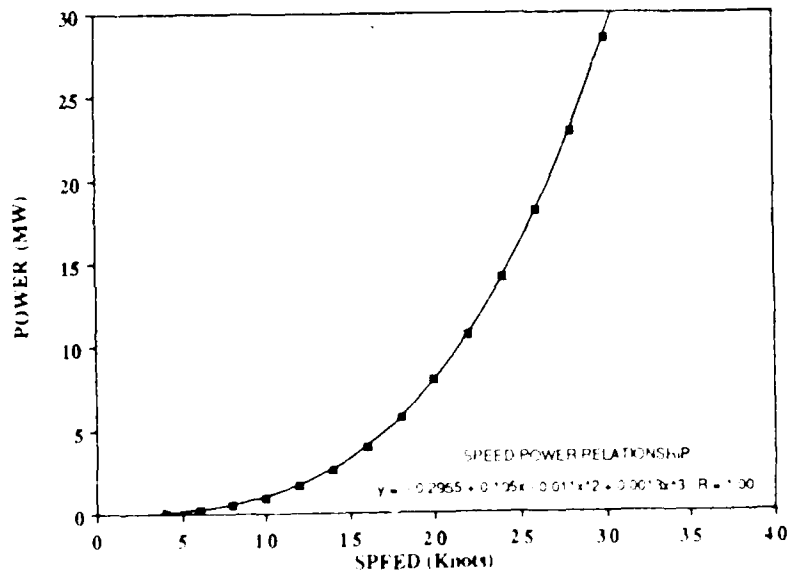

Figure 3-22 SSNX-4 Speed-Power Requirement Curve

Table 3-1 SSNX-1 Speed-Power Calculations

PERFORMANCE ANALYSIS SSNX-1 TABLE 3-1

TABLE 3-1A: Ship and Thruster Data
(SI Units except coefficients)

L =	109.7560			k' =	0.048	Lf =	65
D =	10.06097	A2' =	44.14424	A2 =	46.37	Lpmb =	160
D/L =	0.0917	A3' =	37.128	A3 =	39	La =	135
L/D =	10.90909	A3'/A2' =	0.800690	A3/A2 =	0.841061	Cp =	0.808
		a' =	171.36	a =	180	Cs =	0.875
dR =	1.2	Lc =	18.29268				
Ro =	6.730487	S,fixed =	3350			A,I,avg =	670.7941
Ri =	5.530487	Cd,fixed	0.003				
r0 =	5.030487	Lt =	21.8				
r1 =	4.826	p =	0.027545	Sp =	283.2754		

Seawater Density (kg/m^3) = 1025.9 @ 15 C
u = ship's velocity (m/sec) v = thruster exit velocity (m/sec)

TABLE 3-1B: SURFACE AREAS

Surface	Number	Area (ft^2)	Tot Area (m^2)
Bare Hull (total)	1	32665.58	3038.145
Bare Hull (loss)	2	3158.890	587.2416
Bare Hull (net)		29526.68	2450.903
Sail	1	914.761	85.02760
Fairwater Planes	2	229.873	42.73367
Rudder (upper)	1	377.91	35.12697
Rudder (lower)	1	342.252	31.81753
Stern Planes	2	465.857	86.60339
Emergency Prop	0	0	0
Thrusters (ext)	2	5260.347	977.9052
Thrusters (int)	2	9055.574	1683.442

TABLE 3-1C: COEFFICIENTS OF FRICTION (VARIABLE)

Seawater viscosity (m^2/sec) = 1.19E-06 @ 15 C
Correlation Allowance (del Cf) = 0.0004

Speed(u) (Knots)	Speed(u) (m/sec)	Cf Bare Hull	Cd Bare Hull	Cd Sail	Cd FW Planes	Cd Rud(up)	Cd Rud(low)	Cd Stern Pl	Cd Emer Prop	Cf Thruster	Cd Thruster
4	2.058536	0.00190	0.00239	0.00658	0.00584	0.00603	0.00619	0.00630	0.00804	0.00248	0.00310
6	3.087804	0.00180	0.00229	0.00630	0.00548	0.00567	0.00583	0.00598	0.00742	0.00233	0.00293
8	4.117073	0.00173	0.00221	0.00612	0.00525	0.00543	0.00560	0.00576	0.00702	0.00223	0.00282
10	5.146341	0.00168	0.00216	0.00599	0.00508	0.00526	0.00543	0.00561	0.00674	0.00216	0.00275
12	6.175609	0.00164	0.00212	0.00589	0.00495	0.00513	0.00530	0.00549	0.00652	0.00210	0.00268
14	7.204878	0.00161	0.00209	0.00580	0.00485	0.00502	0.00520	0.00539	0.00635	0.00205	0.00263
16	8.234146	0.00158	0.00206	0.00573	0.00476	0.00494	0.00511	0.00531	0.00620	0.00201	0.00259
18	9.263414	0.00156	0.00203	0.00567	0.00468	0.00486	0.00504	0.00524	0.00608	0.00198	0.00256
20	10.29268	0.00154	0.00201	0.00562	0.00462	0.00479	0.00497	0.00518	0.00597	0.00195	0.00252
22	11.32195	0.00152	0.00199	0.00557	0.00456	0.00473	0.00491	0.00512	0.00588	0.00193	0.00250
24	12.35121	0.00151	0.00198	0.00553	0.00451	0.00468	0.00486	0.00508	0.00579	0.00190	0.00247
26	13.38048	0.00149	0.00196	0.00550	0.00446	0.00464	0.00481	0.00503	0.00572	0.00188	0.00245
28	14.40975	0.00148	0.00195	0.00546	0.00442	0.00459	0.00477	0.00499	0.00565	0.00186	0.00243
30	15.43902	0.00147	0.00194	0.00543	0.00438	0.00455	0.00473	0.00496	0.00559	0.00185	0.00241

Table 3-1 SSNX-1 continued

TABLE 3-1D: CALCULATION OF COEFFICIENTS FOR F(Ao) = 0
(SUBMERGED)

Speed(u) (Knots)	Speed(u) (m/sec)	Cd*S,ref	Ci*Si Ssum
4	2.058536	10.050	10.657
6	3.087804	10.050	10.142
8	4.117073	10.050	9.803
10	5.146341	10.050	9.555
12	6.175609	10.050	9.361
14	7.204878	10.050	9.201
16	8.234146	10.050	9.068
18	9.263414	10.050	8.953
20	10.29268	10.050	8.853
22	11.32195	10.050	8.763
24	12.35121	10.050	8.685
26	13.38048	10.050	8.613
28	14.40975	10.050	8.546
30	15.43902	10.050	8.486

Electromagnetic Parameters

Magnetic field (B) : 8 Tesla
Conductivity (seawater) : 4 Mhos/m

TABLE 3-1D: THRUSTER VOLTAGE, CURRENT, POWER, EFFICIENCY (ACTUAL)
(SUBMERGED)

Speed(u) (Knots)	Speed(u) (m/sec)	Ao (m^2)	Cf(Lm)	Thrust (N)	Drag (N)	Ie (amps)	Ve (volts)	Pe (MW)	"EHP" (MW) ****	Efficiency NpNeNh
4	2.058536	41.95488	0.00430	23166	23166	3832	20.45102	0.072	0.048	0.664
6	3.087804	41.64872	0.00415	49604	49604	8229	31.64733	0.239	0.153	0.642
8	4.117073	41.51188	0.00405	85234	85234	14168	43.50357	0.565	0.351	0.621
10	5.146341	41.41128	0.00398	129807	129807	21612	56.01173	1.109	0.668	0.602
12	6.175609	41.33225	0.00392	183123	183123	30529	69.16272	1.935	1.131	0.585
14	7.204878	41.26725	0.00387	245010	245010	40893	82.94762	3.108	1.765	0.568
16	8.234146	41.21274	0.00383	315382	315382	52690	97.36293	4.700	2.597	0.553
18	9.263414	41.16560	0.00380	394098	394098	65899	112.4001	6.786	3.651	0.538
20	10.29268	41.12446	0.00377	481102	481102	80510	128.0569	9.446	4.952	0.524
22	11.32195	41.08741	0.00375	576216	576216	96499	144.3215	12.760	6.524	0.511
24	12.35121	41.05496	0.00372	679588	679588	113882	161.2052	16.820	8.394	0.499
26	13.38048	41.02520	0.00370	790953	790953	132624	178.6903	21.713	10.583	0.487
28	14.40975	40.99775	0.00368	910248	910248	152716	196.7729	27.532	13 116	0.476
30	15.43902	40.97297	0.00366	1037611	1037611	174173	215.4626	34.383	16.020	0.466

**** Calculated from Thrust (or Drag) * Uo = Power

Table 3-2 SSNX-2 Speed-Power Calculations

PERFORMANCE ANALYSIS SSNX-2 TABLE 3-2

TABLE 3-2A: Ship and Thruster Data
(SI Units except coefficients)

L =	109.7560			k' =	0.048	Lf =	65
D =	10.06097	A2' =	44.14424	A2 =	46.37	Lpab =	160
D/L =	0.0917	A3' =	37.128	A3 =	39	La =	135
L/D =	10.9096	A3'/A2' =	0.800690	A3/A2 =	0.841061	Cp =	0.808
		a' =	171.36	a =	180	Cs =	0.875
dR =	1.2	Lc =	18.29268				
Ro =	6.730487	S,fixed =	3350			A,I,avg =	670.7941
Ri =	5.530487	Cd,fixed	0.003				
r0 =	5.030487	Lt =	21.8				
r1 =	4.826	p =	0.027545	Sp =	283.2754		

Seawater Density (kg/m^3) = 1025.9 @ 15 C
u = ship's velocity (m/sec) v = thruster exit velocity (m/sec)

TABLE 3-2B: SURFACE AREAS

Surface	Number	Area (ft^2)	Tot Area (m^2)
Bare Hull (total)	1	32685.58	3038.145
Bare Hull (loss)	2	3158.890	587.2416
Bare Hull (net)		29526.68	2450.903
Sail	0	914.761	0
Fairwater Planes	2	229.873	42.73367
Rudder (upper)	1	377.91	35.12697
Rudder (lower)	1	342.252	31.81253
Stern Planes	2	465.857	86.60339
Emergency Prop	0	0	0
Thrusters (ext)	2	5260.347	977.9052
Thrusters (int)	2	9055.574	1683.442

TABLE 3-2C: COEFFICIENTS OF FRICTION (VARIABLE)

Seawater viscosity (m^2/sec) = 1.19E-06 @ 15 C
Correlation Allowance (del Cf) = 0.0004

Speed(u) (Knots)	Speed(u) (m/sec)	Cf Bare Hull	Cd Bare Hull	Cd Sail	Cd FW Planes	Cd Rud(up)	Cd Rud(low)	Cd Stern Pl	Cd Emer Prop	Cf Thruster	Cd Thruster
4	2.058536	0.00190	0.00239	0.00658	0.00584	0.00603	0.00619	0.00630	0.00804	0.00248	0.00310
6	3.087804	0.00180	0.00229	0.00630	0.00548	0.00567	0.00583	0.00598	0.00742	0.00233	0.00293
8	4.117073	0.00173	0.00221	0.00612	0.00525	0.00543	0.00560	0.00576	0.00702	0.00223	0.00282
10	5.146341	0.00168	0.00216	0.00599	0.00508	0.00526	0.00543	0.00561	0.00674	0.00216	0.00275
12	6.175609	0.00164	0.00212	0.00589	0.00495	0.00513	0.00530	0.00549	0.00652	0.00210	0.00268
14	7.204878	0.00161	0.00209	0.00580	0.00485	0.00502	0.00520	0.00539	0.00635	0.00205	0.00263
16	8.234146	0.00158	0.00206	0.00573	0.00476	0.00494	0.00511	0.00531	0.00620	0.00201	0.00259
18	9.263414	0.00156	0.00203	0.00567	0.00468	0.00486	0.00504	0.00524	0.00608	0.00198	0.00256
20	10.29268	0.00154	0.00201	0.00562	0.00462	0.00479	0.00497	0.00518	0.00597	0.00195	0.00252
22	11.32195	0.00152	0.00199	0.00557	0.00456	0.00473	0.00491	0.00512	0.00588	0.00193	0.00250
24	12.35121	0.00151	0.00198	0.00553	0.00451	0.00468	0.00486	0.00508	0.00579	0.00190	0.00247
26	13.38048	0.00149	0.00196	0.00550	0.00446	0.00464	0.00481	0.00503	0.00572	0.00188	0.00245
28	14.40975	0.00148	0.00195	0.00546	0.00442	0.00459	0.00477	0.00499	0.00565	0.00186	0.00243
30	15.43902	0.00147	0.00194	0.00543	0.00438	0.00455	0.00472	0.00496	0.00559	0.00185	0.00241

Table 3-2 SSNX-2 continued

TABLE 3-2D: CALCULATION OF COEFFICIENTS FOR F(Ao) = 0
(SUBMERGED)

Speed(u) (Knots)	Speed(u) (m/sec)	Cd*S,ref	Ci*Si @sun
4	2.058536	10.050	10.098
6	3.087804	10.050	9.687
8	4.117073	10.050	9.283
10	5.146341	10.050	9.046
12	6.175609	10.050	8.860
14	7.204878	10.050	8.708
16	8.234146	10.050	8.581
18	9.263414	10.050	8.471
20	10.29268	10.050	8.375
22	11.32195	10.050	8.290
24	12.35121	10.050	8.214
26	13.38048	10.050	8.145
28	14.40975	10.050	8.082
30	15.43902	10.050	8.025

Electromagnetic Parameters

Magnetic field (B) = 8 Tesla
Conductivity (seawater) = 4 Mhos/m

TABLE 3-2E: THRUSTER VOLTAGE, CURRENT, POWER, EFFICIENCY (ACTUAL)
(SUBMERGED)

Speed(u) (Knots)	Speed(u) (m/sec)	Ao (m^2)	Cf(Lm)	Thrust (N)	Drag (N)	Ie (amps)	Ve (volts)	Pe (MW)	"BHP" (MW) ****	Efficiency MpMeMh
4	2.058536	41.63083	0.00430	21949	21949	3686	20.28510	0.068	0.045	0.660
6	3.087804	41.43232	0.00415	46984	46984	7912	31.36044	0.227	0.145	0.638
8	4.117073	41.30042	0.00405	80709	80709	13621	43.06953	0.537	0.332	0.618
10	5.146341	41.20342	0.00398	122887	122887	20774	55.40459	1.055	0.632	0.600
12	6.175609	41.12716	0.00392	173325	173325	29342	68.35669	1.838	1.070	0.582
14	7.204878	41.06472	0.00387	231879	231879	39302	81.91881	2.950	1.671	0.566
16	8.234146	41.01219	0.00384	298438	298438	50636	96.08536	4.458	2.457	0.551
18	9.263414	40.96674	0.00380	372877	372877	63326	110.8489	6.431	3.454	0.537
20	10.29268	40.92700	0.00377	455135	455135	77360	126.2064	8.945	4.685	0.524
22	11.32195	40.89138	0.00375	545075	545075	92721	142.1494	12.076	6.171	0.511
24	12.35121	40.86006	0.00372	642793	642793	109417	158.6850	15.908	7.919	0.499
26	13.38048	40.83110	0.00370	748005	748005	127411	175.7943	20.521	10.009	0.488
28	14.40975	40.80483	0.00368	860801	860801	146713	193.4838	26.008	12.404	0.477
30	15.43902	40.78091	0.00367	981160	981160	167319	211.7523	32.461	15.148	0.467

**** Calculated from Thrust (or Drag) * Uo : Power

Table 3-3 SSNX-3 Speed-Power Calculations

PERFORMANCE ANALYSIS SSNX-3 TABLE 3-3

TABLE 3-3A: Ship and Thruster Data
(SI Units except coefficients)

L =	109.7560			k' =	0.048	Lf =	65
D =	12.19512	A2' =	44.14424	A2 =	46.37	Lpab =	160
D/L =	0.1111	A3' =	37.128	A3 =	39	La =	135
L/D =	9	A3'/A2' =	0.800690	A3/A2 =	0.841061	Cp =	0.808
		a' =	171.36	a =	180	Ca =	0.849
dR =	1.2	Lc =	18.29268				
Ro =	6.73	S,fixed =	3350			A,I,avg =	670.7407
Ri =	5.53	Cd,fixed	0.003				
r0 =	5.03	Lt =	21.8				
r1 =	4.826	p =	0.027478	Sp =	283.2611		

Seawater Density (kg/m^3) = 1025.9 @ 15 C
u = ship's velocity (m/sec) v = thruster exit velocity (m/sec)

TABLE 3-3B: SURFACE AREAS

Surface	Number	Area (ft^2)	Tot Area (m^2)
Bare Hull (total)	1	39757.11	3695.448
Bare Hull (loss)	0	3158.736	0
Bare Hull (net)		36598.37	3695.448
Sail	0	1344.698	0
Fairwater Planes	2	337.9133	62.81850
Rudder (upper)	1	555.5277	51.63664
Rudder (lower)	1	503.1104	46.76442
Stern Planes	2	684.8097	127.3069
Emergency Prop	0	0	0
Thrusters (ext)	0	4839.854	0
Thrusters (int)	2	9054.999	1683.335

TABLE 3-3C: COEFFICIENTS OF FRICTION (VARIABLE)

Seawater viscosity (m^2/sec) = 1.19E-06 @ 15 C
Correlation Allowance (del Cf) = 0.0004

Speed(u) (Knots)	Speed(u) (m/sec)	Cf Bare Hull	Cd Bare Hull	Cd Sail	Cd FW Planes	Cd Rud(up)	Cd Rud(low)	Cd Stern Pl	Cd Emer Prop	Cf Thruster	Cd Thruster
4	2.058536	0.00190	0.00243	0.00658	0.00584	0.00603	0.00619	0.00630	0.00804	0.00248	0.00316
6	3.087804	0.00180	0.00232	0.00630	0.00548	0.00567	0.00583	0.00598	0.00742	0.00233	0.00299
8	4.117073	0.00173	0.00225	0.00612	0.00525	0.00543	0.00560	0.00576	0.00702	0.00223	0.00288
10	5.146341	0.00168	0.00219	0.00599	0.00508	0.00526	0.00543	0.00561	0.00674	0.00216	0.00280
12	6.175609	0.00164	0.00215	0.00589	0.00495	0.00513	0.00530	0.00549	0.00652	0.00210	0.00274
14	7.204878	0.00161	0.00212	0.00580	0.00485	0.00502	0.00520	0.00539	0.00635	0.00205	0.00268
16	8.234146	0.00158	0.00209	0.00573	0.00476	0.00494	0.00511	0.00531	0.00620	0.00201	0.00264
18	9.263414	0.00156	0.00206	0.00567	0.00468	0.00486	0.00504	0.00524	0.00608	0.00198	0.00260
20	10.29268	0.00154	0.00204	0.00562	0.00462	0.00479	0.00497	0.00518	0.00597	0.00195	0.00257
22	11.32195	0.00152	0.00202	0.00557	0.00456	0.00473	0.00491	0.00512	0.00588	0.00193	0.00254
24	12.35121	0.00151	0.00200	0.00553	0.00451	0.00468	0.00486	0.00508	0.00579	0.00190	0.00252
26	13.38048	0.00149	0.00199	0.00550	0.00446	0.00464	0.00481	0.00503	0.00572	0.00188	0.00249
28	14.40975	0.00148	0.00197	0.00546	0.00442	0.00459	0.00477	0.00499	0.00565	0.00186	0.00247
30	15.43902	0.00147	0.00196	0.00543	0.00438	0.00455	0.00473	0.00496	0.00559	0.00185	0.00245

Table 3-3 SSNX-3 continued

TABLE 3-3D: CALCULATION OF COEFFICIENTS FOR F(Ao) = 0
(SUBMERGED)

Speed(u) (Knots)	Speed(u) (m/sec)	Cd*S,ref	Ci*Si @sum
4	2.058536	10.050	10.740
6	3.087804	10.050	10.238
8	4.117073	10.050	9.906
10	5.146341	10.050	9.663
12	6.175609	10.050	9.472
14	7.204878	10.050	9.316
16	8.234146	10.050	9.186
18	9.263414	10.050	9.073
20	10.29268	10.050	8.974
22	11.32195	10.050	8.885
24	12.35121	10.050	8.808
26	13.38048	10.050	8.736
28	14.40975	10.050	8.671
30	15.43902	10.050	8.612

Electromagnetic Parameters

Magnetic field (B) = 8 Tesla
Conductivity (seawater) = 4 Mhos/m

TABLE 3-3E: THRUSTER VOLTAGE, CURRENT, POWER, EFFICIENCY (ACTUAL)
(SUBMERGED)

Speed(u) (Knots)	Speed(u) (m/sec)	Ao (m^2)	Cf(Lm)	Thrust (N)	Drag (N)	Ie (amps)	Ve (volts)	Pe (MW)	"EHP" (MW) ****	Efficiency NpNeNh
4	2.058536	41.88784	0.00430	23345	23345	3854	20.47546	0.072	0.048	0.665
6	3.087804	41.68719	0.00415	50072	50072	8285	31.69841	0.241	0.155	0.641
8	4.117073	41.55343	0.00405	86128	86128	14275	43.58901	0.570	0.355	0 622
10	5.146341	41.45506	0.00398	131272	131272	21787	56.13364	1.121	0.676	0.603
12	6.175609	41.37762	0.00392	185302	185302	30789	69.34133	1.956	1.144	0.585
14	7.204878	41.31417	0.00387	248069	248069	41259	83.18648	3.145	1.787	0.568
16	8.234146	41.26079	0.00383	319464	319464	53179	97.66966	4.759	2.631	0.553
18	9.263414	41.21450	0.00380	399344	399344	66528	112.7824	6.874	3.699	0.538
20	10.29268	41.17403	0.00377	487657	487657	81296	128.5225	9.573	5.019	0.524
22	11.32195	41.13761	0.00374	584235	584235	97462	144.8792	12.937	6.615	0.511
24	12.35121	41.10585	0.00372	689248	689248	115042	161.8649	17.061	8.513	0.499
26	13.38048	41.07622	0.00370	802305	802305	133988	179.4534	22.030	10.735	0.487
28	14.40975	41.04940	0.00368	923560	923560	154316	197.6558	27.945	13.308	0.476
30	15.43902	41.02506	0.00366	1053005	1053005	176024	216.4714	34.911	16.257	0.466

**** Calculated from Thrust (or Drag) * Uo = Power

Table 3-4 SSNX-4 Speed-Power Calculations

PERFORMANCE ANALYSIS SSNX-4 TABLE 3-4

TABLE 3-4A: Ship and Thruster Data
(SI Units except coefficients)

L =	109.7560			k' =	0.048	Lf =	65
D =	10.06097	A2' =	28.20776	A2 =	29.63	Lpab =	160
D/L =	0.0917	A3' =	25.704	A3 =	27	La =	135
L/D =	10.90909	A3'/A2' =	0.867499	A3/A2 =	0.911238	Cp =	0.808
		a' =	171.36	a =	180	Ca =	0.875
dR =	1.2	Lc =	24				
Ro =	4.53	S,fixed =	3350			A,I,avg =	564.1837
Ri =	3.33	Cd,fixed	0.003				
r0 =	5.030487	Lt =	24				
r1 =	4.826	p =	0.020995	Sp =	371.6476		

Seawater Density (kg/m^3) = 1025.9 @ 15 C
u = ship's velocity (m/sec) v = thruster exit velocity (m/sec)

TABLE 3-4B: SURFACE AREAS

Surface	Number	Area (ft^2)	Tot Area (m^2)
Bare Hull (total)	1	32685.58	3038.145
Bare Hull (loss)	0	4109.633	0
Bare Hull (net)		28575.94	3038.145
Sail	1	914.761	85.02750
Fairwater Planes	2	229.873	42.73367
Rudder (upper)	1	377.91	35.12697
Rudder (lower)	1	342.252	31.81253
Stern Planes	2	465.857	86.60339
Emergency Prop	0	0	0
Thrusters (ext)	0	3846.120	0
Thrusters (int)	2	6375.75	1185.259

TABLE 3-4C: COEFFICIENTS OF FRICTION (VARIABLE)

Seawater viscosity (m^2/sec) = 1.19E-06 @ 15 C
Correlation Allowance (del Cf) = 0.0004

Speed(u) (Knots)	Speed(u) (m/sec)	Cf Bare Hull	Cd Bare Hull	Cd Sail	Cd FW Planes	Cd Rud(up)	Cd Rud(low)	Cd Stern Pl	Cd Emer Prop	Cf Thruster	Cd Thruster
4	2.058536	0.00190	0.00239	0.00658	0.00584	0.00603	0.00619	0.00630	0.00804	0.00238	0.00299
6	3.087804	0.00180	0.00229	0.00630	0.00548	0.00567	0.00583	0.00598	0.00742	0.00223	0.00283
8	4.117073	0.00173	0.00221	0.00612	0.00525	0.00543	0.00560	0.00576	0.00702	0.00214	0.00273
10	5.146341	0.00168	0.00216	0.00599	0.00508	0.00526	0.00543	0.00561	0.00674	0.00207	0.00265
12	6.175609	0.00164	0.00212	0.00589	0.00495	0.00513	0.00530	0.00549	0.00652	0.00202	0.00260
14	7.204878	0.00161	0.00209	0.00580	0.00485	0.00502	0.00520	0.00539	0.00635	0.00198	0.00255
16	8.234145	0.00158	0.00206	0.00573	0.00476	0.00494	0.00511	0.00531	0.00620	0.00194	0.00251
18	9.263414	0.00156	0.00203	0.00567	0.00468	0.00486	0.00504	0.00524	0.00608	0.00191	0.00248
20	10.29268	0.00154	0.00201	0.00562	0.00462	0.00479	0.00497	0.00518	0.00597	0.00188	0.00245
22	11.32195	0.00152	0.00199	0.00557	0.00456	0.00473	0.00491	0.00512	0.00588	0.00185	0.00241
24	12.35121	0.00151	0.00198	0.00553	0.00451	0.00468	0.00486	0.00508	0.00579	0.00183	0.00239
26	13.38048	0.00149	0.00196	0.00550	0.00446	0.00464	0.00481	0.00503	0.00572	0.00181	0.00237
28	14.40975	0.00148	0.00195	0.00546	0.00442	0.00459	0.00477	0.00499	0.00565	0.00180	0.00235
30	15.43902	0.00147	0.00194	0.00543	0.00438	0.00455	0.00473	0.00496	0.00559	0.00178	0.00234

Table 3-4 SSNX-4 continued

TABLE 3-4D: CALCULATION OF COEFFICIENTS FOR F(Ao) = 0
(SUBMERGED)

Speed(u) (Knots)	Speed(u) (m/sec)	Cd*S,ref	Ci*Si $sum
4	2.058536	10.050	9.033
6	3.087804	10.050	8.617
8	4.117073	10.050	8.341
10	5.146341	10.050	8.139
12	6.175609	10.050	7.982
14	7.204878	10.050	7.852
16	8.234146	10.050	7.743
18	9.263414	10.050	7.650
20	10.29268	10.050	7.568
22	11.32195	10.050	7.494
24	12.35121	10.050	7.430
26	13.38048	10.050	7.371
28	14.40975	10.050	7.317
30	15.43902	10.050	7.268

Electromagnetic Parameters

Magnetic field (B) = 8 Tesla
Conductivity (seawater) = 4 Mhos/m

TABLE 3-4E: THRUSTER VOLTAGE, CURRENT, POWER, EFFICIENCY (ACTUAL)
(SUBMERGED)

Speed(u) (Knots)	Speed(u) (m/sec)	Ao (m^2)	Cf(Lm)	Thrust (N)	Drag (N)	Ie (amps)	Ve (volts)	Pe (MW)	"EHP" (MW) ****	Efficiency NpNeNh
4	2.058536	29.62312	0.00336	19635	19635	3041	22.37075	0.062	0.040	0.648
6	3.087804	29.46263	0.00322	42141	42141	6527	34.43224	0.206	0.130	0.632
8	4.117073	29.35573	0.00313	72523	72523	11233	47.10560	0.485	0.299	0.616
10	5.146341	29.27705	0.00306	110578	110578	17129	60.38600	0.948	0.569	0.600
12	6.175609	29.21515	0.00301	156143	156143	24190	74.26583	1.646	0.964	0.586
14	7.204878	29.16411	0.00297	209072	209072	32334	88.73696	2.634	1.506	0.572
16	8.234146	29.12132	0.00293	269302	269302	41730	103.7974	3.968	2.217	0.559
18	9.263414	29.08425	0.00290	336708	336708	52181	119.4387	5.710	3.119	0.546
20	10.29268	29.05190	0.00287	411253	411253	63739	135.6595	7.922	4.233	0.534
22	11.32195	29.02265	0.00285	492771	492771	76384	152.4474	10.669	5.579	0.523
24	12.35121	28.99715	0.00283	581423	581423	90132	169.8166	14.023	7.181	0.512
26	13.38048	28.97370	0.00281	676956	676956	104951	187.7472	18.053	9.058	0.502
28	14.40975	28.95200	0.00279	779315	779315	120834	206.2357	22.832	11.230	0.492
30	15.43902	28.93249	0.00277	888649	888649	137795	225.2940	28.443	13.720	0.482

**** Calculated from Thrust (or Drag) * Uo = Power

4. SUBMARINE POWER PLANT

4.1 PRESENT DAY SUBMARINES

At the present time in the U.S., the only type of reactor in service for submarine propulsion is the pressurized-water reactor (PWR). After the immediate success of the U.S.S. Nautilus, in order to test a different type of nuclear reactor, U.S.S. Seawolf was put to sea with a reactor core cooled by a sodium-potasium (NaK) liquid metal. Eventually this ship was converted to the pressurized-water reactor plant due to leaks in the superheater. This lead to the abandonment of non-PWR projects.

Today's nuclear submarine PWR power plant (or a plant using a boiling water reactor) is limited in power by the saturation temperature of water at a given pressure since the energy conversion system is a saturated steam Rankine cycle. New energy conversion systems may further improve the efficiency depending on details of their respective thermodynamic cycles. However, major advances primarily depend on the source temperature.

Although an increase in pressure would raise the saturation temperature and lead to a corresponding thermal efficiency increase, the attendant increase in weight of the primary system and auxiliary equipment may actually decrease the power density.

The same applies to an advanced steam turbine plant.

Reductions in condenser pressure by providing greater surface area for the heat transfer requires a larger condenser. The temperature of the steam is limited by fuel and coolant conditions in the reactor. The use of superheaters can increase the steam temperature by 100 C, increasing thermal efficiency by 7 percent. Another option is to employ a regenerative feed-heating cycles which may increase the thermal efficiency by as much as 10 percent.[22]

These secondary plant improvements are not very attractive in submarine applications because the ship is generally weight limited. Any improvement to the thermodynamic efficiency carries with it a trade-off penalty as indicated in Figure 4-1. Increase in steam pressure improves thermal efficiency of the steam cycle; however, the relative weight of propulsion plant increases. Thermal efficiency of the steam cycle can also be increased by higher source temperatures. This requires higher coolant pressures to prevent boiling in the core; consequently, reactor plant weight increases. The reduction in power density (weight/SHP) of the primary power and propulsion plants outweighs the importance of the improved thermal efficiency. Superheaters and regenerating equipment are generally either bulky or heavy and, therefore, are undesirable for submarine use.

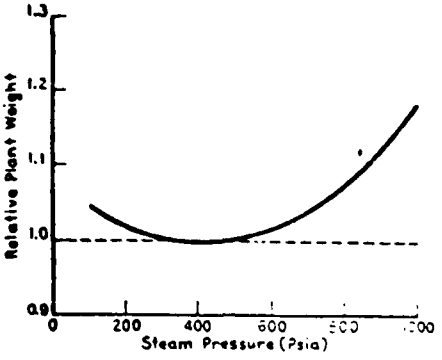

Figure 4-1a

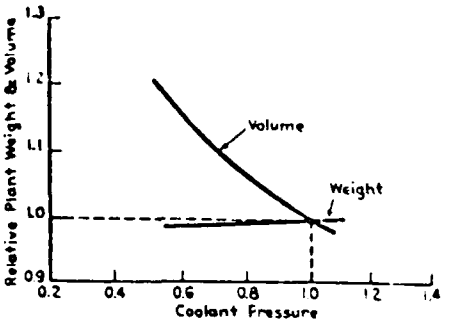

Figure 4-1b

Figure 4-1 (a) Effect of Steam Pressure on Nuclear Propulsion Plant Weight
(b) Effect of Primary Coolant Pressure on Reactor plant Weight and Volume.
(taken from ref. 27)

The design of the PWR plant has been modified several times since the early days of the U.S.S. Nautilus. Starting with U.S.S Los Angeles (SSN-688), the S5W plant was replaced by the larger S6G. An even larger S8G plant was installed on the Trident SSBN.

Regardless of power rating and specifications, the basics of the PWR were preserved in all designs. Whilst details of these reactors have not been released, information is available concerning the land-based power reactor at Shippingport (U.S), which was developed directly from the early submarine reactors.[23] More information on marine plants is available in many publi-

cations concerning the N.S. Savannah[24] and the N.S. OTTO HAHN.[25]

The first reactor core in the Shippingport plant was rated at 231 MW thermal which is approximately double the requirement for a fast attack submarine reactor plant. Reducing the number of primary loops from four to two gives a better model for submarine applications.

The principal elements of the reactor plant are the reactor vessel, containing a nuclear core, and two main coolant loops which circulate the cooling water between the core and the steam generators. A section of the Shippingport reactor is shown in Figure 4-2. The active part of the core is about 1.82 m high and 2 m in diameter and the core is of a "seed and blanket" design. Highly enriched uranium, which forms the seed, is in 1914 zirconium-clad plates. The "blanket" contains the natural uranium oxide enclosed in zirconium tubes.

In the seed, the fuel is an alloy of zirconium and highly enriched (93%) uranium. This alloy is roll bonded with Zircaloy 2 and its final form is produced as plates 1.83 m long, 63 mm wide, 1.8 mm thick. These fuel plates are welded together in groups of 15 to form a sub-assembly. Four sub-assemblies are welded together to form a fuel cell. A cruciform space is left at the center of each fuel cell, in which a control rod operates. The maximum fuel alloy temperature is 400 C and the average temperature is 300 C.

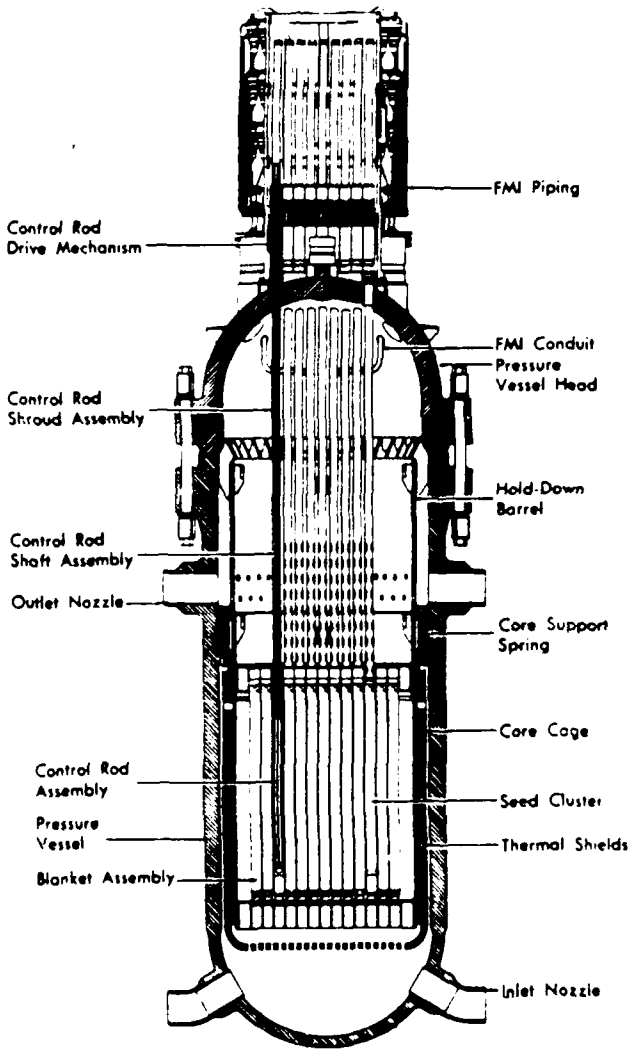

Figure 4-2 Shippingport Pressurized-Water Reactor
(by courtesy U.S. Atomic Energy Commission)
(taken from ref. 23)

The average temperature of the reactor coolant is 273 C. Coolant is circulated through the primary system by the main coolant pumps. The pressure is 13.8 MPa and it is regulated by the pressurizer in the primary loop.

Since the coolant water and suspended materials become radioactive in passing through the reactor core, radiation shielding is required around the portion of the plant which contains the radioactive coolant in order to protect personnel. A separate reactor shield surrounds the pressure vessel; this shield attenuates the direct radiation to allow for reactor compartment entry during shut-down conditions.

The steam produced in the steam generator is used to produce work by expanding across blades in a steam turbine. The steam system, excluding the steam generators, is outside the reactor compartment and this secondary system is nonradioactive. A typical layout of a PWR plant and a secondary system, adopted for submarine propulsion plant, is shown in Figure 4-3.

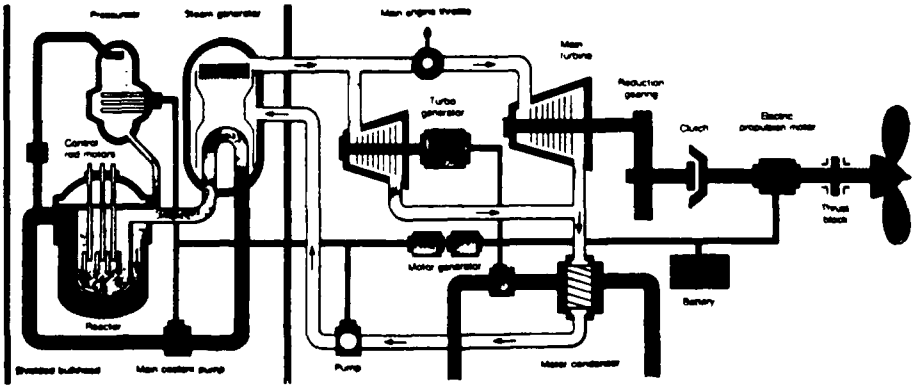

Figure 4-3 Pressurized-Water Nuclear Propulsion System Layout (taken from ref. 15)

The N.S. Savannah reactor plant is very similar. The fuel is U-235 with the enrichment varying from 4.20% in the inner fuel elements to 4.60% in the outer elements in order to flatten the radial power density. The fuel elements (5,248) are assembled in rectangular arrays of 32. The assemblies are contained in a circular cylinder 1.57 m in diameter and 1.68 m high. The pumping power is reduced by a multi-pass flow path through the core. The plant was rated at 70 MW thermal, the primary coolant temperature increases from reactor inlet temperature of 258 C to outlet temperature of 271 C.

The propulsion plant is rated at 25000 SHP. The propulsion machinery is very large and essentially the same as that of a conventional steam-powered ship; hence, it lacks the compactness required for submarine applications. The propulsion system contributes 1,265 tons to the total 4,348 tons power plant weight; the remainder is made up of reactor system (1,665 tons) and shielding (2,418 tons).

The N.S. OTTO HAHN reactor is rated at 38 MW thermal. The propulsion plant is rated at 10000 SHP. The plant is mentioned here because it is a compromise between a pressurized and boiling water reactor as far as the core design is concerned. Unlike the Savannah's design, the location of the steam generators rather high above the core provides sufficient natural circulation of coolant for reactor operation up to 11 MW. The natural convection capability is quite attractive for subma-

rine applications since a very quiet mode of operation is possible.

The nuclear reactor EFDR-80 is an advanced concept related to the reactor of the N.S. OTTO HAHN. The EFDR-80 is an integrated pressurized water reactor with a thermal output of 220 MW. Reactor pressure is at 9.8 MPa, core outlet temperature is 308 C, and the coolant flow rate is 2305 kg/s. The pressure vessel contains core, control rods, primary coolant pumps and steam generator. Pump motors and control rod drives are mounted on the closure head of the pressure vessel. The primary coolant is self-pressurized by means of saturated steam on the free-water surface within the pressure vessel.[28]

Thus with the exception of the primary purification system, all essential components usually in contact with primary water are contained within the pressure vessel. This leads to a particularly safe and compact construction.

The reactor core is a two-zone reshuffling core, consisting of 24 fuel assemblies. The fuel assemblies contain approximately 9 tons of UO_2, with an enrichment of 3.7%. The equivalent core diameter is 1.66 m, and the active height is 1.75 m. Each element has one control rod shaped as a finger absorber using B_4C as absorber material.

The reactor pressure vessel has an inner diameter of 4 m and, without control rod drives, a length of approximately 14 m.

The steam generator is of the once-through type. The steam flow rate amounts 114 kg/s, with steam conditions of 4.4 MPa and 282 C.

The Los Angeles class submarine is capable of speeds in excess of 30 knots plus based on 35,000 shaft horse power.[26] Since the ship's total displacement is only 6,080 tons, the weight of the power plant must be significantly less than that in the N.S. Savannah. Higher power density is achievable only if the secondary steam plant is relatively simple and the shielding requirements are satisfied with a more compact innovative design.

4.2 MHD SUBMARINE POWERED BY A PWR REACTOR

The thermal efficiency of the PWR plants range from 20% to 30% depending on the primary average temperature, condenser pressure, and turbine efficiency. Based on the above and estimating total electric load at 4 MW, the Los Angeles class submarine must be powered by a PWR rated from 76 MW to 113 MW.

An equivalent, but slower, MHD submarine can be constructed with virtually no impact on the present reactor plant. Required modifications involve secondary plant, auxiliary plant, and propulsion train components.

The entire propulsion train from the main turbine to the propeller is eliminated. This necessitates a different design for the emergency electrical propulsion motor. Eliminating the main reduction gear, shaft, and bearings frees significant volume inside the hull and reduces the total weight of machinery equipment by approximately 265 tons. The main steam turbines can be replaced by smaller units since the astern stages are no longer needed due to MHD thrust reversal capabilities.

The electrical power for MHD thrusters comes from electrical generators coupled directly to the main propulsion turbines. Each generator consists of a 15-phase, round rotor, oil cooled synchronous alternator with an integral rectifier.

To demonstrate the full range of MHD propulsive capabilities, the ability to operate in split, half

power, astern, and combined modes is essential. This is achieved by connecting port and starboard electrical systems by a complex switching network. Large safety breakers are not needed in this design; should faults occur in the propulsion circuitry, alternator field excitation is reduced. The summary of electrical component characteristics for a possible MHD thruster design is provided in Table 4-1.

Table 4-1 Electrical Component Characteristics for MHD Propulsion

Generator:	14.9 MW, 298 V, 50 kA, 3600 rpm.
Alternator:	Synchronous, 15-phase, round rotor, oil cooled.
	1.91 m long, 1.32 m diameter, 5.56 tons
Rectifier:	1.70 m long, 0.94 m diameter, 2.52 tons
Conductor:	Coaxial, copper, 0.26 m diameter,
	1.29 A/m^2, $1.92*10^{-7}$ ohm/m
Switches:	.26 ton each, 0.72 m long, 0.34 m diameter

Further weight and space savings can be achieved by eliminating ship service turbo generators. With a proper transformer network, ship's power can be supplied by the main generators. The ship's power network, based on N.S. Savannah electrical data, requires approximately 2 to 4 MW of electrical power. A conservative approach is to install the main turbines and generators with a 4 MW increased capacity so the ship can operate safely on

reduced power supplied by one side with the other being down for maintenance. Figure 4-4 shows a simple diagram of a MHD propulsion electrical layout.

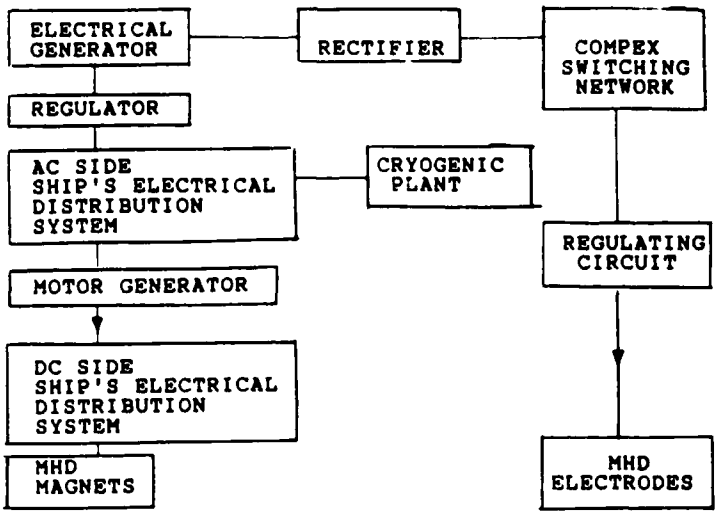

Figure 4-4 Simplified MHD Propulsion Electrical Layout

The electrical connections to the magnets will be discussed later in conjunction with the cryogenic plant. The cryogenic plant power requirements were estimated at 200 kW. The other major electrical load is due to resistive losses in the electrical connections from the generator to the electrodes and magnets. These losses depend on the size, length, and the type of conductor used. Assuming resistive losses and generator losses not varying appreciably from the mechanical losses of the eliminated equipment, the value of SHP for MHD submarine remains at 35,000 HP (26.1 MW).

By examining Figures 3-21 through 3-24 it can be

concluded that MHD propulsion has a lower propulsive coefficient for all four submarine options selected. With a present SSN-688 PWR power and design, a speed of 30 knots is not achievable.

SSNX-1 (baseline with sail and external MHD thruster) is capable of 27 knots top speed. To achieve a speed of 30 knots the PWR thermal power must be increased by about 30 MW. If the external thruster is designed neutrally buoyant about 200 tons can be added to the ship. The power density for a PWR plant is about 120 lb/SHP.[27] Hence, only 10 MW increase within the weight constraint is possible. The resultant maximum speed is 28.5 knots. This is predicated on an assumption that a 33-ft diameter hull is adequate to handle the 10 MW increase in PWR thermal power.

SSNX-2 (same as option 1 but with a retractable sail) is capable of 28 knots top speed. Because the retractable sail takes up significant volume, further increase in PWR thermal power may not be feasible.

SSNX-3 (40-ft beam, retractable sail, internal MHD thruster) is capable of about 27 knots top speed. The PWR power has to be increased by 35 MW to achieve the speed of 30 knots. The Ohio class submarine has a 60,000 SHP PWR plant enclosed in a 42-ft beam[15]; the 40-ft beam is adequate for a 54,800 SHP plant. After adjustment for internal volume for a MHD thruster, the SSNX-3 has an available volume of 59,000 ft^3. Using 3.5 ft^3/SHP from reference (16) allows for a 69 MW increase in reactor

power. Even with the additional reserve buoyancy margin added on, the SSNX-3 is capable of achieving 30+ knots if the thermal power of the installed PWR is about 140 MW.

SSNX-4 (baseline with sail and internal MHD thruster) is capable of 29 knots top speed. This ship is volume limited and will require a significant engineering effort to minimize the impact of reduced internal volume on mission capabilities. Further increase in PWR power to achieve 30 knot maximum speed is not feasible.

Table 4-2 Performance Summary of MHD Submarine Powered be PWR and Steam Turbine (35,000 SHP)

	SSN-688	SSNX-1	SSNX-2	SSNX-3	SSNX-4
Top Speed (kts)	32.0	27.0	28.0	27.0	29.0
Reactor Power (MW)	-	100	100	100	100
Maximum Reactor Power Installed (MW)*		110	100	140	100
Maximum Speed (kts)**		28.5	28.0	30.0	29.0

* Maximum installed reactor power based on the ship's displacement or volume constraint

** Speed that corresponds to the maximum installed reactor power

4.3 A COMPARISON OF ADVANCED REACTOR POTENTIALS

A comprehensive survey was conducted of current reactor concepts to assess some of the more advanced versions. None of the reactors considered in this survey was designed for submarine use; the purpose was not intended to find reactor concepts directly transferable to submarines, but to identify the desirable features of each concept for future submarine applications.

The LMFBR is characterized by liquid sodium coolant with good heat transfer properties and a fast neutron spectrum. The sodium necessitates the use of an intermediate cooling loop to prevent sodium-steam reaction, although the future LMFBR's may use a double-walled heat exchanger instead. The oxides fuels will probably be replaced by either metal fuels (Pu-U alloy or U metal), nitride or carbide fuels in the near future.

The HTGR is a helium cooled thermal converter reactor. The fuel can be U-235, U-233, or plutonium. The fuel is in the form of microspheres which are coated, bonded, and pressed into particles which are placed in a graphite block. Similarly prepared thorium oxide is converted in the reactor to U-233. This reactor can be coupled to a steam cycle, a direct-cycle gas turbine, or a MHD generator.

The GCFR is a helium-cooled high-gain breeder reactor. It has a larger fissile inventory but a higher breeding ratio than LMFBR. The fuel is similar to an

LMFBR but the remaining components are similar to those of an HTGR. Thorium or U-238 breed U-233 or Pu-239 which could be recycled in either thermal or fast reactors.

The MSBR is a fluid fueled reactor. The fluoride fuel salt flows through the system and also serves as a primary coolant. Moderation is provided by graphite slabs. This reactor has special corrosion problems and an extremely high radiation field for which appropriate techniques must be developed.

The LWBR is basically a PWR with a special core. The fuel is U-233 and thorium oxides. Reactivity is controlled by moving fuel assemblies.

A HWR such as a CANDU reactor is both heavy-water moderated and heavy-water cooled. Natural uranium oxide can be used. This reactor uses fuel bundles containing UO_2 pellets in Zircaloy tubes. The fuel and coolant pass through horizontal pressure tubes. A disadvantage is that more tritium is produced than in a LWR because of the use of D_2O as a coolant.

A comparative survey was limited to three major areas.[28] The first area covers the rating of reactor systems with respect to fuel cycle components. The LMFBR and CANDU stand out as significantly more economical than other competitors.

The second area considers the environmental impact of the advanced reactor systems. The major conclusion is that the LWR is generally the least environmentally attractive technology even though it is clearly capable

of satisfying current regulations. The ranking of HTGR would increase appreciably with use of a heavier thorium loading. Development of the gas-turbine or MHD generator in conjunction with closed-cycle dry cooling would reduce water consumption and thermal discharge to water by roughly an order of magnitude. In these categories the HTGR would then clearly be superior to the other systems.

The concern for the reactor safety is the final area of interest. The criteria for grading the alternative advanced reactor systems all relate to the potential for major release of radioactive materials to the environment. The MSBR and HTGR show a distinct advantage in this category.[28]

Functionally the advanced fission reactor systems can offer improvements compared to LWR. Cost, safety, and environmental considerations, while different for each of the advanced concepts, suggest possible development strategies for the future. The base program includes the development of the LMFBR, and HTGR to accompany the LWR.

4.4 SPECIAL CONSIDERATIONS FOR NAVAL REACTORS

Requirements for naval reactors differ from those of both commercial ships and those of land-based plants. Propulsion plants for naval nuclear submarine differ from those for commercial ships in at least two important areas: (1) they must be designed and built to operate reliably and safely under conditions of combat shock; (2) they must be able to continue producing power following a partial casualty since loss of power in an engagement could rapidly lead to loss of the ship.

In contrast to nuclear land-based plants, the ship and its power plant are exposed to additional accelerations and inclinations induced by sea motions and ship maneuvers. The design values for additional accelerations are in the range of 1 g, and for inclinations up to 45 degrees. The shock requirements are even more stringent and have to be applied to the reactor and all safety related components. Extreme climactic conditions have also to be taken into consideration.

The heave and pitch motions are minimum near the geometrical center of the parallel middle body of the submarine. Maximum hull diameter and minimum acceleration levels dictate the exact location of the reactor compartment.

Additional provisions have to be made for ship accidents, such as collision, grounding, capsizing, sinking, and fire. A special collision barrier and grounding pro-

tection structure in the reactor area protects the reactor against mechanical damages due to collisions and grounding (up to design levels).

Sufficient ship stability under all loading conditions has to be provided. In spite of all safety measures, sinking of a vessel can not, of course, be absolutely excluded. Therefore, flood openings in the safety enclosure are provided to avoid collapse and breech of the reactor due to outer sea pressure. The integrity of the enclosure must be maintained even after sinking.

Contrary to a nuclear land-based power plant, specific conditions aboard ship for the installation and operation of a nuclear propulsion plant have to be considered. Each ship is exposed to vibrations excited by sea motion, oscillating propeller forces and auxiliary machinery. The excitation frequencies range from below 1 Hz up to 80 Hz. Conversion to MHD propulsion should eliminate the major source of these vibrations; some provisions to protect the nuclear equipment are still required.

The submarine structure cannot be assumed as perfectly rigid. Due to the movement of the vessel in heavy seas, and different loading conditions, the whole ship structure deforms. These deformations can be significant during rapid depth excursions resulting in compression or expansion of the cylindrical hull. This causes interactions between the ship and the reactor plant. The interactions place significant limitations on the

arrangement of the reactor compartment. Minimizing rigid piping connections favors an integrated modular unit which is not rigidly mounted to the hull. What may be the ultimate challenge in designing a submarine reactor plant is the limited space aboard ship which requires a compact reactor design. The localized heavy weight of the reactor requires special attention to the ship's longitudinal strength, trim and stability.

When at sea, a submarine operates in isolation and the propulsion plant must be maintained by the ship's force. Therefore, a sufficient number of redundant auxiliary and emergency systems are required for energy supply (in a case of equipment failure or ship accident). It is expected that the reactor subsystem power density (lb/SHP) of an equivalent reactor plant converted for marine applications will be larger than the power density for its land-based counterpart.

Due to maneuvering requirements, a rapid change of the load factor is necessary for ship reactors. Crash stop maneuvers are possible with changing rates up to 4% of full power per second.

Due to space limitations inside the hull, the secondary shield has to be more compact and more effective per unit of thickness. Ideally, ship tanks filled with fuel and compensated with water can be utilized to form a secondary shielding boundary.

4.5 SELECTION OF ADVANCED REACTOR PLANT FOR AN MHD SUBMARINE

The cost, the safety and the environmental impact are important attributes in selecting the most suitable reactor plant for an MHD submarine. However, the above survey used no ranking items to express the ability of the various reactors to be used as a power source for naval applications. The purpose of this section is to establish the potential of the various reactor concepts to provide higher outlet temperature.

The first goal of this section is to assess each type reactor system for its potential as a submarine power source in terms of the three important factors: weight power density, volume power density, and outlet temperature, and to select the best combination of the various concepts.

The second goal of this section is to compare the relative merit of the coolant materials for removing energy from the reactor core. Because of high reactor outlet temperatures, water and many organic compound coolants were not considered due to low saturation temperature and chemical instability.

In order to establish the basis for comparison of weight and volume power density, several plants were examined (ref. 29). This study was conducted in 1971, hence it was based on an outdated reactor technology. It is assumed here that the core power density of a similar

and newer designs has not changed significantly from the values reported in Table 4-3. To see the relative merits of the reactor concepts, two PWR were also included in Table 4-3.[29] In order to estimate the ratio of reactor weight to SHP, the same shielding configuration was used in all reactor concepts, i.e., 4-in (0.1 m) thickness of lead and 6-ft (1.83 m) thickness of B_4C.

Table 4-3 Assessment of Reactor Technology

(taken from ref. 29)

Reactor	Type	Power (MWT)	Coolant			Fuel			
			Type	T_{in}/T_{out} (°F)	Pressure (psia)	Compos.	Enrich. (Wt%)	Burn Up (MWD/Ton)	In. Loading (lb-U^{235})
SRE-1	Therm.	20	Na	500/950	55	Metal	2.30	2,500	183
HNPF	Therm.	250	Na	670/945	55	UO_2-U^{235}	3.50	11,300	1500
EBR-II*	Fast	62.5	Na	700/900	80	Metal	49	24,000	798
Fermi	Fast	265	Na	550/800	100	Metal	28	6,000	1067
1000 MWe	Fast	2,465	Na	797/1095	75	(U-Pu)C	9.8-11.8	100,000	5770
Kaiser-GCPR	Therm.	125	CO_2	463/1000	370	UO_2	3.04	10,000	1051
ORNL-GCPR	Therm.	700	He	450/1000	300	UO_2	2.03	7,350	5339
DRAGON-GCR	Therm.	20	He	662/1380	294	(U-Th)C	15.16		44
SNAP	Inter.	2.17	Li	1640/1740	~100	UN	92.7	25,000	400
MSPR*	Inter.	840	--	1075/1210	83	UF_4+ThF_4	90%$U^{233}F_4$	--	1329
N.S. Savannah	Therm. (PWR)	63.5	H_2O	496/520	1750	UO_2	4.4	7,352	687
CNSG	Therm.	62.4	H_2O	493/517	815	UO_2	4.19	16,000	1300

Reactor	Core Power Density	Net MWe / Gro.MWt	Reactor, Shield†, Containment Vessel		
			Size (ft) Dia./Height	Power Density (lb/SHP)	Weight (ton)
SRE-1	4.16	28.6	23/25	239	870
HNPF	4.09	29.5	34/36	46	2100
EBR-II*	8.90	26.4	18/18	41.4	1416
Fermi	1066	35.5	28.5/42	10.3	1226
1000 MWe	543	40.6	28.5/46	2.95	1800
Kaiser-GCPR	1.187	35.2	30/32	48.5	1300
ORNL-GCPR	1.75	32.1	62 sph.	42.5	5825
DRAGON-GCR	13.90	440	23.5/26	155	736
SNAP	50.15	465	14/8.3	150	92
MSPR*	80	40.6	22/26	6	960
N.S. Savannah	25.5	23.5	35/50	275	2450
CNSG	19.4	24.0	20/38	77	685

*No pressure vessel available.

†Shielding is estimated based on submarine application.

From the three reactor types examined (thermal, intermediate, and fast), thermal reactor has the lowest volume power density (26 kW/L). Fast reactor (200 kW/L) and intermediate reactor (50-200 kW/L) may be considered as better candidates for submarine application.

For naval application, breeding is not a major concern. However, the same technology is applicable to the design of non-breeding compact reactors. If the bulky blanket were eliminated from the fast breeder reactor and replaced by a reflector/shield, the core size and weight can be reduced.[29]

The liquid metal cooled (Na, Li), gas cooled (He, CO_2), and molten salt reactor concepts can achieve outlet temperatures in excess of 1000 F (537 C). Since the thermal efficiency increases with high outlet temperatures, these reactor concepts are an obvious choice.

The MSPR is the only fluid fueled reactor in Table 4-3. The weight reported for MSPR does not include additional shielding for the heat exchanger and the fission product removal systems. This reactor would be a good choice if the power requirement was higher than 400 MW. At lower power levels sodium cooled solid fuel reactor is superior.[29]

Gases have relatively poor heat transport characteristics, but allow for higher coolant temperatures. The combination of graphite as moderator with gaseous coolant results in attractive neutron characteristics. Two examples of such combination are Kaiser-GCPR which is

cooled by CO_2 and ORNL-GCPR which is cooled by helium. These reactors are considered thermal and operate at lower temperatures. Employing several advanced fuel element concepts (fuel slug, fuel capsule, or fuel particle) and coating materials (BISO and TRISO), the maximum fuel design temperature can reach about 1400 C (3000 R) with average coolant outlet temperatures around 840 C (2000 R).[29]

At present, most gas cooled reactor concepts still suffer from low volume power density (kW/L) and relatively modest temperature. On the other hand, gas has no phase changes, has smooth changes in characteristics with temperature, stability, and compatibility with structural materials. If the high temperature obstacle is overcome, gas cooled reactor is a good candidate for future submarine use.

With its excellent heat transfer properties and compatibility with structure materials, sodium cooled (need to increase system pressure to about 2.1 MPa) and lithium cooled (slightly above atmosphere pressure) reactors can be easily operated at 840 C.[29]

The compactness and mature technologies for the liquid cooled reactor plant makes it an outstanding candidate for submarine use. For instance, the thermal reactor (SRE) with less than 3% enrichment is contained in a reactor tank 3.35 m diameter and 5.8 m height. The EBR-II (a pool type concept) with 49% enrichment and the primary heat exchanger and recirculating system all sub-

merged in sodium (with helium or argon cover gas) tank, the system occupied a volume of 7.92 m diameter by 7.92 m height. This system, if converted to a loop-type system, can be reduced to 3 m diameter and 5.5 m height.[29]

The SNAP-10 reactor uses high enrichment solid fuel and liquid metal as coolant. It was developed for space applications. If slight modifications are made in the core design and proper shielding is added it has a potential for submarine use.

From the above discussion, both liquid metal and gas cooled reactor technologies offer considerable potential as energy sources in future MHD submarine. The sodium cooled reactor is a first choice due to higher efficiency. However, if direct coupling is feasible (e.g., gas turbine or MHD generator, then both reactors provide equal potential for use.

The feasibility of direct coupling was demonstrated by Westinghouse in their 1972 study of a ship powered by a lightweight nuclear propulsion (LWNP) system.[30 31] Key assumptions used in this study included a ship displacement of 2,000 tons, a maximum mission duration of 6 months, a power plant design lifetime of 10,000 EFPH, and a power plant specific weight less than 15 lb/SHP at 140,000 HP (104 MW). Design included compliance with federal regulations on radiological safety and containment integrity following a 30-knot collision.

The shielding design for a liquid metal or a gas cooled reactor will be approximately the same since it

is based on a typical reactor core neutron spectrum. The core neutron flux was computed on a two-group (below 1.35 Mev and above 1.35 Mev) approximation.[29] For a 100 MW core first group was $1.61*10^{14}$, and the second group was $5.86*10^{14}$ for a total flux of $7.47*10^{14}$. For a 200 MW core the total neutron flux increased to $9.62*10^{14}$. A typical diagrammatic representation of pressure vessel and shielding is shown in Figure 4-5. Different combinations of shielding materials are possible to reduce secondary emission to 0.5 MR/hr. For a most compact shield about 0.1 m thick lead for high energy gamma radiation, and 1.8 m thick B_4C for thermal neutron absorption was selected.

SHIELD MATERIALS, DIMENSION, AND WEIGHT
FOR 100 MWt HE COOLED REACTOR

	Pb - B_4C	Pb - L B	Pb - B_2O	Pb - B - C	Concrete -B
Y-shield thickness (cm)	9	30	25	17	--
Neutron shield thickness (cm)	170	180	180	222	193
Total shield weight (Mt)	159	125	135	230	233

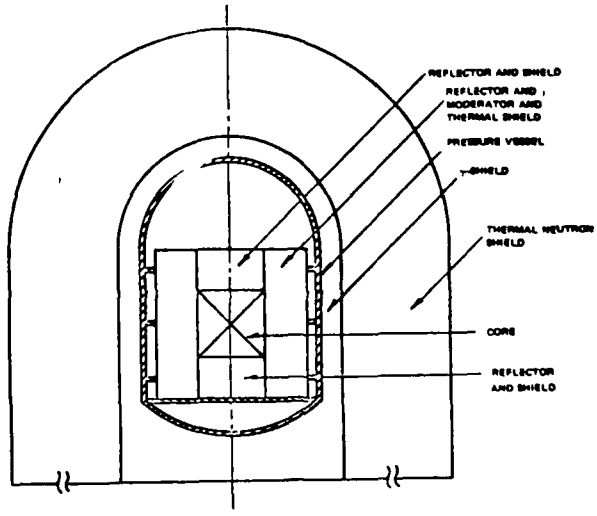

Figure 4-5 Shield for 100 MW Helium Cooled Reactor (taken from ref. 29)

A compact core design configuration is shown in Figure 4-6. The primary shield for thermalizing fast neutrons consists of two layers of BeO which also serve as the thermal shield.

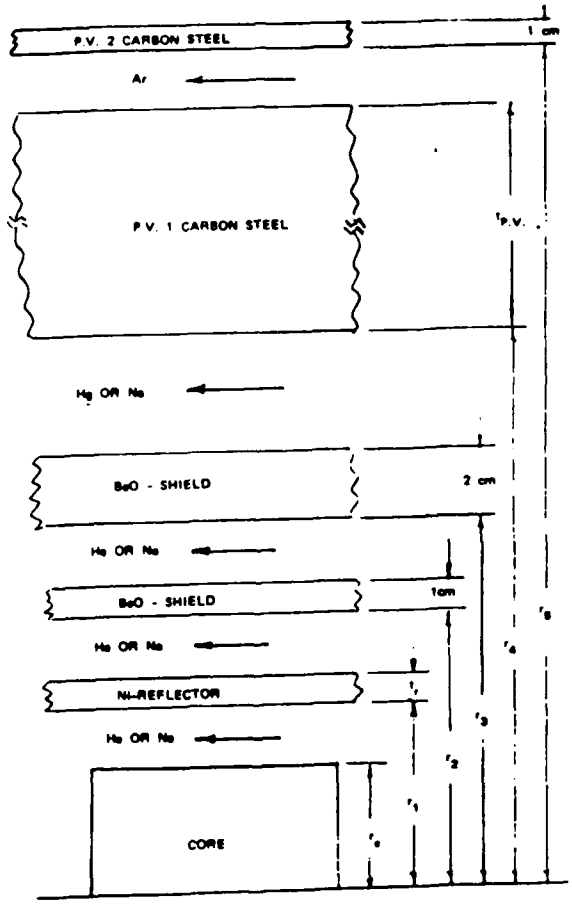

Figure 4-6 Compact Core Design Configuration for HTGR or Liquid Metal Reactor (taken from ref. 29)

4.6 GAS COOLED REACTOR LIGHT WEIGHT PROPULSION SYSTEM

Among gaseous coolants, inert gases are considered the best in terms of material compatibility and temperature limitations. Helium has the best combined heat transfer and heat transport properties.

The fuel material must have a high melting point and good thermal conductivity. This excludes metal fuel, and a ceramic type of fuel, such as UO_2 and UC, should be selected; UC may be the best choice due to its superior conductivity.

The design for the fuel clad may require refractory metals if canning is necessary. However, if canning is not required, ceramic coating of the fuel using carbides of niobium, silicon, tantalum, and titanium may be considered.[29]

A fast or a hard spectrum intermediate reactor at 100 MW to 400 MW with 1094 C coolant mean temperature and cooled by 10.3 MPa helium was examined in reference (29). The reactor core life was assumed to be 18,000 EFPH. The reactor is to be used with either a high temperature gas turbine or a high temperature MHD generator conversion systems. Preliminary data for a helium cooled light weight reactor and reactor subsystem is summarized in Table 4-4. Figure 4-7 is a schematic diagram of two different power conversion systems using a gas turbine or a MHD generator.

Table 4-4a Preliminary Design Data for Helium Cooled Reactor (taken from ref. 29)

	Unit	100 MWt	200 MWt	300 MWt	400 MWt
U^{235}	Vol%	15.337	11.927	10.236	9.264
U^{238}	Vol%	15.963	12,413	10.654	9.642
S. S.	Vol%	17.444	14.920	12.810	10.536
He	Vol%	49.500	60.740	66.300	69.500
Core dia.	cm	70.5	90.5	105.5	118.0
Core height	cm	70.5	90.5	105.5	119.0
Reflector thickness	cm	1.50	2.55	3.25	3.00
Primary shield thick's	cm	5.0	5.0	5.0	5.0
Pressure vessel thick's	cm	12.0	12.0	12.0	12.0
Pressure vessel dia.	cm	121.6	147.6	164.0	176.0
Pressure vessel ht.	cm	232.2	291.7	336.0	368.0
Cont. vessel thick's	cm	1.0	1.0	1.0	1.0
Cont. vessel dia.	cm	123.6	149.6	166.0	178.0
Cont. vessel ht.	cm	236.2	293.7	336.0	370.0
Reactor core wt	ton	4.1	6.9	9.4	11.7
Reactor vessel wt.	ton	5.30	8.4	11.0	13.2
Total reactor wt.	ton	10.1	17.0	23.0	28.0
Core power dens.	MW/ℓ	0.363	0.344	0.325	0.310

Table 4-4b He Cooled Reactor Subsystem Power Density (taken from ref. 29)

		100 MWt	200 MWt	300 MWt	400 MWt
Y-shield (Pb)		6.6	9.4	11.4	13.0
Neutron shield (B_4C)	1	295.3	343.6	377.0	403.5
	2	262.6	287.9	338.6	354.9
	3	190.9	233.3	262.2	284.5
Reactor		10.1	17.0	23.0	28.0
Control and safety system		2.1	3.5	4.7	5.8
Piping system	--	30.0	42.0	52.0	60.0
Misc wt.	--	20.0	28.0	35.0	40.0
Total reactor subsystem	1	364.1	443.5	503.1	550.3
	2	311.4	387.8	464 7	501.7
	3	259.7	333.2	388.3	431.3
Net output power in HP (η=0.42)		56,300	112,600	168,900	225,200
Power density lb/HP	1	14.2	8.7	6.6	5.6
	2	12.2	7.6	6.1	4.9
	3	10.1	6.5	5.1	4.2

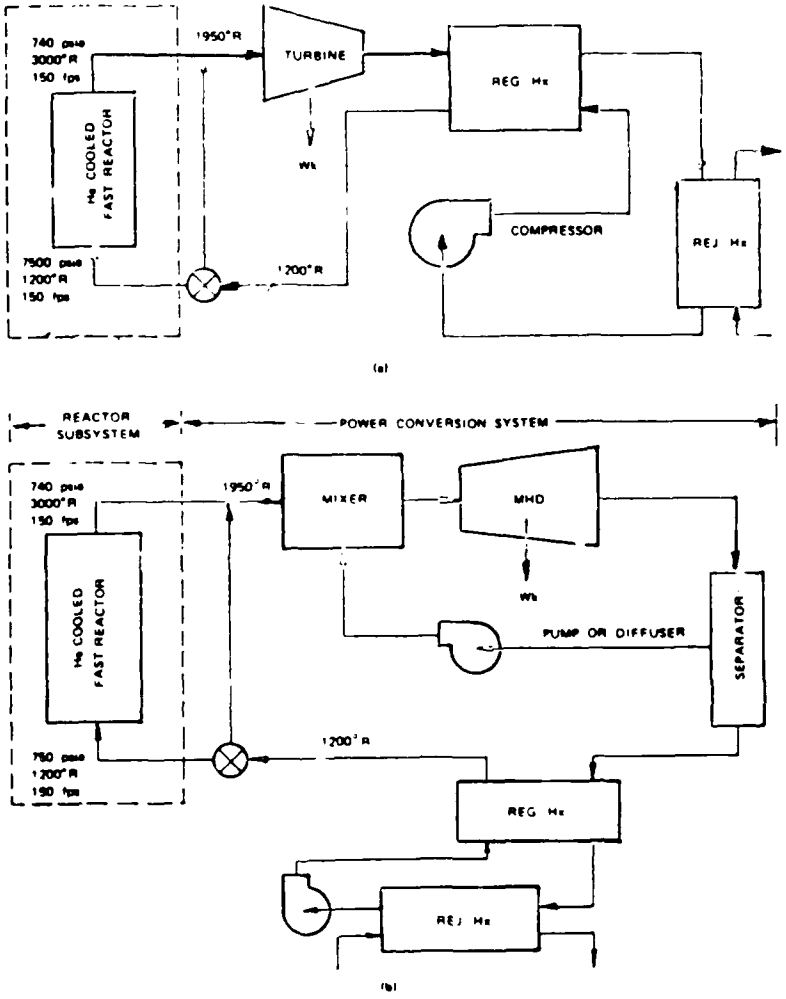

Figure 4-7 Schematic Diagram of Typical Helium Cooled Reactor Coupled with (a) Gas (He) Turbine (b) Liquid Metal MHD Generator (taken from ref. 29)

In a previously mentioned Westinghouse feasibility study, following appropriate trade-off studies, a Nuclear Engine for Rocket Vehicle Application NERVA-type

reactor and a closed-cycle helium gas-turbine power conversion system were selected for this application.[30] Superconducting motors and generators are chosen to permit transfer of large blocks of power throughout the ship.

Reactor outlet conditions of 927 C and 10.3 MPa are selected after consideration of cycle and materials requirements and technology. The nuclear reactor (rated at 104 MWt), along with the two power conversion packages, radiation shielding, and containment, is shown in Figure 4-8. This unit is 9.75 m long, 5.9 m wide, and 10.4 m high. The auxiliaries, not shown in this figure, are estimated to require 331 m^3 additional volume.

The entire primary system is enclosed by a thick-walled containment vessel and consists of two cylinders joined in the form of an inverted "T". The 50 mm thick vertical cylinder immediately surrounds the reactor assembly, while the lower 152 mm thick cylinder surrounds the turbomachinery, emergency cooling system, control gas storage bottles, and power conversion equipment.

The number of external connections is minimized and includes means for positive sealing to ensure protection against release of fission products in the event of an accident.

Like NERVA, the reactor consists of a gas-cooled, graphite moderated, epithermal core with coated fuel particles dispersed in graphite elements; it has a lat-

eral support system to maintain core bundling and beryllium radial reflector with control drums. The operating temperature required TRISO-design fuel particles. This feature enhances retention of fission products within the fuel particle itself and substantially increases the overall safety of the system.

The specific weight of the power plant including all auxiliaries is less than 12 lb/SHP. The study reveals that the plant could also be designed with an arrangement whereby the turbomachinery and heat exchangers would be separated and more accessible, but with significant weight and size penalties.

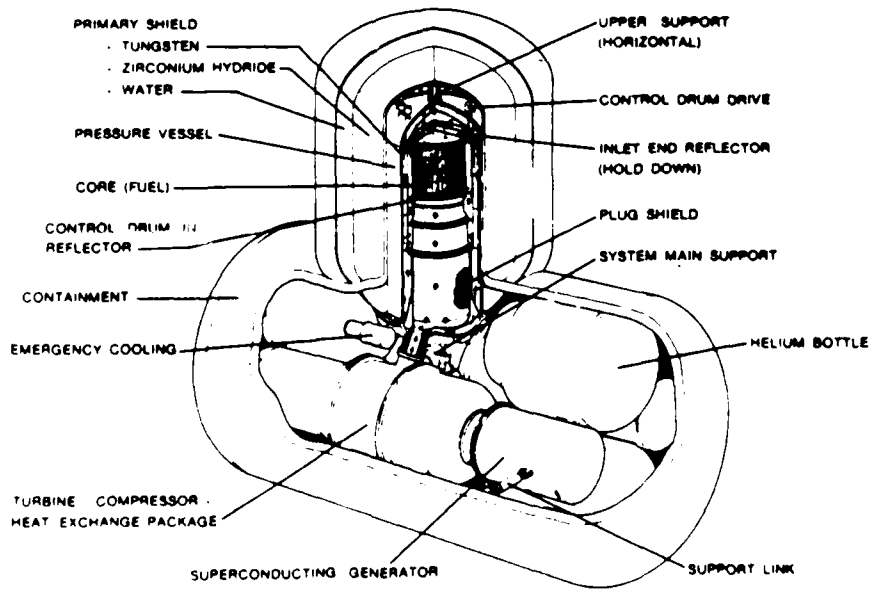

Figure 4-8 Layout of LWNP Power Plant

(taken from ref. 30)

The development of the LWNP conceptual design indicated that a lightweight nuclear propulsion power plant with direct coupling was feasible and could be developed with minimal risk and reasonable R&D costs.

A concept similar to the Westinghouse's is being developed by the MIT Nuclear Engineering Department. This design eliminates essentially all piping connections by enclosing the core in several cylindrical shells. The space between the cylindrical shells provides for a helium path to and from the power conversion systems. Elimination of piping connections results in an arrangement which has a superior shock resistance. The results of this study are soon to be published by Richard D. Lantz.

With a gas turbine coupled to a superconducting generator, the MHD propulsion electrical system is almost identical to the one described in Section 4.2. The major difference is that a superconducting generator is selected and is enclosed in the containment vessel. The electrical output of the generator can be connected to the AC side of the ship's electrical system, but the majority of the electrical power is rectified and connected to the voltage regulating system in the switching circuit for the MHD propulsion.

With a MHD generator in the power conversion system, DC electrical power is generated. Therefore, rectification is not required. The power required for the ship's electrical distribution system can be connected to the

DC side of the power distribution system with its own voltage regulator. The size of the motor generators depend on the electrical load distribution of the ship; a need for some adjustments in the present design are anticipated.

Based on the preliminary calculations, the thermal efficiency of the power plant is 42%. Assuming that this value is correct and allowing 4 MWe for ship's power and electrical losses, 38 MW is available for the MHD propulsion with a 100 MW reactor. Using this system, all four variant submarines from Section 3.3 are capable of 30+ knots top speed, with SSNX-4 being the fastest.

Table 4-5 MHD Submarine Powered by HTGR Performance Summary

	SSNX-1	SSNX-2	SSNX-3	SSNX-4
Reactor Power (MWt)	100	100	100	100
Top Speed (knots)	30.5	30.8	30.3	31.3

4.7 LIQUID METAL COOLED REACTOR LIGHT WEIGHT PROPULSION SYSTEM

Liquid metals are better heat transfer media than gases or water and can be used at high temperatures, while their good thermal conductivity maintains an even fuel temperature. Liquid sodium has desirable physical properties by having a low melting temperature (98 C) and boiling temperature (883 C) that is much higher than for water. A low melting point eutectic of sodium and potassium (-11 to 19 C depending on sodium concentration) has been preferred for cooling purposes.

Some special problems arise with the use of liquid metals; if any of the structural materials are soluble in liquid metal, it is found that it tends to precipitate out in the cold parts. This process, known as mass transfer can cause failure in a hot region and blockages in cold parts. Stainless steel, zirconium, niobium and vanadium are satisfactory in this respect for use with sodium. Of these, niobium and vanadium must be used for canning materials at operating temperatures above 550 C.

Any measurable level of oxygen in sodium reacts with stainless steel and zirconium at high temperatures; special precautions must be taken to keep the oxygen level to less than 5 p.p.m.

Induced radioactivity in sodium is rather high and relatively long-lived. This may preclude direct coupling to a MHD generator and may require an intermediate heat

exchanger to confine the primary coolant in a small area.

The compactness and high power density of the core (5 to 10 times that of LWR) implies that imbalances between heat production and heat removal can lead to rapid changes in core temperature. Indeed it is the protection against mismatches between power and flow, and the analysis of their consequences, which form the central issues in fast reactor safety. Therefore, the LMFBR design generally includes two independent, diverse, and functionally redundant reactor shutdown systems to insure that off-normal conditions requiring scram are reliably terminated. The safety features and accident analysis of LMFBR are covered in reference (32).

The light weight reactor design for a MHD submarine should be similar in most respects to a commercial or an experimental LMFBR but with the necessary modifications to account for a much higher outlet temperature than in any state of the art design.

The higher temperature in the LMFBR require that creep rupture effects and thermal fatigue be considered in the design. Thermal transients are severe both in terms of total temperature and the rate of temperature change. One example of the use of high temperature design technology in the Clinch River Project is in the design of the upper internals structure located immediately above the core. 138 to 167 C temperature differences at the fuel blanket and fuel control interface

subject the upper internal structure to severe thermal stripping. A mixing chamber was developed to protect the downstream components from thermal fatigue.[33]

Four LMFBR designs will be discussed briefly. The light weight LMFBR plant for a MHD propulsion will probably be a hybrid of those four designs. The first one is JOYO because it is designed for 100 MW power capacity and it is a two-loop design. Second one is EBR-II because, through painful experience, it has been optimized to handle frequent power transients as would be expected in submarine operations. Third one is FFTF because of higher operating temperature. The final design is PRISM because it utilizes reactor modular construction and its core can easily adapt to a higher temperature fuel.

JOYO (Japan) is a sodium cooled fast breeder reactor fueled with mixed oxide of plutonium and uranium. The reactor is loop type and has two identical cooling circuits, each having a heat removal capacity of 50 MW. Each circuit consists of a primary loop, intermediate heat exchanger and secondary loop.[34] JOYO's cooling system layout, shown in Figure 4-9, may be ideal for submarine applications. Both in the primary and secondary loop the coolant flow rate is 306 kg/sec. All the piping and equipment circuits in the primary loop are double-walled so any leakage will be retained in the space in between.

The four main pumps, all in the cold leg of the

cooling circuit, are of a mechanical type and use hydrostatic bearings of sodium. The intermediate heat exchanger is of the shell and tube type, with a free surface of sodium. The pressure on the secondary side is higher to prevent radioactive contamination of the secondary loop in the event of leakage across the heat exchanger. All the pumps used in a secondary system are of a electromagnetic type. With an energy conversion system substituting for the air blast cooler, this plant can power an MHD submarine.

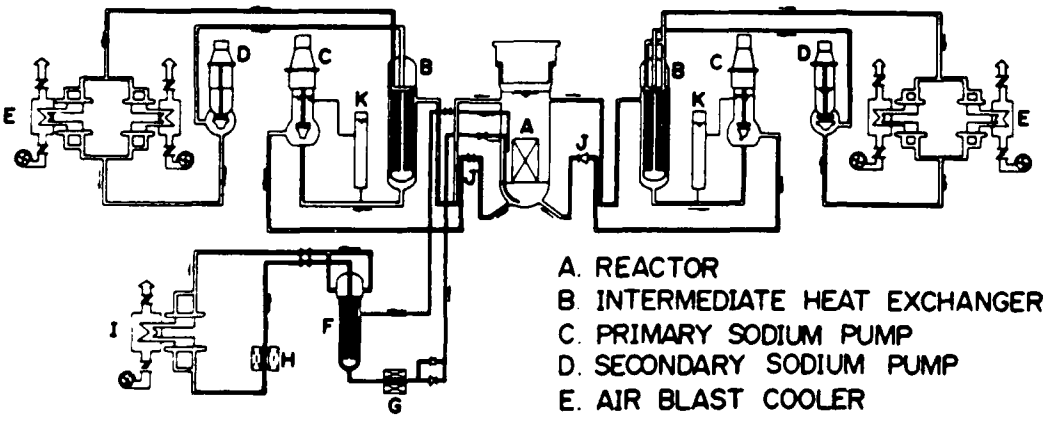

Figure 4-9 JOYO Reactor Cooling System Diagram

(taken from ref. 34)

Many of the problems experienced in EBR-II design have been attributed to the large number of temperature cycles due to changing power levels. The number of start-ups, shutdowns, and scrams of the reactor definitely affects the failure rate in the power plant. Therefore, this design has been modified to handle frequent power cycling. This capability is certainly required in a submarine reactor plant. A similar design may have been employed on U.S.S. Seawolf since the reactor plant of EBR-II is coupled to a conventional steam plant.

The design of EBR-II is, in principle, very similar to JOYO. The primary system uses two centrifugal pumps which operate in parallel to supply 0.57 m^3/sec of 371 C sodium at 0.42 MPa to the reactor core.

The reactor is designed for 62.5 MW thermal power with the reactor outlet temperature of 473 C. The EBR-II driver fuel element comprises a U-235 fissium metallic fuel pin, sodium-bonded to stainless steel cladding. Similar elements, but with a shorter fuel pin, are used for control-rod and safety-rod subassemblies. All primary equipment, including the intermediate heat exchanger, is enclosed in a reactor vessel, Figure 4-10.

The Fast Flux Test Facility (FFTF) is a primary test facility for LMFBR fuel and materials. The unique test capabilities of the FTFF permit testing fast breeder fuels and materials with core component sizes, temperatures, neutron fluxes and sodium environment prototypic of LMFBR's. The knowledge that is gained can be directly

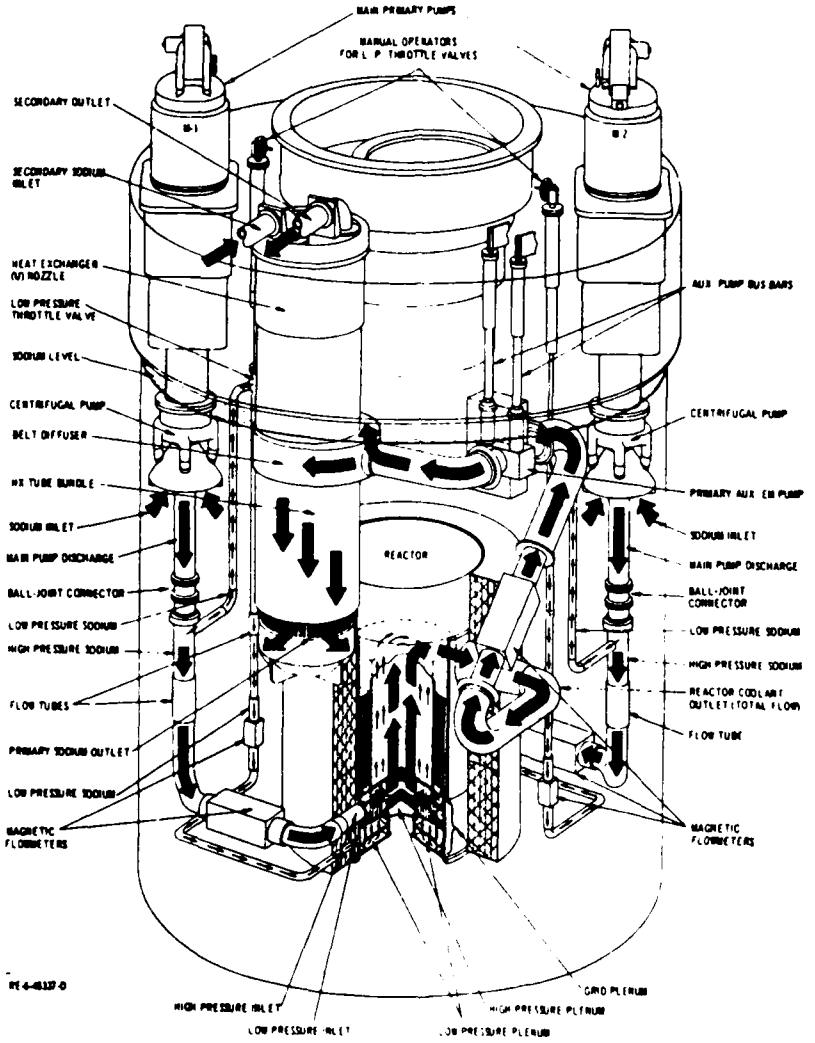

Figure 4-10 EBR II Primary Tank

(taken from ref. 53)

applied to the construction of a light weight LMFBR with outlet temperatures of 830 C which is not very far from the present temperature limit of 660 C.[53]

Since FFTF is a test reactor, there is no requirement for a radial breeder blanket of UO_2 fueled assemblies surrounding the mixed oxide fuel region of the core. The same approach can be taken for a submarine design resulting in space and weight savings.

An FFTF driver fuel assembly is 3.66 m long and consists of 217 fuel pins mounted as a fuel pin bundle contained within a hexagonal duct tube. The fuel pins are arranged on a triangular pitch with a pitch-to-diameter ratio of 1.24. Figure 4-11 shows a FFTF driver fuel pin

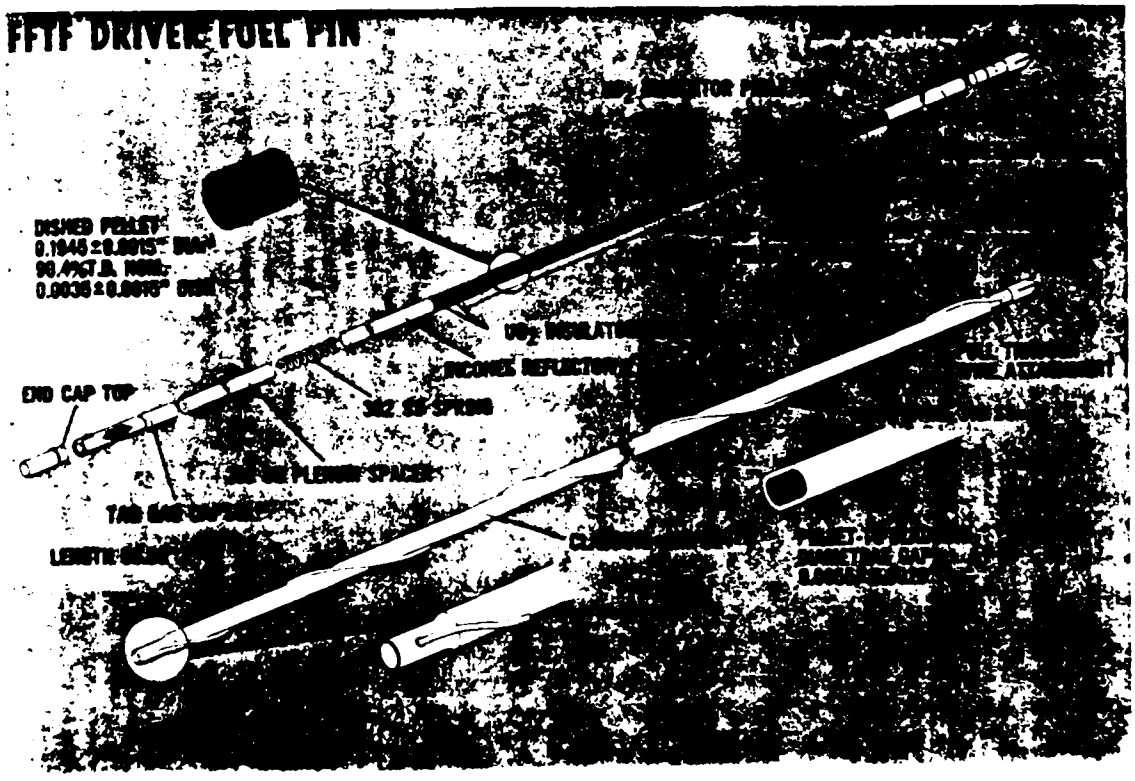

Figure 4-11 FFTF Driver Fuel Pin

(taken from ref. 53)

The Power Reactor Inherently Safe Module (PRISM) is an innovative advanced reactor design program headed by General Electric with other major nuclear industry participation. The paramount objective of the PRISM design concept is the simultaneous achievement of favorable safety and economics. PRISM is inherently stable under abnormal events, such as loss of cooling and even failure of the scram function. This allows for the deletion of the numerous conventional auxiliary and engineering safety systems.[35]

The small module makes it relatively simple to place the whole nuclear reactor primary system on a flexible foundation to achieve good shock protection and easy integration with hull movement.

The module is rated at 155 MWt and weighs about 800 tons. The height is 18.3 m but could be re-designed to fit a submarine hull. Primary sodium is circulated through the core and the shell side of the intermediate heat exchanger by electromagnetic pumps. This design uses an intermediate sodium loop connected to a steam generating plant; however it could be easily replaced by a helium cooling loop.

The reference fuel for PRISM is metallic U-Pu-Zr alloy. The ferritic alloy HT9 is used for cladding and fuel channels to minimize the swelling associated with long burnups. Metal fuel is chosen because of the excellent negative reactivity feedback it provides for loss of cooling and transient overpower events. Oxide fuel is

being retained as a backup, pending the outcome of the metal fuel development program. The design allows for a quick fuel change-out with no modification in internal equipment required.

This design operates at lower temperatures (426 C) but it is designed for a 982 C limit for in-core sodium boiling temperature. Figure 4-12 shows PRISM reactor module and PRISM core.

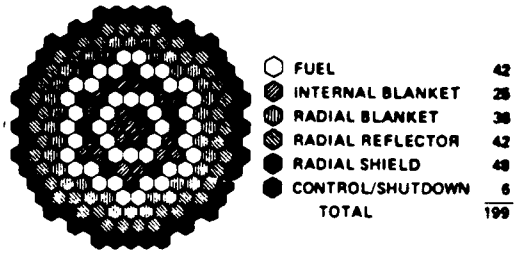

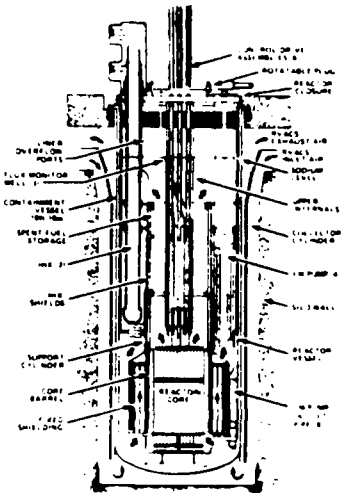

(b) (a)

Figure 4-12 PRISM (a) Reactor Module (b) Core (taken from ref. 35)

In LMFBR the reactor core life and criticality are the major factors affecting the size and weight of the reactor. Because of this, the reactor can be made more compact by increasing fuel loading and enrichment. If further materials development can be made to accommodate higher reactor operating temperatures (830 C), a LMFBR can be made very compact with an energy conversion system such as gas turbine or MHD electrical generator.

A preliminary design of LMFBR with a helium second-

ary loop at 815 C (1,500 F) has been investigated in reference (29). This design is based on a homogenized one-group model that, for a 100 MW reactor, the vessel size was estimated at 0.91 m diameter by 1.98 m height. Similar designs are considered for LMFBR up to 400 MW power.

The shielding design for LMFBR was evaluated using the same two-group approximation used in HTGR computations; the outer neutron shield thickness for LMFBR was 150 mm less than for HTGR.

Due to the high activity of Na-24, an intermediate heat exchanger is used to transfer energy from the sodium primary coolant to the helium secondary. The preliminary design data for intermediate heat exchanger for sodium cooled reactor coupled with gas turbine or LM-MHD power conversion system are listed in Tables 4-6a and 4-6b respectively.

Table 4-6a Preliminary Design of U-Type Intermediate HX for Na Cooled Reactor Coupled with a Gas Turbine Energy Conversion System (taken from ref. 29)

	Unit	100 MWt	200 MWt	300 MWt	400 MWt
No. of tubes		1,051	2,102	3,153	4,204
Overall heat transf. coef.	$\frac{BTU}{ft^2 hr\text{-}^\circ F}$	331	331	331	331
Eff. heat transf. area	ft^2	13,224	26,448	39,672	52,896
Eff. tube length	ft	24	24	24	24
Estimated Hx O.D.	ft	4.50	6.33	7.83	9.00
Estimated Hx length	ft	18	18	18	18
Estimated Hx volume	ft^3	262.4	490.7	691.0	276.5
Estimated Hx weight	lb	33,500	52,800	70,000	86,000

Table 4-6b Preliminary Design of Intermediate Heat Exchanger for Na Cooled Reactor with LM-MHD Energy Conversion System (taken from ref. 29)

	Unit	100 MWt		200 MWt		300 MWt		400 MWt	
		Na-Hx	Na-Hx	Na-Hx	Na-Hx	Na-Hx	Na-Hx	Na-Hx	Na-Hx
Tube size O.D.	in -gage	1.0-#16	.75-#16	1.0-#16	.75-#16	1.0-#16	.75-#16	1.0-#16	.75-#16
ℓ - ℓ distance	in.	1.25	1.00	1.25	1.00	1.25	1.00	1.25	1.00
Log.-mean temp.	--	78.0	109.7	78.0	109.7	78.0	109.7	78.0	109.7
No. of tubes	--	509	1,002	1,018	2,005	1,527	3,008	2,035	4,010
Overall heat transf. coef.	$\frac{BTU}{ft^2-hr-°F}$	2,633	331	2,633	331	2,633	331	2,633	331
Eff. heat transfer area	ft^2	1,026	3,610.9	2,048	722.15	3,072	10,832.6	4,096.5	14,443.5
Eff. tube length	ft	8.84	18.34	8.84	18.34	8.84	18.34	8.84	18.34
Estimated Hx O.D.	ft	3.0	3.00	4.00	4.58	4.83	5.58	5.67	6.25
Estimated Hx length	ft	14.84	24.34	14.84	24.34	14.84	24.34	14.84	24.34
Estimated Hx volume	ft^3	106.6	417	186.5	936.7	271.9	623 x 2	376	936.7 x 2
Estimated Hx weight	lb	9,072	40,440	13,934	74,930	17,696	108,600	21,863	136,600

Preliminary design data for sodium cooled reactor and reactor subsystem is listed in Table 4-7. The weights summary includes the added weight of heat exchangers and primary coolant recirculation pump. The net output power for the cycle was adjusted for the additional power required tc operate primary pumps.

Figure 4-13 is a schematic diagram of two system layouts. Direct coupling with an MHD generator (Figure 4-13b) may be achievable with significant weight and space savings. This set-up may develop significant restrictions on generator maintenance due to radiological considerations. The MHD generator would have to be located in the reactor compartment and significant downtime for the reactor plant could result; preventive or corrective maintenance would require reactor plant shut-

Table 4-7a Preliminary Design Data for Na Cooled Reactor (taken from ref. 29)

	Unit	100 MWt	200 MWt	300 MWt	400 MWt
Core dia.	cm	63.5	66.0	69.0	71.5
Core height	cm	63.5	66.0	69.0	71.5
Reflector thickness	cm	1.0	1.0	1.0	1.0
Primary shield thick's	cm	4.0	4.0	4.0	4.0
Pressure vessel thick's	cm	5.0	5.0	5.0	5.0
Pressure vessel dia.	cm	91.5	96.0	97.0	99.5
Pressure vessel ht.	cm	195.6	202.5	210.7	217.6
Cont. vessel thick's	cm	1.0	1.0	1.0	1.0
Cont. vessel dia.	cm	93.5	96.0	99.0	101.5
Cont. vessel ht.	cm	197.6	204.5	212.7	219.6
Reactor core wt.	ton	3.3	3.7	4.3	4.7
Reactor vessel wt.	ton	0.782	0.805	0.843	0.853
Total reactor wt.	ton	4.6	5.1	5.7	6.2
Core power dens.	MW/ℓ	0.497	0.886	1.163	1.393

Table 4-7b Sodium Cooled Reactor Subsystem Performance (taken from ref. 29)

		100 MWt	200 MWt	300 MWt	400 MWt
r-shield (Pb)		6.0	6.3	6.7	7.0
Neutron shield (B_4C) (Mton)	1	207.2	213.1	217.1	222.0
	2	167.9	173.4	177.6	182.0
	3	130.0	136.1	139.0	144.0
Reactor (Mton)		4.6	5.1	5.7	6.2
Control and safety system (Mton)		2.1	3.5	4.7	5.8
Heat exchanger (Mton)		15.2	24.0	31.8	39.1
MHD MHD* (Mton)		22.8	40.4	56.5	72.0	
Reactor pump (Mton)	~	1.0	2.0	3.0	4.0
Piping system (Mton)	~	40.0	56.6	69.1	80.0
MR shield and misc. wt. (Mton)	~	40.0	56.6	69.1	80.0
Total reactor subsystem weight (Mton)	1	316.1 323.7*	365.2 381.6*	407.6 422.2*	444.1 477.0*
	2	278.8 284.4*	327.5 343.9*	368.1 382.8*	404.1 437.0*
	3	238.9 246.5*	288.2 304.6*	329.5 334.2*	366.1 399.0*
Net output power (~40.41) MW		55,000	110,000	164,900	219,800
Power density lb/MW	1	12.04 12.33*	7.30 7.63*	5.44 5.77*	4.43 4.77*
	2	11.07 11.38*	6.33 6.88*	4.91 5.26*	4.06 4.37*
	3	9.56 9.86*	5.76 6.09*	4.40 4.73*	3.86 3.99*

*Reactor subsystem performance for a two-phase liquid metal MHD conversion system.

down. Far more operational and design flexibility is possible if an intermediate heat exchanger is used. The schematic of this alternate design is shown in Figure 4-14.

The gas turbine energy conversion system (Figure 4-13a) requires an intermediate heat exchanger since the turbine operates on helium gas. The turbine can be located in the reactor enclosure with a design similar for the Westighouse HTGR. The option to locate the turbine outside the reactor compartment will add weight and space to the system but allow easy access for maintenance.

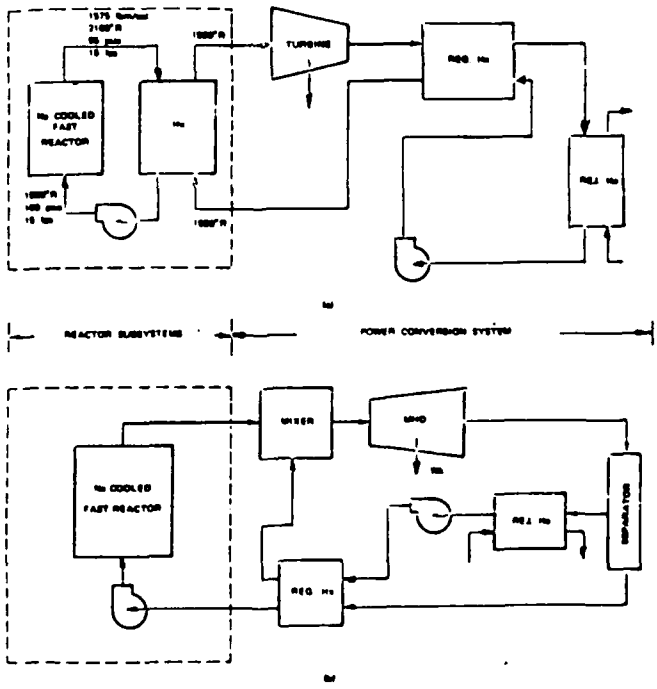

Figure 4-13 Na Cooled Reactor Coupled with (a) Gas Turbine (b) LM-MHD Energy Conversion System (taken from ref. 29)

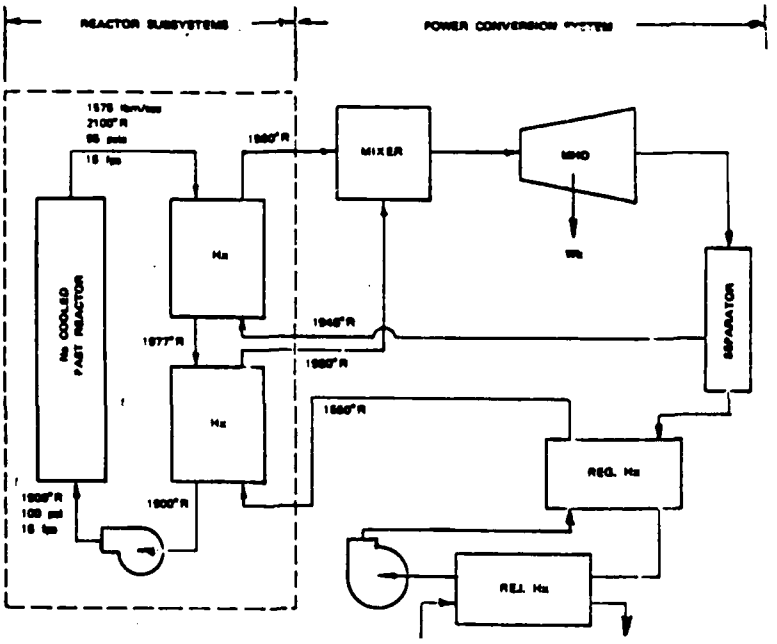

Figure 4-14 Na Cooled Reactor Coupled Indirectly with LM-MHD (taken from ref. 29)

The electrical system for MHD propulsion and ship's electrical service is identical to that described in the HTGR light weight propulsion system design.

With an estimated thermal efficiency of 41%, 37 MW is available for the propulsive power. All four variant submarines, if powered by this plant, are capable of 30+ knots top speed, Table 4-8.

Table 4-8 MHD Submarine Powered by LMFBR Performance Summary

	SSNX-1	SSNX-2	SSNX-3	SSNX-4
Reactor Power (MW)	100	100	100	100
Top Speed (knots)	30.4	30.7	30.2	31.1

4.8 CONCLUSIONS AND RECOMMENDATIONS FOR LIGHT WEIGHT PROPULSION SYSTEMS

Light water reactors are inherently bulky and have low power density. The PWR technology is fully developed and modified, through years of evolution, to provide a very reliable source of nuclear energy for submarine use. The PWR is limited in terms of maximum source temperature and high power density (lb/SHP). The existing reactor technology indicates that LMFBR and HTGR plants can be developed with much higher source temperature and core power density. High efficiency and low power density characteristics are desirable for marine use, particularly in submarine applications.

With further materials development and technological advances in gas turbine and MHD power generation, the thermal efficiency of the light weight propulsion system can be significantly increased.

A significant degree of uncertainty still exists since the analyses are derived from land-based reactor technology. It is anticipated that sea-going reactor plants will have increased power density (lb/SHP) due to structural requirements and conservative auxiliary systems design.

The results of the reference (29) feasibility study suggest that LMFBR and HTGR systems coupled with advanced energy conversion systems are equally attractive. Figures 4-15 (a) through (d) compare the relative

merits of the two designs selected. With the exception of a slightly lower efficiency, LMFBR may be a better choice of the two for submarine use.

A more detailed preliminary reactor design should be carried out with the emphasis on the modifications required for marine application. This study should consider the increased shock resistance criteria for a combatant vessel.

Based on the selected conversion system, the feasibility and means of direct coupling to the power source must be established. Certainly more effort is required in the development of a closed cycle MHD generator and a closed cycle gas turbine along with their control systems.

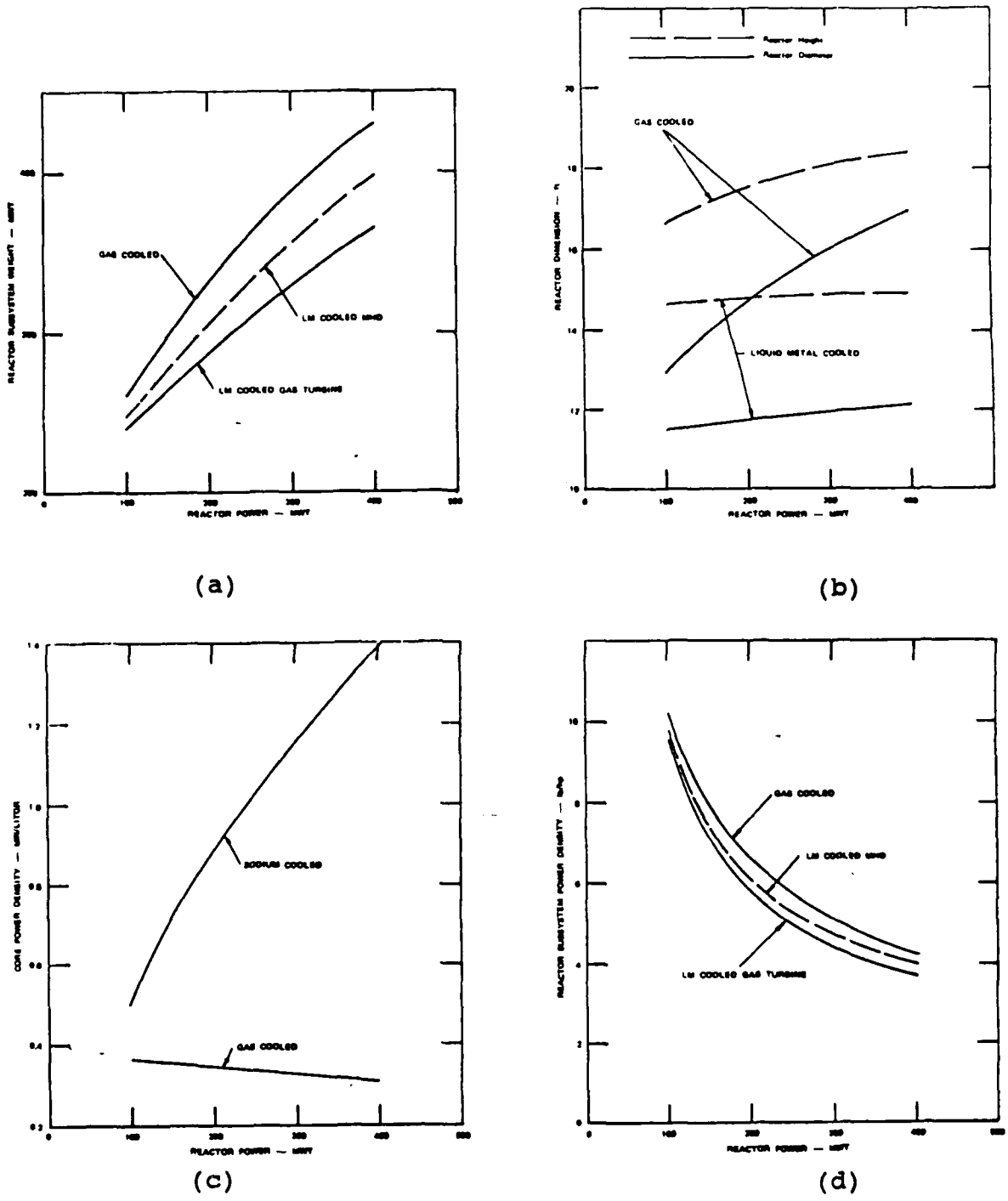

Figure 4-15 Estimated (a) Weights (b) Size (c) Core Power Density (d) Reactor Subsystem Power Density versus Thermal Power Level for Advanced Power Systems (taken from ref. 29)

5. MAJOR MHD PROPULSION ENERGY CONVERSION AND AUXILIARY SYSTEMS CONSIDERATIONS

5.1 OVERVIEW OF MECHANICAL AND ELECTRICAL CONSIDERATIONS

The final design of the nuclear power plant (HTGR or LMFBR) and the energy conversion system (gas turbine or MHD generator) has a major impact on the submarine nuclear and non-nuclear auxiliary systems. Since further technological development is required, the exact auxiliary support is not well defined. The discussion here is limited to the components that provide direct support for the two power plant energy conversion cases (the closed cycle liquid metal MHD generator and the closed cycle gas turbine).

The MHD propulsion concept eliminates the entire conventional propulsion drive train. With the LM-MHD generator or the gas turbine energy conversion system, only a small auxiliary steam plant is needed. The size of the reactor compartment depends on the method of coupling between the reactor and the energy conversion system. The same features determine the design and location of auxiliary support equipment.

The major non-nuclear auxiliary support system is a cryogenic plant. A shipboard cryogenic system must be added to provide cooling for the MHD superconducting magnets (MHD thrusters and MHD generator). In addition,

with a gas turbine energy conversion system, a superconducting electrical generator magnet is supplied. Other MHD and superconducting applications, if desired, can also be supported by the central cryogenic plant.

Other mechanical systems in a current nuclear submarine designs are affected significantly by the MHD propulsion. These are the sea water/fresh water cooling system, the lube oil system, and the emergency propulsion system.

The role of the main sea water and fresh cooling water system remains unchanged. A rejection heat exchanger is used for waste heat and is in common to all energy conversion systems proposed. The rejection heat exchanger replaces the main condenser, used in a conventional steam plant, unless fresh water intermediate cooling is required. In addition, the cryoplant and gas turbine compressors, the DC power support system breakers, and pumps in the energy conversion system require cooling water.

Although the cooling load on the ship's lube oil system is reduced by elimination of the main propulsion train components, the system is tasked with cooling the rectifiers, coaxial transmission lines connecting the MHD electrodes to the power source, and miscellaneous additional equipment. The key components and their arrangement remain virtually unchanged.

Since the main shaft is eliminated, a provision for alternate emergency propulsion is required. Supercon-

ducting motors are precluded due to their high vulnerability after a casualty to the cryogenic support system.

The final design and safety features of the ship's reactor plant will have a major impact on the ship's electrical distribution system. However, other major electrical features, such as split plant, motor generators connecting DC and AC buses, protection of vital busses, emergency diesel generator and emergency power from the ship's battery, are not affected.

The issue of how the electrical power for propulsion is integrated with the ship's electrical distribution system was addressed in Chapter 4 and will not be repeated here. The electrical power supply to the superconducting magnets, the magnet protection system, and the stored energy in the magnet, are the main considerations of this chapter.

This chapter also examines the major features of the main and auxiliary mechanical systems required for MHD propulsion. The study is limited to the energy conversion system, the cryogenic plant, the main sea water system and the emergency propulsion system.

Since a high magnetic field strength is associated with the MHD propulsion magnets, the last section of this chapter estimates the magnitude and effect of magnetic flux leakage external and internal to the hull. Personnel and equipment safety, and magnetic signature, are considered since they are equally important in a submarine design evaluation.

5.2 ENERGY CONVERSION SYSTEM USING A CLOSED-CYCLE MHD GENERATOR

With HTGR and LMFBR nuclear plants operating with high reactor temperatures, the liquid-metal MHD (LM-MHD) generator and the closed cycle gas turbine energy conversion systems give the best results in terms of efficiency and compactness. These four possible power plant combinations are equally attractive for providing electrical power for the MHD propulsion. Efficiency of the energy conversion system can be increased with a small steam bottoming plant which may be needed to power ship service electrical generators and provide steam to the ship's distilling plant.

A closed-cycle MHD generator with liquid metal working fluid was selected for the energy conversion system; however, it should be mentioned that a close-cycle MHD with gaseous working fluids is a strong candidate as well. Over the past several years, both liquid metal and gaseous MHD designs have been a subject of intensive research.

Direct coupling of the MHD energy conversion system gas with HTGR reactor seems impossible with a gaseous MHD design. Argon or helium gas must be seeded with cesium to ensure adequate conductivity. After passing through a MHD generator, cesium must be separated. Inevitably, small concentration of cesium would remain in the working gas; this requires a separation of gas

streams and an intermediate heat exchanger to prevent contamination of the reactor plant. These complications are eliminated with a two-phase LM-MHD closed cycle energy conversion system.

The closed-cycle liquid-metal MHD system is similar to the inert gas system in its recirculation of the generator working fluid and in requiring a heat exchanger which operates at peak cycle temperature. However, it differs greatly in getting an electrically conducting working fluid by means of liquid metal flow (providing electrical conductivity that is essentially independent of fluid temperature).

The basic liquid metal MHD cycle operates by driving the liquid through the magnetic field with a gas. In some instances, the desired velocity is maintained by leaving the gas in the liquid for further expansion in the MHD duct and nozzle. Four of the options that exist for embodying this cycle in concept are: (1) Nozzle fluid acceleration and gas separation (separator type), (2) Injector-condenser (two-phase condensing type), (3) Bubbly flow (Brayton-type-cycle), and (4) Slug flow (same principle as bubbly flow).[42]

Present technology and experience have indicated that the two-component Brayton-type cycle offers the simplest technology. On this basis, the Brayton cycle is selected for the liquid metal MHD energy conversion system.

The major items of the MHD loop are the mixer, the

MHD channel (including superconducting magnet), the nozzle separator, and the liquid metal primary pumps. The other major loop components include the helium compressor(s) and the interfacing heat exchangers. Figure 5-1 shows a closed-cycle liquid metal MHD energy conversion plant using liquid sodium and helium gas. This design is based on a Westinghouse MHD design for a non-nuclear commercial power plant. Not included in the schematic are some power conversion components (inverters, transformers, and circuit breakers) and the liquid-metal auxiliary systems (such as purification, emergency dump, and storage).[49] Figure 5-1 is almost identical to Figure 4-14 if a primary heat source heat exchanger is replaced by reactor subsystem. This shows that, in principle, a commercial power generating MHD plant can be modified to fit the specifications required for a submarine power conversion system.

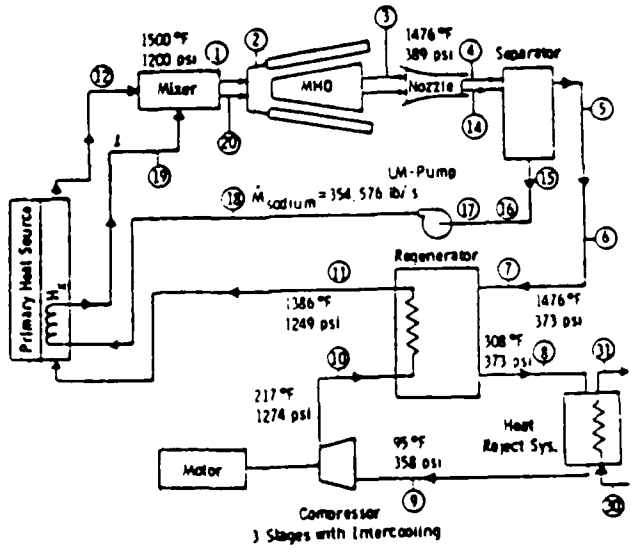

Figure 5-1 Westinghouse Liquid-Metal MHD Power Plant (taken from ref. 41)

It should be noted that in HTGR direct cycle the helium gas heats the liquid metal in the mixer. The opposite is true in LMFBR direct or indirect cycle where liquid sodium transfers heat to the helium gas in the heat exchanger. One way or another, the helium gas is injected as a uniform dispersion of bubbles (occupying over half the volume of the two-phase flow) into the liquid metal in the mixer. The bubbles and liquid flow together as a two-phase mixture through the MHD generator. The liquid provides the necessary electric conductivity and, because it has much greater heat capacity than the helium bubbles, maintains the gas temperature nearly uniform as the bubbles expand through the generator. The bubbles provide the compressibility needed to convert heat to energy in an expansion engine. After leaving the MHD generator, the gas and liquid metal are separated in the separator. The gas is cooled and then recompressed. The cycle is completed by liquid metal and helium gas returning to the mixer; the exact path depends on the reactor plant selected and it is intuitive by examining Figures 4-7, 4-13 and 4-14. The compressor and the heat exchanger designs are based on a conventional design. Higher temperatures may require use of refractory metals for structural materials. The mixer, the generator duct, the separator, and the diffuser are integrated in a housing of the MHD generator. This assembly is shown in Figure 5-2.

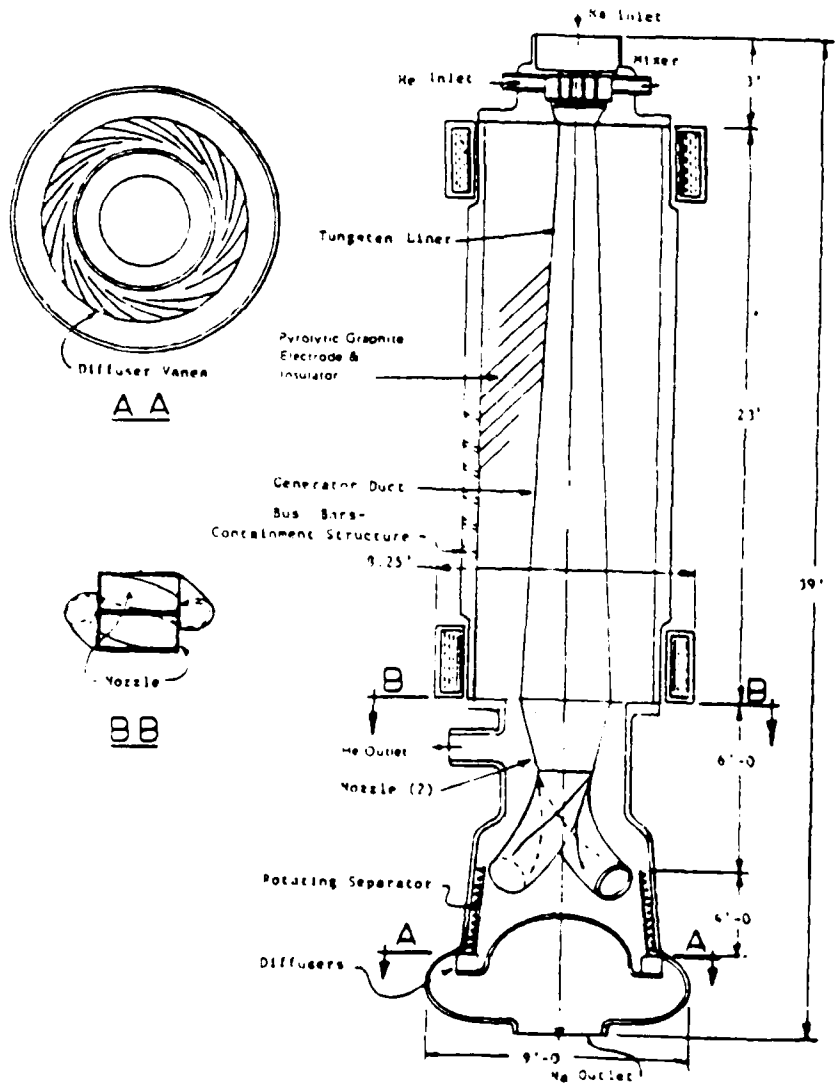

Figure 5-2 General Electric MHD Power Module with Nozzle-Separator-Diffuser

(taken from ref. 43)

The superconducting magnet (2T to 6T) is cooled by the central cryogenic system. A relatively high magnetic field is selected to minimize the frictional effects on generator performance. For a fixed flow rate, generator efficiency increases as the field strength and, hence, power density is increased.[42] The generator duct is rectangular in cross section, with the distance between electrodes remaining constant while the flow area increases to maintain a given two-phase velocity. The electrodes are made of pyrolitic graphite (PG). PG is also used for insulator and containment because it is an excellent material for high-temperature service, actually increasing in mechanical strength with increasing temperature up to 4,500 F (2480 C).[43] PG is not compatible with liquid metals, so a layer of tungsten or molybdenum must be flame-sprayed on the duct surface and the ends of the housing.

The mixer is flame-sprayed over its entire surface with an electrical insulator (Al_2O_3) and covered with thin coating of tungsten. The fluid flows straight through the mixer at nearly constant velocity to minimize pressure drop, and the gas is injected by series of tubes. A homogeneous two-phase flow is formed about one foot before the generator duct inlet.

Separation of two-phase flow is accomplished by impinging the mixture tangentially onto the inner surface of the cone, as indicated in the Figure 5-2, causing the cone to rotate. The large centrifugal force con-

centrates the gas in the center of the cone.

The MHD generator is provided with its own control, alarm, and monitoring system. Indications are integrated in the ship's electrical control console located in the maneuvering control space. The control, indication, and purification systems for a MHD generator are very complex and beyond the scope of this study. Reference (42) provides an excellent summary of the MHD generator auxiliary systems.

The electrical power produced is DC. It is practical to use this power, after voltage regulation, directly for the MHD propulsion. About 4 MW is required for the ship's electrical distribution system. If the connection is made on the AC side of the distribution system then a power inversion process is required.

The inverter system chosen must provide an appropriate interface between the MHD generator and the AC power grid over a wide range of operating conditions, and be flexible and reliable. Solid state inverters of both line-commutated type and force-commutated type are presently under development.[44] A block diagram of the rotary inverter system is shown in Figure 5-3.

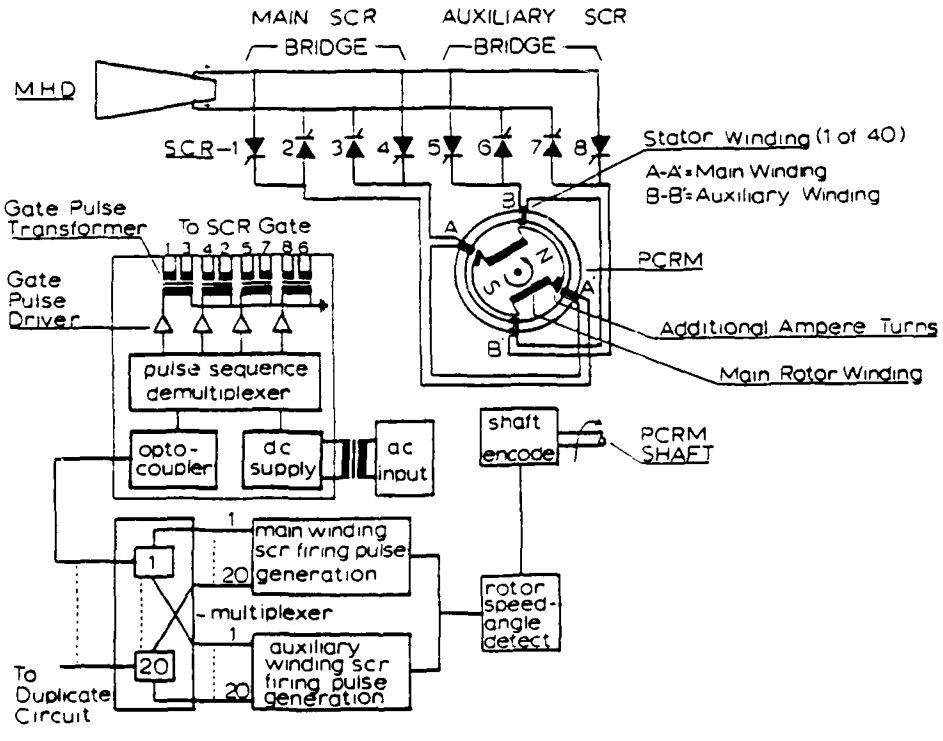

Figure 5-3 Block Diagram of the Rotary Inverter System

(taken from ref. 44)

5.3 ENERGY CONVERSION SYSTEM USING A CLOSED-CYCLE GAS TURBINE

Outstanding among the many advantages claimed for the closed cycle is the possibility of using a high pressure (and hence a high gas density) throughout the cycle, which results in reduced size of turbomachinery and enable the power output to be altered by a change of pressure level in the circuit. This form of control ensures that a wide range of loads can be accommodated without alteration of the maximum cycle temperature and hence with little variation of overall efficiency.

Owing to its high temperature level the waste heat generated by the plant can be used further, especially for remote heating. Another possibility is to use this heat in a second thermodynamic process. In both cases the overall efficiency factor of the plant is raised still higher.

The state of the art of a closed-cycle helium gas turbine plant (proposed in Chapter 4) is such that further development is necessary. Three main areas of research, necessitated almost exclusively by the higher temperatures, are required. The first area concerns materials in the region of the core, continuing with the metallic or ceramic materials for the hot gas pipework, ducts and liners. The long service lives of nuclear power plants and the rapid pressure changes impose stringent requirements on the insulation.

The second area consists of studies on the behavior of the fission products in the integrated cycle. As the escape of gaseous and solid fission products from HTGR fuel elements cannot be prevented completely, accurate information on the release, transport and deposition of fission products is indispensable. A design with an intermediate loop (with lower efficiency and power density) is more conservative and more desirable for a submarine use.

The third area consists of component-specific problems which must be solved before the plant can be built. This includes primarily the turbine with its shaft seals and cooling systems, and the design of its inlets and connections. The heat exchange apparatus presents problems at the connections, quite generally owing to the large dimensions of the components.

A generic description of the power plant, without reference to plant size, is presented here based on similar designs that operate at lower temperatures. A simple Brayton cycle process is necessary to respond to the design requirements and objectives. Consequently, the process illustrated schematically in its most simplified form in Figure 5-4 is selected. Basically, the concept consists of a reactor plant coupled with a simple Brayton cycle. An intermediate heat exchanger is used with both reactor plants, hence indirect coupling is in effect. Figure 5-4a is an example of HTGR with a closed cycle gas turbine energy conversion system. The

power for the main helium compressor comes directly from a turbocharger in the primary helium loop. This setup is not possible if LMFBR is used. The power for the primary sodium pumps comes from the ship's distribution system, Figure 5-4b.

A double wall heat exchanger, located in the reactor compartment, is used for intermediate heat transfer. The heat exchanger is of counter-flow double-walled tubular design. The heat exchanger also employs double tubesheets. The inner-wall cavities are connected to a leak detector.[45]

The energy conversion module houses the secondary helium turbomachinery and superconducting generator, air compressors, and a combined precooler/inter-cooler unit. To maximize efficiency, a high pressure turbine drives the high pressure compressor and the low pressure turbine drives the low pressure compressor and the generator.

Hot gas exiting the intermediate heat exchanger is passed to the HP turbine through a thermally insulated duct and then enters the LP turbine. The exhaust of this turbine is fed to the heat exchanger and flows upwards over the outside of the axial flow heat exchanger tubes. From the top of the heat exchanger pod the gas is ducted to the top of the cooler pod where it enters the precooler section and flows downwards over the outside of the axial flow water tubes.

On reaching the bottom of the precooler section the

gas is passed through a short duct to the LP compressor. The compressor discharges into a second short duct which connects with the inter-cooler which comprises the bottom section of the cooler unit. Cooling water (probably fresh water) is arranged to flow upwards inside the cooler tubes, giving a counter flow configuration.

From the inner-cooler the gas enters the HP compressor which discharges to the top end of the heat exchanger using a counter flow arrangement. After regeneration the gas returns to the intermediate heat exchanger.[46]

The control module includes direct connections to the low pressure storage tank and helium make up gas bottles. The helium blowers in this module provide a backup capability for removing decay heat from the reactor following a normal shutdown by providing flow through the secondary side of the intermediate heat exchanger. The helium gas bottles can be connected directly to the primary loop of HTGR for short-term backup capabilities.

Depending on the design, the gas turbine operates between 3,000 and 3,600 rpm and is coupled to the generator through a reduction gear. The turbine is not self-starting and requires a starter motor. The primary turbomachinery is started pneumatically with the aid of gas injection at the turbine blade tips. The gas is supplied from the high pressure gas accumulator of the primary system.

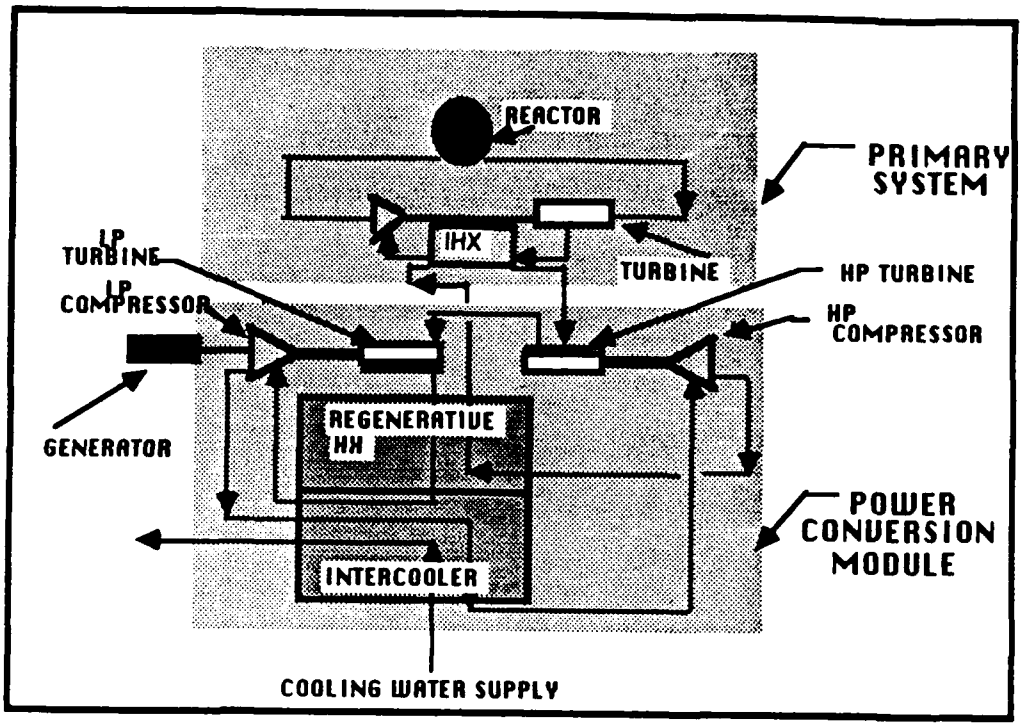

Figure 5-4a HTGR with Closed-Cycle Gas Turbine

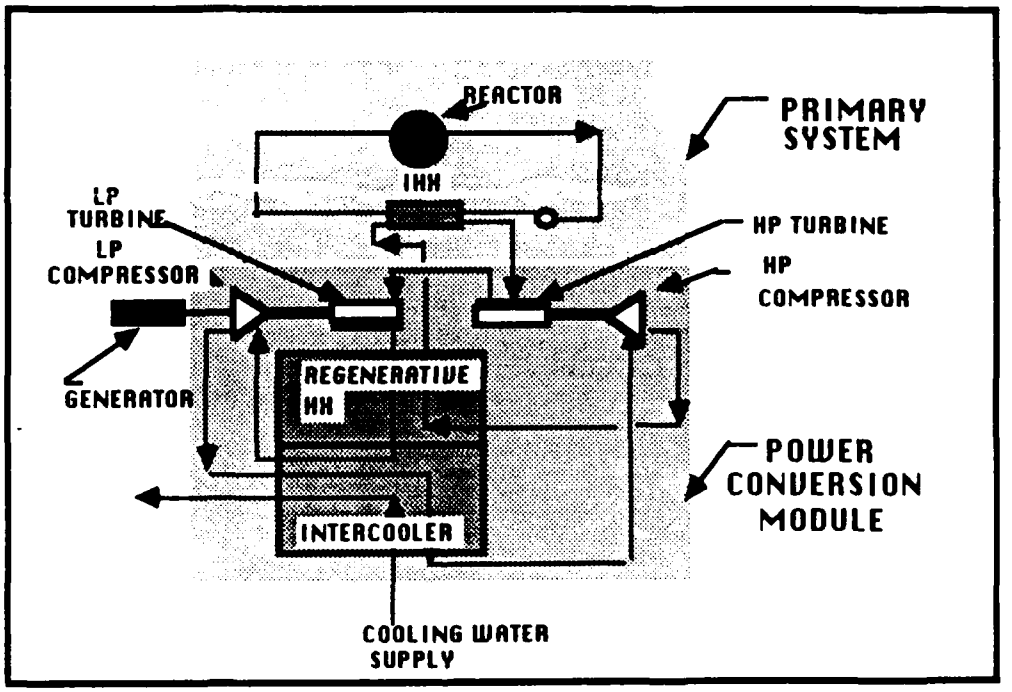

Figure 5-4b LMFBR with Closed-Cycle Gas Turbine

The electrical system consists of the generator, transformer, switchgear, breakers and protective devices. The generator is a two-pole synchronous machine. The field winding, located on the rotor, is supplied with DC current via a slip-ring brush assembly. The armature is located on the stator and is wound in such a way as to produce a three-phase sinusoidal voltage. The two-pole field winding is made of niobium titanium, an alloy possessing superconducting properties when subjected to a magnetic field of about 5 T. The field winding is submerged in a bath of liquid helium. When evaporated, the helium gas also cools the radiation shield. The central cryogenic plant can supply the cooling required.[47] Figure 5-5 shows a major cooling components of the rotor.

The integrated control, monitoring, and alarm circuit indications for the gas turbine and superconducting generator (beyond the scope of this study) are displayed on the ship's control console in the maneuvering spaces.

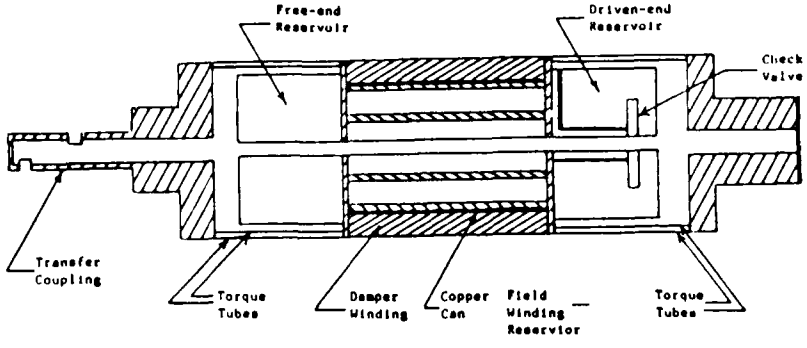

Figure 5-5 Major Cooling Components of the Superconducting Generator Rotor

(taken from ref. 47)

5.4 CRYOGENIC PLANT

Liquid helium temperatures (4.2 K at 1 atm of pressure) are essential for the operation of present day superconductors of niobium titanium (NbTi) alloys, as well as for the newer superconducting alloys of niobium tin (Nb_3Sn) which are still in the development stage.[37] Although some of these materials are superconducting around 16 K, they can not operate at liquid hydrogen temperatures (20 K). Liquid helium is firmly established as the cryogenic fluid for superconductors.

It takes only 1 Wh of equivalent heat energy to vaporize 1.4 liter of liquid helium and, since it takes approximately 4 kWh to produce 1 liter of liquid helium from a liquifier, the losses must be kept to an absolute minimum. The system requires minimum piping runs and significant thermal insulation.

A superconducting generator (30 MW rating) will require up to 10 liters of liquid per hour, depending on the size and construction of its field system.[37] The heat load of the MHD propulsion magnets on the cryogenic system can be calculated for a given design using energy data derived from experimentation or available magnetic applications. There is an additional heat load due to cooling of the electrical leads connecting the magnet to the power supply.

The size of the cryogenic equipment can be determined from existing equipment by 0.7 power scaling.[38]

For the MHD propulsion magnet and electrical leads, the heat load is estimated to require 20 liters of liquid helium per hour. Table 5-1 shows estimated heat loads of a typical commercial size magnet systems with design operating currents of 5 kA, 10 kA and 50 kA. The estimated conductor splice heat load is conservatively high and subject to revision when more experience is obtained on splice losses in high current superconducting windings.[40]

Table 5-1 Cryogenic Characteristics of Baseline Design MHD Magnet System (taken from ref. 39)

Electrical leads	5kA	10kA	50kA
4.5 K Flow g/s	.695	1.39	1.80
78 K Flow g/s	-	-	5.0
Heat Leak from Environment			
Radiation	8W	8W	8W
Conduction	10W	10W	10W
Heat Leak to Stack	5W	5W	5W
Conductor Splices	12.5W	50W	1250W
Total Heat Load	35.5W	73W	1273W
Total Liq. He Consumption	20L/hr	40L/hr	52L/hr

The most commonly used cooling method is known as pool boiling. A pool of liquid helium is maintained in the lower part of the coil cryostat and the coil is cooled to below the critical temperature by a combina-

tion of heat transfer directly to the liquid for the immersed part of the coil and into the coil boil-off vapors for the exposed part. The cold vapor is also used to cool the coil leads and the heat intercept shield within the cryostat, before being returned to the helium compressor. The biggest advantage of the pool boiling method is that there is no requirement to maintain total immersion of the coils which may be difficult in a rolling ship.

On a submarine, the helium inventory is limited; therefore, the cryogenic plant must be of cyclic design with a minimum tolerance for leakage. A closed cycle for the cryogenic system requires a refrigeration process. The helium vapor returning from the load transfers its cooling capacity across the heat exchanger of a liquifier to assist in the production of more liquid, then it is returned to the compressor for recycling through the liquifier.

The cool-down of a superconducting coil system requires the extraction of large quantities of heat energy in the initial stages, gradually reducing as the temperature of the coils and cryostat approaches the normal working temperature. The cool-down will normally take place in port using an outside supply of cryogent. Nevertheless, the shipboard cryoplant must have a cool-down capability following an inadvertent magnet coil quench, which generates a large amount of heat as the magnetic field within the coil collapses. The final tem-

perature of the cold mass, after a quench from full field, is expected to be approximately 100 K.[37]

When a superconducting coil quenches, a large amount of heat is generated in a very short time and this is usually sufficient to vaporize the entire liquid helium content of the coil cryostat. This may be as much as 50 liters equivalent to 38 m^3 of gas at normal temperature and pressure. Because of the speed at which the gas evolves during a quench, it must first be stored and then compressed over a longer period of time. The large containment vessel required for the low-pressure boil-off gas is a major obstacle to quench gas recovery in a submarine system.

Leakage losses can be kept to acceptably low levels by proper system design and good fabrication techniques. However, the unpredictable quench of a magnet, or a liquifier failure could result in some loss if the system is equipped with over-pressure vents. Obviously, the quantity of helium gas makeup must be sufficient to provide continuous cryogenic plant operation even after a quench.

If the helium supply to an operating superconducting magnet is interrupted (as in the case of liquifier failure), the magnet will remain superconducting until essentially all the liquid helium in the dewar is lost. The thruster can therefore operate normally for some 6 to 8 hours following an interruption in helium supply. This period can be extended with a larger liquid helium

storage inventory, larger dewar, and larger helium gas storage tank.

Two large compressors of the oil flooded screw type, each capable of steady state capacity of cryogenic system ranging from 20 to 30 liters per hour, is a minimum requirement for a submarine cryogenic plant. The upper limit is based on cooling the MHD thruster magnet, MHD generator magnet or the superconducting generator magnet. Ideally, a three or four compressors design provides the most operational flexibility; one or two units remain on stand-by. Two compressors should be running simultaneously, each supplying one side of a duplicate cryogenic plant. The compressors can be cross-connected to allow for operational cycling; however, a split lineup is the normal operating mode. The cross-connect concept, may under certain conditions, cause serious interference problems. One such possibility is the introduction of contaminants from one system to another, leading to an eventual shutdown of both. Another possibility is that the quenching of one magnet (or a segment) could cause excessive pressure fluctuations and associated temperature variations in the second, due to a common low pressure suction line.

A shipboard helium management system must include a suitable and compatible helium liquifier. Its capacity must be adequate for supplying the entire heat load and to assist cool-down of the dewar in a reasonably short time. The cryogenic plant has two identical liquifiers.

Figure 5-6 is a schematic diagram of one such liquifier concept. It features three reciprocating expansion engines (E-1 through E-3) for normal steady state liquid production. The large cool-down expansion engine (E-4) is operated only during system cool-down. The liquifier operates between two constant pressure levels; namely, about 1.7 MPa (250 psig) on the high-pressure side and about 13.7 kPa (2 psig) on the low-pressure side.[37]

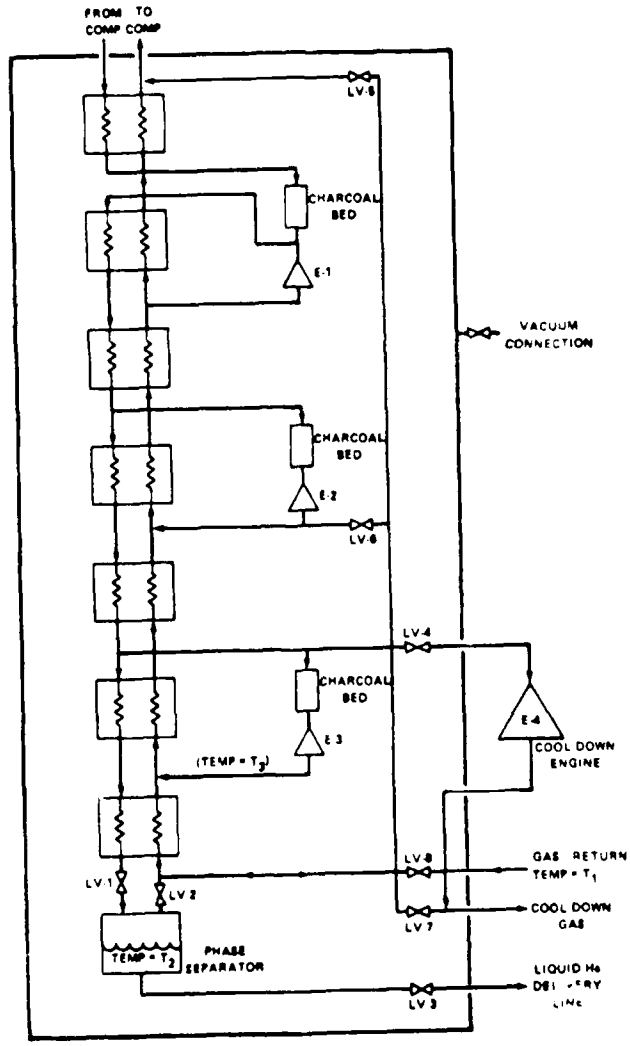

Figure 5-6 Shipboard Helium Liquifier

(taken from ref. 37)

Each liquifier supplies one side. If one fails, an operational unit can be cross-connected. This introduces a possibility of cross contamination. The only solution is to have a third stand-by liquifier which has no direct access to either side, Figure 5-7.

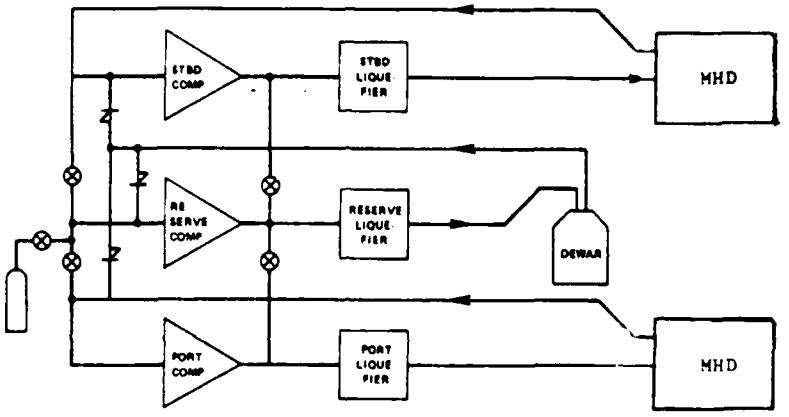

Figure 5-7 Cryogenic Plant with Reserve Liquifier (adopted from ref. 37)

A submarine is limited in volume; therefore, two liquifiers may have to suffice. Compressors in general require significant preventive maintenance, and a conservative approach is to have four compressors. A proposed shipboard helium system schematic is shown in Figure 5-8.

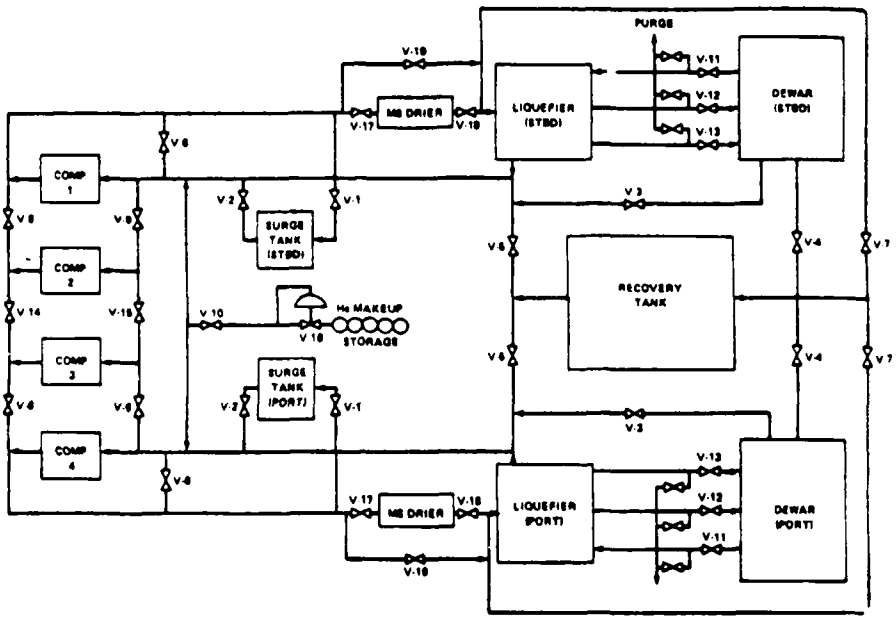

Figure 5-8 Proposed Shipboard Helium System
(taken from ref. 37)

Most commercial superconducting magnet designs use two different cryogenic mediums. Liquid nitrogen is used to cool the thermal radiation shield of the magnet and also for precooling in the refrigerator. This system is more efficient than using a secondary helium gas loop. This two-cryogent system is not practical for submarine use because it requires a separate inventory of liquid nitrogen. Table 5-2 is a summary of cryogenic data for a typical superconducting magnet design rated at about 40 MW using liquid helium cryogent only.[39]

Table 5-2 Cryogenic Data for ETF-MHD Magnet Design (taken from ref. 39)

Cryogenic data:		
Operating temperature at winding	(K)	4.5
Operating temperature, thermal shield	(K)	102
Coolant, thermal shield	—	He gas
Heat loads LHe region, not incl. leads	(W)	39[a]
LHe for lead cooling at design current	(ℓ/hr)	60
Materials of construction:		
Winding substructure	—	SS 310 S
Insulation	—	Epoxy/glass
Superstructure	—	SS 310 S
Liquid helium vessel	—	SS 310 S
Thermal shield	—	Al 5083
Vacuum vessel	—	Al 5083
Design stresses:		
Winding substructure	(MPa)	379
Superstructure (tension)	(MPa)	379
Superstructure (bending)		379
Pressure rating		
Liquid helium vessel		
Normal operating	(atm)	1.3

Reliability and failure modes for cryogenic system components are of particular importance since the entire main propulsion system availability depends on it. A mean time between failure (MTBF) of about 10,000 hours is considered reasonable for refrigerator heat exchangers. Screw compressors are expected to run 12,000 hours without down time. Turbo-expanders and reciprocating expanders should be accessible for repair and replacement of parts. Typical time allowance for parts replacement is from 4 to 8 hours.[40]

It is expected that magnet operation can continue using stored liquid helium or cross-connecting port and starboard plants. Expected MTBF for cryogenic components

is summarized in Table 5-3. The uptime of more than 99% and more than 50,000 hours of failure free operation in a mobile environment is advertised by the Intermagnetic General Corporation for its superconducting magnet cooled by cryogenics. This indicates that the MHD propulsion is potentially highly reliable.

Table 5-3 Expected MTBF for Cryogenic Components (taken from ref. 40)

	MTBF
Compressor	12,000 hrs
Compressor Oil Removal System	12,000 hrs
Refrigerator Cold Box	
Heat Exchanger Plugging	20,000 hrs
Turbine	8,000 hrs
Reciprocating Expander	4,000 hrs
Insulating Vacuum	50,000 hrs
Valves	20,000 hrs
Liquid Helium Storage Vessel	50,000 hrs
Gaseous Helium Storage Vessel	50,000 hrs
Vacuum Jacketed Piping	50,000 hrs
Liquid Nitrogen Storage Tank	50,000 hrs
Warm Piping and Valves	50,000 hrs

The entire system is self-regulated. The electrical control system receives electrical inputs from level detectors and activates the network for solenoid control valves. A centralized control panel for monitoring cryogenic parameters should be located in the maneuvering spaces.

It should be mentioned here that the most common reason for magnet quenching is due to friction between windings. With the thrusters being external to the hull,

they will be subjected to significant vibration; therefore, those superconducting magnets are more susceptible to a quench than a magnet resting on a stationary foundation.

In order to prevent any damage to the windings or to the cryostats, an active interlock will trip the power supplies in case of quenches, overheating of current leads or abnormal liquid helium level. This protection network is described in the section on MHD thruster magnet system.

5.5 SEA WATER COOLING SYSTEM

Present nuclear submarine designs use a pressurized water reactor plant with a Rankine cycle secondary steam system. The major function of the main sea water is to provide cooling water to condense the steam from the ship's turbines and the steam plant auxiliary equipment.

After removing the heat the sea water is pumped overboard. It is anticipated that the main sea water cooling system will be arranged in similar port and starboard loops in the engine room. Each loop has a pump that takes suction from the sea through a strainer and associated hull valves. After passing through the condenser and, possibly other heat exchangers, the sea water is discharged overboard. The main sea water system is augmented with an auxiliary sea water cooling system which provides cooling to sw/fw heat exchangers.

The heat rejected in the main condensers corresponds to about 70% of the PWR thermal power, hence, the mass flow rate of the main sea water system is relatively large. Large pumps or several smaller pumps are required to overcome the headloss in the cooling system. These pumps are of the rotary vane centrifugal type since positive displacement pumps are not known for their high mass flow rate capabilities. Rotating equipment is undesirable for submarine use since complex vibration damping systems are required to prevent the transmission of unwanted sound to the ambient surroundings.

With HTGR or LMFBR replacing PWR, the heat rejection takes place in a heat exchanger which does not depend on a high vacuum as is required for a condenser. Therefore, higher temperature sea water can be used as a heat sink. For this reason, the main sea water system is replaced by a larger auxiliary sea water system which, in addition to its normal cooling loads, provides adequate cooling for the energy conversion system. The number of hull penetrations is reduced, the drag on the hull is reduced, and the sea water cooling system becomes more compact.

The auxiliary sea water system is split into port and starboard with two sea water intakes. An intermediate sw/fw heat exchanger may be required for cooling the energy conversion heat exchangers. After passing through all heat exchangers, sea water is pumped overboard through a common discharge. Because the propulsion train and the propeller is eliminated, the sea water discharge may be located at the cone section of the after body.

The auxiliary sea water system pumps can be replaced by MHD pumps which are larger in size, but quieter. The efficiency of such pumps is very low because of the small flow area. Major advantages include the lack of vibrations, ease of maintenance, and a reduction in the water-tight integrity boundary because the pump is integrated with the sea water piping.

Higher temperature sea water has a better conductivity, hence, the efficiency of the MHD sea water pumps

can be increased by locating them downstream of all the heat exchangers.

Cooling for the sea water MHD pumps comes from the central cryogenic system. Port and starboard sea water cooling systems can be cross-connected. A total loss of the sea water cooling is very unlikely. A loss of cryogenic plant will reduce the cooling load to a minimum; ship service motor generators and the nuclear support systems which require uninterrupted cooling to maintain plant safety. To increase reliability, a much smaller cooling system, independent of the cryogenic cooling, can be provided. Another alternative is to integrate the emergency propulsion system with the sea water cooling system.

5.6 EMERGENCY PROPULSION SYSTEM

Emergency propulsion is normally provided for by an electrical motor coupled to the propulsion shaft. Since the shaft is eliminated other means of emergency propulsion are required. In this study, the emergency propulsion requirement is set at 6 knots top speed. The power curves (from Chapter 3) predict that 500 HP is adequate for this function if the MHD thruster operates in emergency mode.

When submerged, emergency propulsion is achieved by powering the MHD thrusters with the ship's battery for a limited period. On or near the surface, emergency power can also be provided by the diesel generator. The stored energy in the MHD thrusters can also be used for emergency power. Draining the stored energy from the MHD propulsion magnets lowers both magnetic field strength and efficiency; but nevertheless remains a viable emergency option.

The magnets (or a segment of a magnet) can always be recharged after main power is restored. A loss of operation on both thrusters has the same consequence as a loss of the propulsion shaft on a current submarine design, and results in a loss of emergency propulsion. A major drawback is low efficiency of the MHD propulsion, hence a large load on the ship's battery. For this reason a redundant emergency propulsion unit can be installed. This unit can be removed after the safety and

reliability of the MHD propulsion is fully demonstrated.

The propeller drag can be eliminated if the propulsion motor and the propeller are installed inside the ship's hull. A small induction motor with a propeller riding inside the sleeves of the stator winding is being developed.[48] This design eliminates shafting and the entire assembly fits in the cone of submarine after-body (where the cone's interior surface acts just like a propeller duct). The lateral suctions can be faired during normal operation.

The ship's sea water cooling system discharges to the duct of the emergency propeller. With the emergency propulsion suction shutters closed, the emergency propulsion can take a suction on the sea water cooling system, Figure 5-9.

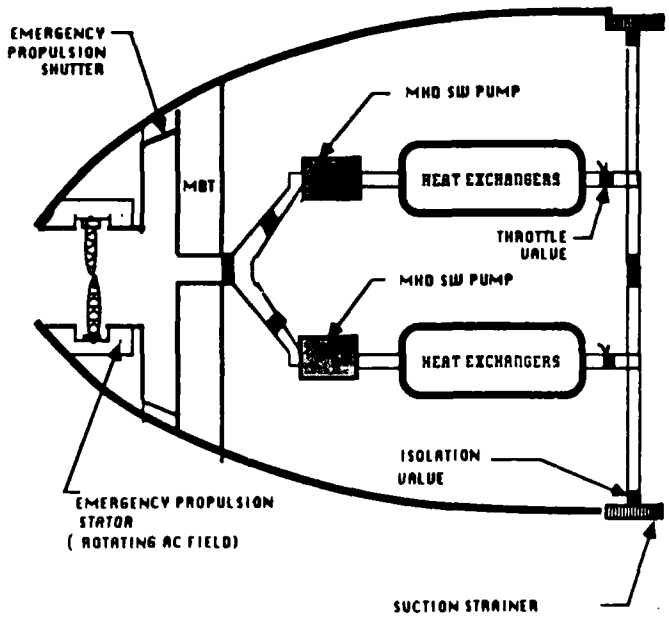

Figure 5-9 Sea Water Cooling System and Emergency Propulsion

5.7 MHD THRUSTER MAGNET SYSTEM

The method for connecting superconducting magnet of a MHD thruster to its power supply depends on the design philosophy. One such design philosophy is to utilize the stored energy in the magnet as a possible emergency source of electric power. This results in a direct electrical connections to the coils, hence, a significant additional cooling load on the cryogenic plant. On the other hand, direct connections allow for fast charging and discharging of the magnet which deems to be necessary for submarine applications.

Figure 5-10 shows a simplified schematic of a MHD thruster magnet electric network. Charging the magnet is accomplished by providing DC power to the MHD magnet power supply. The necessary power can come from the ship's electrical distribution system, directly from the energy conversion system, or an external source. Electrical lineup requires closing of the dump switch contacts and leaving the emergency power switch open on all contacts.

The superconducting magnet is protected from overheating by the resistor bank which may be external to the hull. This method of discharging is used only if the magnets recovery from a quench is not possible; magnet quenches on all coils and the cryogenic cooling is threatened. The electrical lineup is accomplished by shutting the dump switch and closing the circuit in the

emergency power switch.

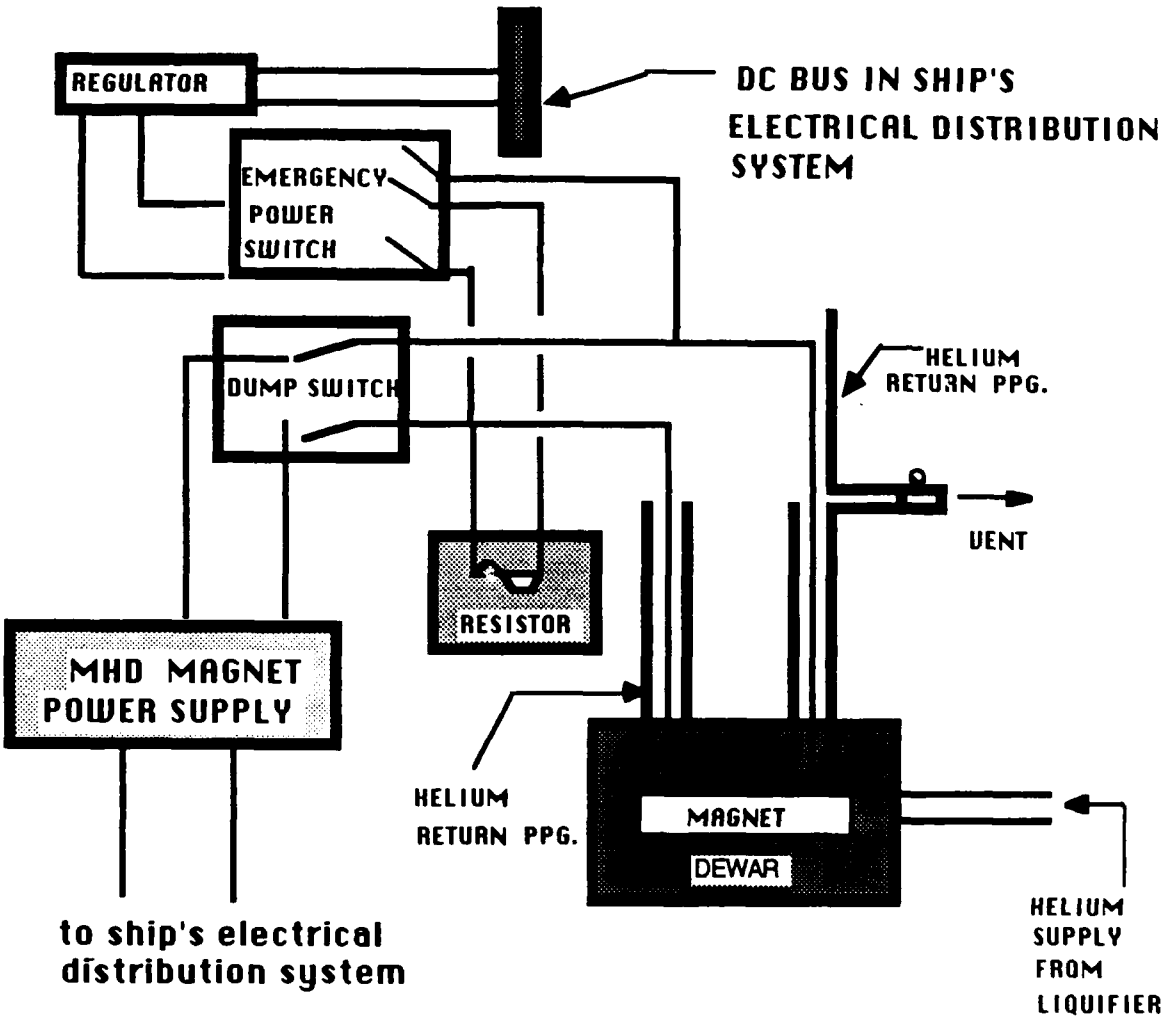

Figure 5-10 MHD Magnet Electrical Network

The stored energy in the magnet E_s is calculated by:

$$E_s = 0.5 L_m I^2 \quad ;$$

where L_m is inductance and I is the total current in the magnet. The MHD thruster magnet is a modified version of AVCO's magnet which was evaluated by the General Dynamics at 1.5 Giga-Joules of stored energy when fully charged.[36] The modifications include current variation in the coil to make the magnetic field in the MHD channel more uniform with radius and have no bearing on the stored energy in the magnet.

The rate of discharge follows Ohm's Law; therefore, a regulator is required to match the voltage of the ship's electrical distribution system. The stored energy in the magnet can be used as an emergency power source by closing the dump switch and the emergency power switch with a dump resistor left on open circuit. With the thruster segmentation, any segment(s) of the magnet can be discharged and, the power can be used to energize the operational segments of the MHD thruster.

The stored energy in the magnet is directly proportional to the square of magnetic field strength in a magnet. The top 50% of stored energy is easy to recover and can be recovered with very fast rates. The next 25% of energy recovery is rate limited, and the remainder of the stored energy is not recoverable.[36] The amount of recoverable stored energy in the magnet is significant enough to provide enough energy for the emergency propulsion system to drive the ship to the surface. To

ensure a high rate of energy transfer, direct electrical connection to the magnet coils are required.

If the stored energy of the magnet is not considered necessary to augment the emergency power, then the heat load on the cryogenic system can be reduced by coupling the magnetic coils indirectly with its power supply. This is accomplished with a superconducting rectifier-type flux pump. A simplified schematic of such a design is shown in Figure 5-11.

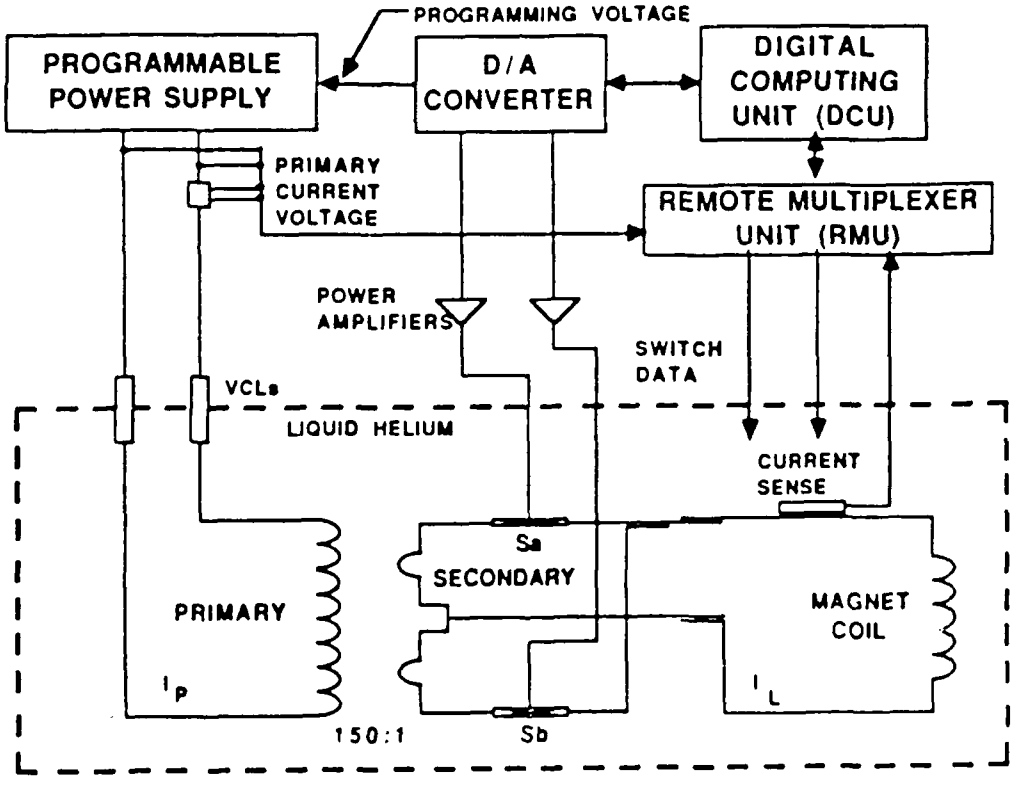

Figure 5-11 Flux Pump for Magnet System

(taken from ref. 50)

A flux pump is a high current power supply operating in a superconducting mode that is used to charge the magnet. The flux pump consists of a front end transformer that takes energy from a low current AC power conditioner source via two helium vapor cooled leads. The high current transformer secondary employes a pair of superconducting switches to rectify the magnetic current.

The flux pump controller houses the avionics required for controlling the refrigeration system, the flux pump system, and the magnet. It consists of a real time digital computing unit, a programmable power supply for the flux pump, and the two much smaller programmable power supplies for the superconducting switch heaters.[50] Schematic of a magnet system power supply and integrated control is shown in Figure 5-12.

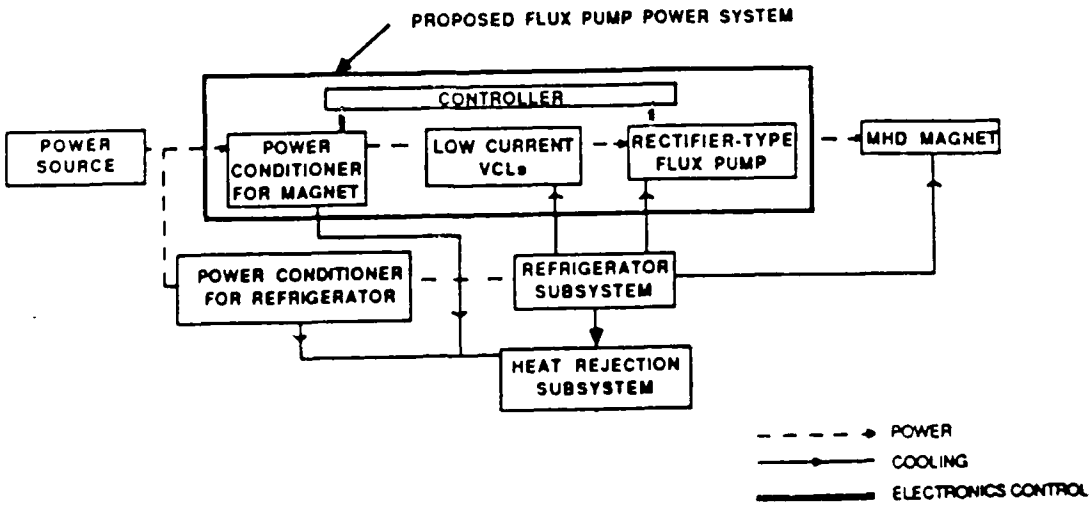

Figure 5-12 Magnet System Power Supply

(taken from ref. 50)

The superconducting MHD propulsion magnets are charged and then disconnected from the flux pump power system by a superconducting (persistent) switch. The resistance of the superconducting magnet is negligible and a periodic charging is accomplished by allowing the superconducting switch to go normal and closing a switch on the magnet power supply, Figure 5-13.

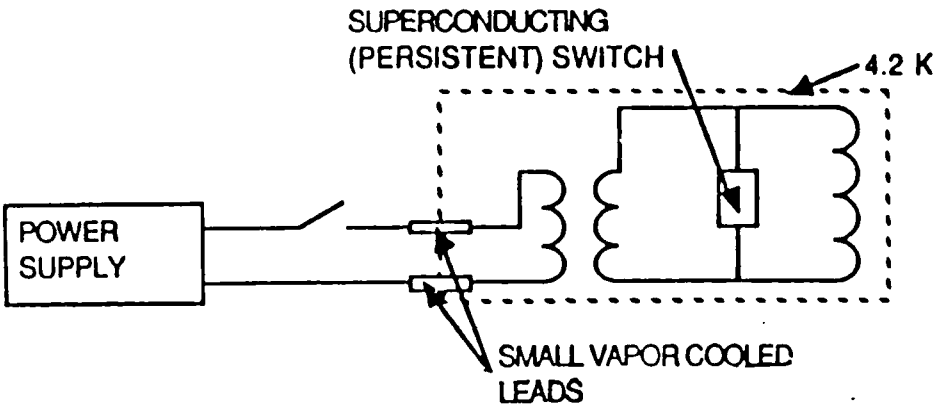

Figure 5-13 Superconducting (persistent) Switch for Magnet Charging System
(taken from ref. 50)

The monitoring system for the MHD propulsion magnets is a simple one since the design is made inherently safe. Indication of the temperature, pressure and flow rate of the cryogenic supply and return are considered sufficient. Addition of a magnetic field detectors or magnetic coil voltage sensors may improve the means of early detection of a MHD flow-train emergency or a fault

in the magnet itself. The heat generation and transfer from a very small section of magnet winding in the normal state can be arrested before adjacent sections of the magnet are affected.

Copper-to-superconductor ratio, heat flux and helium-to-conductor-metal volume ratio are criteria often used as measures of the stability, and hence the reliability of magnet windings. In the past, conservative winding designs for MHD magnets have usually involved copper-to-superconductor ratios in the range of 6 to 30, heat fluxes of less than 0.4 W/cm^2 and helium-to-conductor ratios of at least 0.2.[51]

All magnet designs incorporate substructures which provide an individual support for the conductors and transmit magnetic loads from conductor to containment vessel. Substructure design stress may be as high as 125 MPa. Consequently, the containment vessel (superstructure) experiences large stresses. These stresses are compounded by hydrostatic pressure stresses and the stress due to the temperature gradient across the containment wall. Proper design and periodic non-destructive testing are required to achieve high confidence factor in the structural integrity of a MHD thruster.

5.8 MHD THRUSTER MAGNETIC FRINGE FIELDS

The (unshielded) superconducting magnet will, when charged, produce relatively high DC magnetic fringe fields in the region around it. This field is reduced by shielding and the proper design of magnet assembly. The annular toroid configuration is selected for a MHD magnet because the high magnetic field is confined to the annulus and the leakage outside the annulus is very small.

The field decreases exponentially as one moves away from the magnet, dropping off approximately as the reciprocal of the distance cubed for a single coil design. Increasing the number of coils (n) results in a faster field drop rate. At a distance x away from the magnet, magnetic field is estimated by:

$$B(x) = B(0)x^{-(2n+1)} \quad ,$$

hence, the magnet should have as many coils as the MHD propulsor volume and weight limitations will allow.

The superstructure of a MHD thruster and submarine hull provide some shielding. Additional shielding to reduce fringe fields to very low levels is prohibitively expensive and adds significant weight and volume to the structure. Based on AVCO's calculations, Figure 5-14 shows the magnetic field profile for a MHD propulsion system as a function of distance from the submarine axis of symmetry.[36] Magnetic field strength interior to the hull is difficult to calculate due to shielding provided

by the hull itself and any other shielding materials adjacent to the hull. However, AVCO predicts very low magnetic fields of about .05 gauss at 0.5 m measured radially inward from the ship's pressure hull. This corresponds to 10% of the earths magnetic field.

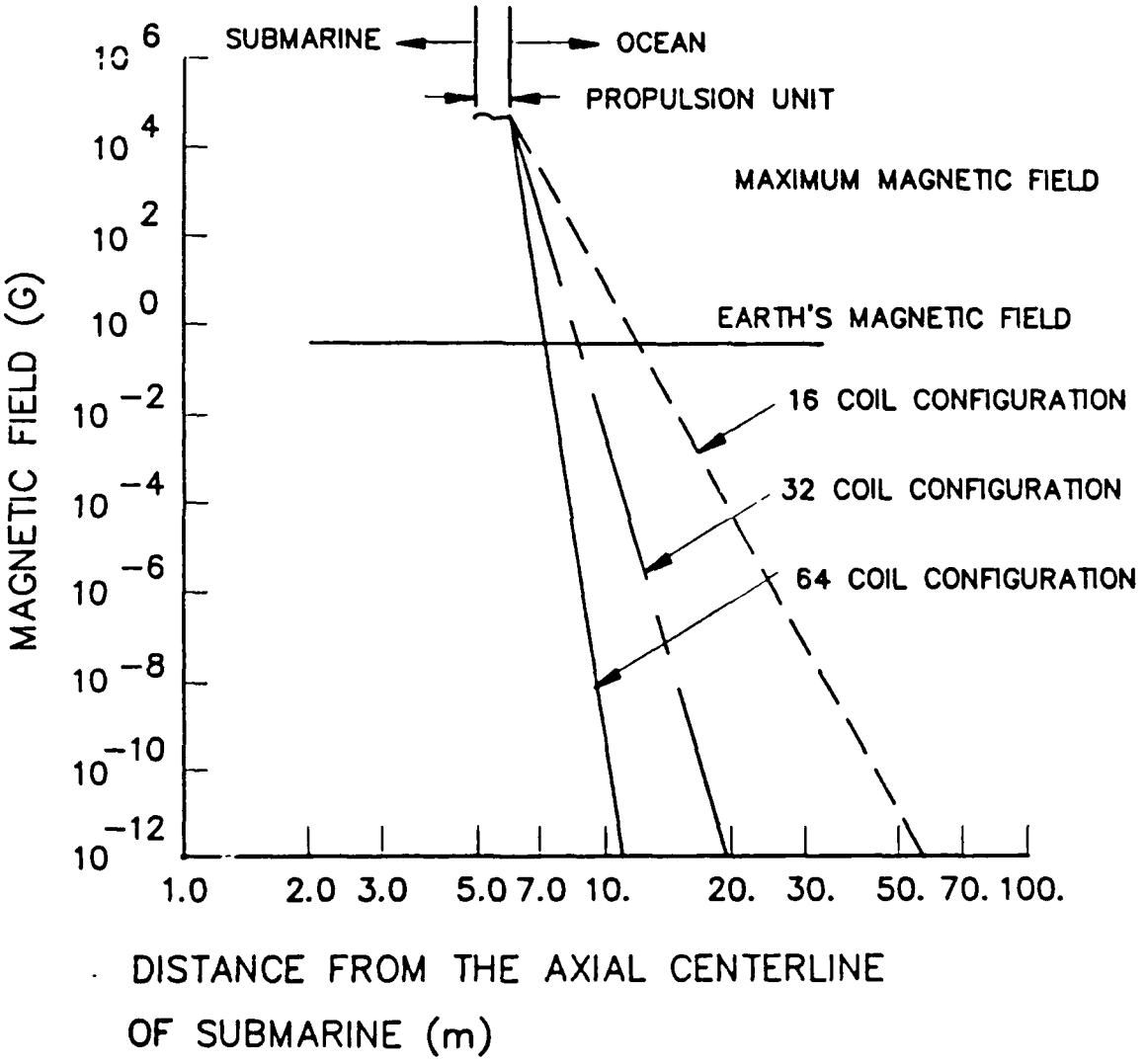

Figure 5-14 Magnetic Field Profile for MHD Propulsion System (courtesy of AVCO Inc.)

The magnitude of fringe magnetic field axially outward from an inlet nozzle and diffuser of a MHD thruster is unknown. Magnetic field may be very high near the active channel but will fall off much more rapidly with distance because the magnet's vertical cross-section is much smaller than its horizontal cross-section. However, this must be taken into account in the design and location of the after escape trunk.

Because of relatively low magnetic fields exterior to the hull, magnetic signature generated is not a major concern. Magnetic field interior to the ship can be reduced by proper arrangements to maximize internal shielding.

In the past, personnel exposure to high DC magnetic fringe fields has occurred on many occasions with no observable adverse effects. However, there has not yet been sufficient experience and medical investigation to serve as the basis for any final personnel exposure criteria. The specification prepared by M.I.T under subcontract from NASA for an MHD Test Facility is used as interim criteria for personnel and equipment exposure to magnetic fields.[52]

The standards are limited to constant DC fields. Submarine personnel are assumed to be in good health as is required by submarine medical qualifications. Limits for approved personnel are:

(1) Exposure for entire work-days 0.01 T

(2) Exposure for 1 hour or less 0.1 T

(3) Exposure for 10 minutes or less 0.5 T

For unapproved personnel (not a crew member) exposure limit is reduced to a magnetic field of less than 0.0005 T (no time limit).

Hand tools and portable equipment for use inside the 0.01 T perimeter must be of non-magnetic type or determined to be suitable for use in the presence of high fields.

DC magnetic fields may have serious adverse effects on the functions of equipment with moving parts, especially if the equipment operation is based on small electromagnetic forces. Also, even if there is no limit on environmental field from a functional standpoint, the forces on ferromagnetic parts must be considered.

Rectifiers, transformers, power supply controls, transducers, and electrical sensors must be arranged as to minimize the impact of magnetic interference on their performance. If arrangement in a location remote from a magnet is not possible, the magnetic fields should be aligned as to limit the interference. Devices such as strain gages are less critical and may only require proper compensation.

Very little experience or test data is available to date and suppliers may be unable to specify environmental field limits. Magnetic field of 0.05 T is considered an upper range for mechanical equipment such as pumps, compressors, refrigerators, etc. AVCO's experience shows that HP-1000 computer operation is not affected by a

magnetic field of 3 gauss; however, electronic monitors experienced a shift in the display. A field of 40 gauss had no impact on operation of mechanical pumps and similar equipment.[36]

The most practical and economical means of coping with fringe fields appears to be the separation of personnel and sensitive equipment from the magnet by appropriate distances. The use of local shielding, for example around a particular item of equipment or control station, may be appropriate in cases where remote location is impossible or has serious disadvantages.

6. CONCLUSION AND OPINIONS

The MHD propulsion and MHD power generation are still in their early developmental stages. With the present efforts in the SSN-21 new fast attack submarine design, employing conventional propulsion, it is doubtful that the U.S. Navy will risk a MHD prototype in the near future.

SSN-21 will be powered by a reactor similar in design to the power plant on a Los Angeles-class submarines but more powerful (60,000 SHP).[54] Presently, the PWR and steam energy conversion system remains as the most attractive submarine propulsion power system. Therefore, it is doubtful that the U.S. Navy will make significant contribution in the development of a more advanced power plant. Major progress is anticipated to come from the commercial power plant applications. The progress made in the past two decades suggests that the commercial advanced reactor technology should be well established by the 21st century. Only if successful, will the advanced reactor plants and advanced energy conversion systems receive the interest and support from the U.S. Navy.

It has already been noted that for an attractive nuclear gas turbine plant or nuclear MHD generator plant, further reactor development is required. The special features introduced by the gas turbine are primarily a call for higher pressures and an incentive to

provide the highest temperatures which the turbine plant itself can accommodate. Development in the desired direction is already proceeding. More particular aspects of the combined plant which might affect the reactor design are those of fault consequences, and of control. Here, analytical work does not suggest that there would be any major or urgent effect on the main aims of reactor development. Hence, the major obstacle to overcome is in the field of material engineering. To achieve 3000 K reactor temperatures, new materials which exceed present limitations must be developed.

The most optimistic estimates do not exceed a working fluid temperature of 2000 K. It is difficult to project when material technology will allow the temperatures recommended in this study. Judging by the present progress, the required high temperature materials may be available as early as the first decade of the 21st century.

The LM-MHD energy conversion system, in its development, is slightly behind the gas turbine technology. It may be said that MHD generators, being heat engines, are in competition with other energy-conversion technologies such as gas turbines, alkali-metal-vapor turbines and steam turbines. MHD will be successful if it can show advantages with respect to other energy-conversion technologies. If not adopted as the energy conversion system for future submarines, the MHD power generation may still be used in an energy topping applications with

some other energy conversion system such as steam turbine.

MHD propulsion can be coupled to the existing PWR with the steam turbine energy conversion system. Top speed of 30 kt. is achievable with a PWR rated about 130 MW. Recent advances in magnet design, primarily the development of new materials capable of superconducting at higher magnetic flux densities, make construction of powerful, compact magnets a practical reality.

Superconducting magnets of 6-10 T have been built. Japan is at the forefront of the world in magnet design. These magnets were not designed to operate in the hostile environment of the sea which is more severe with respect to temperature, humidity, and vibrations. The development of equipment for marine use is very near; demonstration will soon be available with Japan's MHD research progressing on schedule.

The cryostat design for naval use requires modifications based on the projected operational depth and exposure to shock. The structural requirements are presently under development with the lead of the MIT National Magnet Laboratory.

Cryogenic plant technology is limited to mobile operational units; however, adaptation to naval use is not considered a major problem. More emphases is needed on greater compactness and lighter weight required in devices and equipment developed for on-ship use.

The effect of fringe magnetic fields on personnel and equipment requires a great deal of research. Powerful magnets have been built, but an accurate assessment of biological damage caused by high magnetic fields is a statistical issue and will take time to quantify. Equipment performance evaluation, when subjected to high magnetic field, should become automatic as power producing applications take full advantage of superconducting technology. When equipment is purchased, the equipment suppliers should be requested to specify the maximum field in which the equipment can be operated safely without adverse effect on performance. This, undoubtedly, will escalate the cost of submarine equipment. Finally, internal arrangement and local shielding requirements bring a new meaning to submarine integrated engineering and architecture.

A large scale prototype is required to establish the validity for further research in MHD propulsion for submarines. The primary application of the MHD thruster concept is as a very quiet propulsion of submerged vessels. The turbulence in a MHD duct and the gas production may result in noise levels above those presently anticipated. Although, some problems may be eliminated in future designs and the thruster's signature reduced to very low levels, reliability can only be demonstrated through service performance.

REFERENCES

1.Grundy, R. F., Magnetohydrodynamic Energy For Electric Power Generation, (Noyes Data Corporation, Park Ridge, NJ,1978) pp. 2-10

2. Way, Stewart, Electromagnetic Propulsion For Cargo Submarines, Journal of Hydronautics, Vol. 2, NO. 2, pp. 49-57, April 1968

3. Langone, John, Yashiro Saji And His Magnetic Ship, Discover, pp. 42-48, April 1985

4. Taussig, R., A Foreign Technology Assessment Of Superconductor Technology Applied To MHD Ship Propulsion, Spectra Technology, Inc., STI #1705.01, December 1988

5. Coombe, R. A., Magnetohydrodynamic Generation Of Electrical Power, (Chapman and Hall, London, 1964) pp. 34-52

6. Sutton, Sherman, Engineering Magnetohydrodynamics, Series in Mechanical Engineering, (McGraw-Hill, New York, NY, 1965)

7. Meng, J. C. S., A Superconducting Electromagnetic Thruster for Underwater Propulsion, DARPA/NUSC Progress Review, Newport, RI, January 1989.

8. Cott, D. W., Daniel, R. A., MHD Propulsion for Submarines, Idaho National Engineering Laboratory, Idaho Falls, Idaho 1988, CDIF #2DOE-MHD-D140

9. Meng, J. C. S., A Demonstration Test of a Superconducting Electromagnetic Thruster Within Eighteen Months, Naval Underwater System Center, Newport, Rhode Island, 1988

10. Doragh, R. A., MHD Flow in a Rectangular Channel with Applications to a Marine Propulsion System Using Superconducting Magnets, M.I.T. Thesis, 1963

11. Rosa, R. J., Magnetohydrodynamic Energy Conversion, (McGraw-Hill, New York, NY, 1968) pp. 50

12. Comstock, L. P., Principles of Naval Architecture, (The Society of Naval Architects and Marine Engineers, New York, NY, 1967) pp. 299

13. Ibid, pp. 387-397

14. Sabersky, Acosta, Hauptmann, Fluid Flow, a First Course in Fluid Mechanics, (Macmillian Publishing Co., Inc., New York, NY 1964) pp. 260

15. Miller, D., Jordan, J., Modern Submarine Warfare, (Military Press dist by Crown Publishers Inc., New York, NY, 1987)

16. Electric Boat Division, The Feasibility and Design of Nuclear-Powered Submarine Tankers, (General Dynamics Corporation, Grotton, Connecticut, December 1958) MA-1718

17. Loid, P., Bystrom, L., Hydronamic Aspects of the Design of the Forward and Aft Bodies of the Submarine, (The Royal Institution of Naval Architects, London, May 1983) paper #19

18. Mc Donnell Douglas Corporation, The Transition Analysis Program System, (Naval Sea System Command, June 1976) N00024-75-6-7205

19. Jackson, H. A., Submarine Parametrics, (The Royal Institution of Naval Architects, London, May 1983) paper #3

20. Meng, J. C., Huynh, Q., Castano, J., Superconducting Electromagnetic Thruster for Marine Applications, Naval Underwater Systems Center, Newport, Rhode Island, June 1988

21. Backhaus, O., Nozzle Propellers for Large Ships, Lectures, (Ingenieur-Buro Kort, London, April 1971)

22. Haywood, R. W., Analysis of Engineering Cycles, (Pergamon Press, Elmsford, NY, 1975) pp. 120-143

23. Shippingport Pressurized Water Reactor, (Addison-Wesley Publ. Co., Reading, Mass., 1958)

24. N.S. SAVANNAH Safety Assessment, Vol I-Engineering and Construction, prepared for USAEC and Mar Ad by Babcock and Wilcox, Atomic Energy Division, August, 1960.

25. Woisin, G., Safety Features in Germany's Nuclear Ship, Safety at Sea International, Sept/Oct, 1968.

26. Jane's Fighting Ships 1987-1988. (Janes Publishing Company, Ltd., London, England, 1987)

27. Brooks, R. M., Light-Weight Nuclear Propulsion Applications to High Performance Naval Ships, M.I.T Thesis, June, 1976

28. Pardue, W. M., Denning R. S., A Comparison of Advanced Reactor Potentials, ASME-ANS International Conference on Advanced Nuclear Energy Systems, March 14-17, 1976, (The American Society of Mechanical Engineers, New York, N.Y., 1976) pp. 159-177.

29. Proceedings of the Submarine Technology Workshop, University of Rhode Island, W. Alton Jones Campus, August 1974.

30. Jones, A. R., A Very High Temperature Reactor (VHTR) Technology, Proceedings of the 10th Intersociety Energy Conversion Engineering Conference, vol. 1. New York: Institute of Electrical and Electronics Engineers, 1975, pp. 329-337.

31. Thompson, R. E., Lightweight Nuclear Power Plant Applications of a Very High Temperature Reactor (VHTR), Proceedings of the 10th Intersociety Energy Conversion Engineering Conference, vol. 1. New York: Institute of Electrical and Electronics Engineers, 1975, pp. 1089-1097.

32. Symposium on the Thermal and Hydraulic Aspects of Nuclear Reactor Safety, vol. 2., Liquid Metal Fast Breeder Reactors, The American Society of Mechanical Engineers, New York, N.Y. 1977.

33. Fillnow, R. H., The Breeder Reactor-A Manufacturer's Viewpoint, Fission Breeder Reactor Energy Seminar, The Institute of Electrical and Electronics Engineers, March 26-27, 1979, pp. 88-98.

34. Hara, T., Kosugi, H., Joyo Construction and Preoperational Test Experience, ASME-ANS International Conference on Advanced Nuclear Energy Systems, The American Society of Mechanical Engineers, New York, N.J., March 14-17, 1976, pp.13-28.

35. Salerno, Tippets, Gyorey, Prism-Modular Power Reactor and Passive Safety Features, Proceedings of the Joint ASME-ANS Nuclear Power Conference, The American Society of Mechanical Engineers, New York, N.Y. 1988, pp. 211-219

36. Swallom, D., Sadovnik, I., Personal Communication, AVCO Inc., Everett, MA., January, 1989.

37. Messinger, H., Clarke, P., Bowen, W., Helium Management Aboard Navy Ships Equipped with Superconductive Electric Propulsion Systems, DTNSRDC report PAS-81/17, Annapolis, MD., February, 1982

38. Kirtley, J., Personnal Communication, M.I.T., Cambridge, Mass., January, 1989

39. MHD Magnet Technology Group, MHD Magnet Technology Development Program Summary, Plasma Fusion Center, M.I.T., Cambridge, MA., November, 1983, pp. 221-231

40. Ibid. pp. 107-109

41. Grundy, R. F., Magnetohydrodynamic Energy for Electric Power Generation, (Noyes Data Corporation, Park Ridge, NJ., 1978) pp. 86-108

42. Proceedings of a Symposium on Magnetohydrodynamic Electrical Power Generation, Vol. 1, Closed Cycle MHD with Gaseous Working Fluids, (International Atomic Agency, Vienna, 1968)

43. Grundy, R. F., Magnetohydrodynamic Energy for Electric Power Generation, (Noyes Data Corporation, Park Ridge, NJ., 1978) pp. 190

44. Specialists Meeting on Coal Fired MHD Power Generation 1981, (The Institution of Engineers, Australia, Paragon Printers, Fyshwick, ACT 1981) No. 81/13, pp. 7.3

45. 21st Intersociety Energy Conversion Engineering Conference, Advancing Toward Technology Breakout in Energy Conversion, (American Chemical Society, Washington, DC., 1986) pp. 272-298

46. Proceedings Series, Advanced and High-Temperature Gas-Cooled Reactors, Proceedings of a Symposium held by the Interantional Atomic Energy Agency, October, 1968 (IAEA, Austria, February, 1969) pp. 295-314

47. Chafe, J. N., Helium Flow System for a 10 MVA Superconducting Generator, M.I.T. Thesis, June, 1984

48. Bagley, D., Personal Communication, David Taylor Research Center, Annapolis, MA., March, 1989

49. Grundy, R. F., Magnetohydrodynamic Energy for Electric Power Generation, (Noyes Data Corporation, Park Ridge, NJ. 1978) pp. 150-160

50. Swallom, D., McClaine, A., Conceptual Design of a Space-Based Nuclear Magnetohydrodynamic Power Generator for Directed Energy Weapons, Phase 1 Final Report DE-AC03-86SF16507 prepared by AVCO Research Laboratory, Inc., May, 1987

51. MHD Magnet Technology Group, MHD Magnet Technology Development Program Summary, Plasma Fussion Center, M.I.T., Cambridge, MA., September, 1984

52. MHD Magnet Technology Group, MHD Magnet Technology Development Program Summary, Plasma Fussion Center, M.I.T., Cambridge, MA., November 1983, pp. D1-D7

53. 1976 ASME-ANS International Conference on Advanced Nuclear Energy Systems, (The American Society of Mechanical Engineers, New York, N.Y., March, 1976)

54. Providence Sunday Journal, January pp. B1, by Robert Becker